Modeling of Ethanol Metabolism and Transdermal Transport

Gregory Daniel Webster

Thesis submitted to the faculty of the
Virginia Polytechnic Institute and State University
in partial fulfillment of the requirements for the degree of

Master of Science
In
Mechanical Engineering

H. Clay Gabler, PhD (Chair)
Stefan M. Duma, PhD (Co-Chair)
J. Wallace Grant, PhD

May 28, 2008
Blacksburg, Virginia

Keywords: Transdermal, Ethanol, Alcohol, Modeling, Ignition Interlock, Alcohol Sensor

Modeling of Ethanol Metabolism and
Transdermal Transport

Gregory Daniel Webster

ABSTRACT

Approximately 14,500 people were killed in traffic crashes where the driver was legally intoxicated in 2005, constituting 33% of all traffic fatalities that year. While social efforts to reduce the number of traffic fatalities have shown to be moderately successful, alcohol has remained a factor in 40% of all traffic deaths over the past decade. Transdermal ethanol detection is a promising method that could prevent drunk driving if integrated into an ignition interlock system; potentially preventing 90 million drunk driving trips a year in the US. However, experimental data from previous research has shown significant time delays between alcohol ingestion and detection at the skin which makes real time estimation of blood alcohol concentration via skin measurement difficult. Using a validated model we studied the effects that body weight, metabolic rate and ethanol dose had on the time lag between the blood alcohol concentration and transdermal alcohol concentration. The dose of alcohol ingested was found to have the most significant effect on the skin alcohol lag time. Additionally, custom transdermal ethanol sensors were designed and fabricated and a pilot study on human subjects was conducted to determine if inexpensive transdermal ethanol sensors could be used to detect alcohol in drivers.

Table of Contents

List of Figures

List of Tables

Acknowledgments

I would like to thank Amanda Covey for her help with everything from ordering the parts that I needed to build the sensors to managing the money used to compensate our test subjects. This project would not have been possible without her help.

I would like to thank Stephanie Comas for her help with the Human Subject testing and for her help with the data collection and analysis.

I would like to thank my parents for their support during my two years at Virginia Tech.

I would like to thank my advisor, Clay Gabler, for all of his support and guidance throughout my graduate career and for his interest and support of the study presented in this thesis.

I would like to thank my Center for Injury Biomechanics lab mates, in particular Doug Gabauer, Craig Thor and Qian Wang who certainly made day to day activities interesting. I would also like to thank Sarah Manoogian and Eric Kennedy for their help and advise concerning both research and career issues.

Chapter 1. Introduction

In 2005, approximately 14,500 people were killed in car crashes where the driver was legal intoxicated. This toll comprised 33% of all traffic fatalities in 2005 (NHTSA, 2006). Efforts to reduce the number of alcohol related fatalities have included increasing the presence of law enforcement personnel on the roads, stiff criminal and financial consequences if caught driving under the influence of alcohol and increased media coverage of the problem. These social solutions to prevent drinking and driving have significantly reduced the percentage of alcohol related traffic fatalities. As shown in Figure 1-1, between 1982 and 1992 alcohol related traffic fatalities dropped from 60% to 40% of all traffic fatalities. However since the early 1990's the influence of alcohol in traffic deaths has reached a plateau, constituting approximately 40% of all traffic fatalities. This stagnation suggests that social efforts to prevent drinking and driving may have reached the limit of their effectiveness.

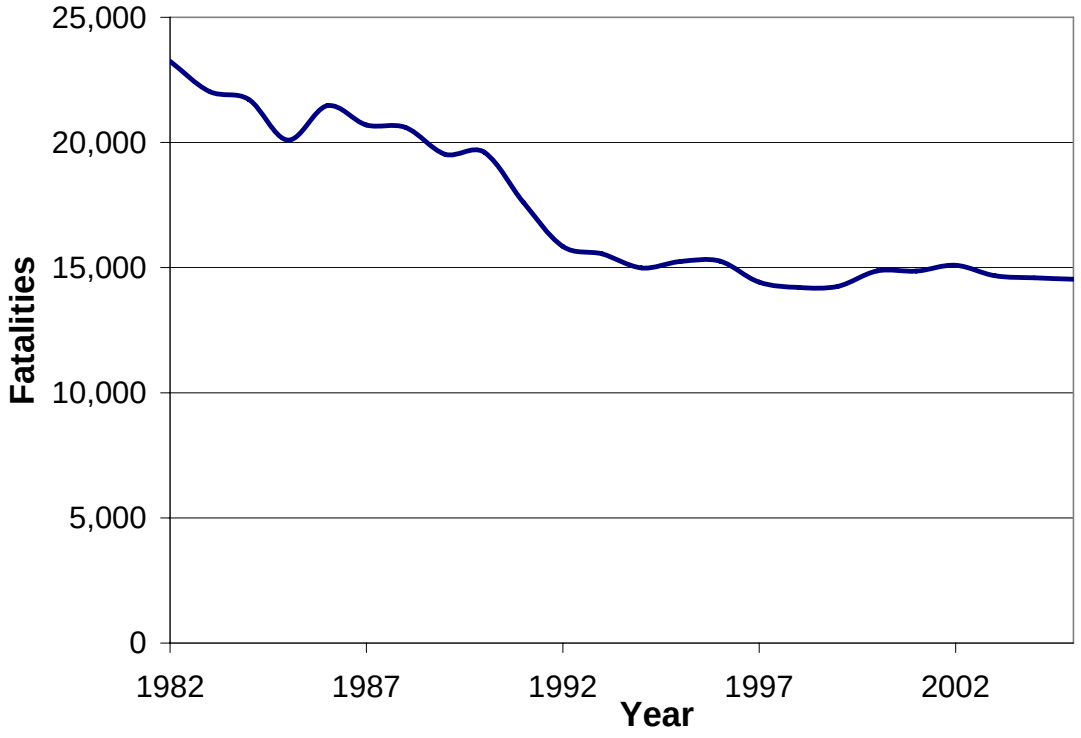

Figure 1-1. Alcohol Related Traffic Fatalities per Year

The best way to reduce the number of alcohol related traffic fatalities is to prevent people from driving drunk to begin with. One aggressive method to eliminate drunk driving would be to fit every highway vehicle with an ignition interlock device that would prevent the vehicle from starting if it sensed that the driver was intoxicated (MADD, 2006). The deployment of such a device would prevent the estimated 90 million drunk driving trips that Americans make every year (IIHS, 2006). The greatest challenge widespread deployment of alcohol ignition interlocks face is the development of a non-invasive method to detect if the driver is intoxicated. Nearly 40% of Americans do not drink alcohol at all; therefore a detection method that requires extra attention from the driver prior to every start of the vehicle will inconvenience a large section of the population not responsible for alcohol related crashes and will most likely not be tolerated by the public.

1.1. Physiologic Response to Alcohol

Alcohol, once ingested, enters the stomach. From here, the alcohol slowly empties into the small intestines. The small intestines are highly vascular and the alcohol that enters from the stomach is quickly absorbed into the blood steam. The first stop the alcohol makes in the blood stream is the liver, via the portal vein. The liver is the site of over 90% of all ethanol metabolism in the body. Some of the alcohol that enters the liver from the stream is eliminated by this metabolism, however much of the alcohol that first enters the liver is passed on to the rest of the body via the blood stream. The heart continues to circulate the alcohol in the blood stream allowing the alcohol to travel about the body where it is absorbed by the body tissues including, muscle and skin tissue. Alcohol also affects neurotransmitter communication in the brain which is largely responsible for the euphoric feeling experienced when a small to moderate amount of alcohol is consumed. Consumption of alcohol can also affect ones ability to maintain balance, coordination or even breathing when large quantities of alcohol are consumed (Ramchandani, 2001).

For legal purposes, the level of intoxication is determined by measuring the concentration of ethanol in a person's blood. Typically this is achieved by drawing blood and analyzing the concentration of alcohol in the head space above the sample. Blood alcohol concentration (BAC) is expressed as a percentage of alcohol by mass in a specific volume of blood, with the unit of g/dl. Human tolerance to alcohol varies between individuals however BACs higher than 0.40 often result in alcohol poisoning or death. A BAC of 0.08 or higher is considered legally drunk in all 50 States. Table 1-1 gives the generally accept clinic symptoms and the corresponding BAC.

Table 1-1. Stages of Alcohol Intoxication (adapted from NIAAA, 1994)

BAC (g/100 ml of blood or g/210 l of breath)	Stage	Clinical symptoms
0.01 - 0.05	Subclinical	Behavior nearly normal by ordinary observation
0.03 - 0.12	Euphoria	Mild euphoria, sociability, talkativeness Increased self-confidence; decreased inhibitions Diminution of attention, judgment and control Beginning of sensory-motor impairment Loss of efficiency in finer performance tests
0.09 - 0.25	Excitement	Emotional instability; loss of critical judgment Impairment of perception, memory and comprehension Decreased sensory response; increased reaction time Reduced visual acuity; peripheral vision and glare recovery Sensory-motor incoordination; impaired balance Drowsiness
0.18 - 0.30	Confusion	Disorientation, mental confusion; dizziness Exaggerated emotional states Disturbances of vision and of perception of color, form, motion and dimensions Increased pain threshold Increased muscular incoordination; staggering gait; slurred speech Apathy, lethargy
0.25 - 0.40	Stupor	General inertia; approaching loss of motor functions Markedly decreased response to stimuli Marked muscular incoordination; inability to stand or walk Vomiting; incontinence Impaired consciousness; sleep or stupor
0.35 - 0.50	Coma	Complete unconsciousness Depressed or abolished reflexes Subnormal body temperature Incontinence Impairment of circulation and respiration Possible death
0.45 +	Death	Death from respiratory arrest

1.2. Current Detection Methods

Currently, there is only one BAC detection method that can reliably measure a person's BAC without drawing blood. By measuring the concentration of alcohol present in a person's exhaled breath it is possible to achieve an indirect measurement of the person's BAC. Pulmonary ventilation is an essential biologic function that delivers oxygen to and removes carbon dioxide from the blood stream.

When a person takes a breath the inhaled air fills small sac-like structures in the lungs called alveoli. The alveoli are the basic structure in lung tissue and are highly perfused, as the lungs receive nearly 100% of the total cardiac output. Oxygen is transported to the blood stream and carbon dioxide is transport to the inhaled air by diffusion across the alveolar wall. When alcohol is present in the blood stream, it also diffuses across the alveolar wall from the blood stream to the air. It has been observed that 0.7% of the ethanol consumed is excreted through the breath (Ramchandani, 2001). Experimental studies have shown that the concentration of alcohol in blood is 2448 times the concentration of alcohol in expelled air (Jones and Andersson, 2003). This relationship allows the BAC of a person to be indirectly measured via the concentration of alcohol in their breath.

There are a number of commercially available devices designed to calculate BAC by measuring the alcohol content in a person's expelled breath. These devices are called Breath Alcohol Dectors, and example breath alcohol detector is shown in Figure 1-2.

Figure 1-2. Breath Alcohol Detector

Professional breath alcohol detectors use an electrochemical fuel cell to detect the concentration of ethanol present. Figure 1-3 is a diagram showing the components of a basic alcohol fuel cell. The fuel cell's main component is the porous middle layer sandwiched between coatings of platinum on either side. The porous middle layer has an electrolyte treatment. When a sample of gas containing alcohol is applied over the top layer of platinum, it is oxidized via an applied catalyst on the surface of the platinum. This chemical reaction frees electrons and hydrogen ions. The hydrogen ions are allowed to pass through the porous middle layer allowing the freed electrons to flow along the top layer of platinum through a load resistor and down to the bottom layer of platinum. The hydrogen ions that pass through the porous middle layer combine with oxygen on the bottom layer to form water. The movement of electrons produces a current. A measurement of this current can be used to assess the amount of alcohol applied to the top layer of platinum, if the volume of gas is known, than concentration can be calculated.

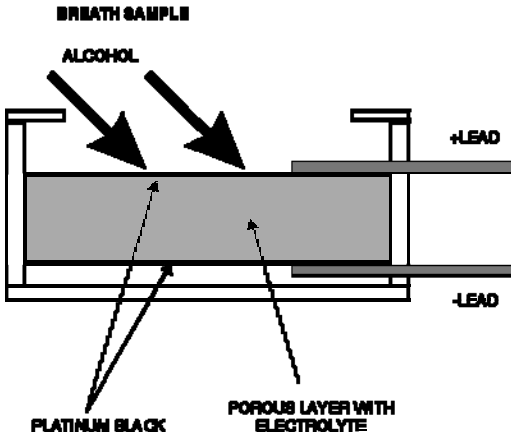

Figure 1-3: Alcohol Electrochemical Fuel Cell

To use a typical breath alcohol detector, the subject is required to blow into a sampling tube for a prescribed amount of time. Pressure and flow sensors contained in the device ensure the fuel cell is given enough sample to make an accurate measurement. The computer contained in the device measures the voltage produced by the electrochemical fuel cell and uses an algorithm to calculate the subject's blood alcohol concentration.

Currently available ignition interlock systems use breath alcohol detectors to sample the driver's breath alcohol concentration prior to starting the car. If the detector senses a high enough concentration of alcohol in the driver's breath the ignition interlock system will act like a switch, preventing the engine from starting. Current breath sensing interlock systems are cumbersome, expensive and carry the stigma of being a convicted 'drunk driver.' Additionally, the breath alcohol test can take up to a minute to perform, adding considerable time to the process of starting the car. As a result, installation of ignition interlocks using breath alcohol detectors in every vehicle would most likely not be tolerated by the public due to that added cost and inconvenience.

1.3. New Detection Methods

The installation of ignition interlocks in every vehicle might be better accepted by the public if the detection was performed non-invasively. A non-invasive detection method would essentially be transparent to the driver requiring no special effort or action on the part of the driver. Several non-invasive technologies are being investigated as part of cooperative research and development effort headed by the Automotive Coalition for Traffic Safety (ACTS). These technologies include tissue spectroscopy, transdermal sensors, ethanol vapor sensors and ocular movement sensors (Pollard, et al, 2007).

Transdermal ethanol sensing, which is the focus of this research, detects the alcohol that diffuses from the blood stream to the surface of the skin. It has been shown that 0.1% of the ethanol consumed is lost through sweat (Ramchandani, 2001). In addition to sweat, ethanol is also absorbed by the skin from the blood and transported to the surface of the skin where it exits the body. The presence of a small, but detectable, concentration of alcohol at the surface of the skin presents a unique opportunity which could allow the concentration of alcohol below the skin, in the blood stream, to be estimated.

The integration of transdermal ethanol sensors into the steering wheel or other skin contact surface of a vehicle could allow an interlock system to measure the concentration of alcohol at the surface of a driver's skin. However, a reliable relationship between skin and blood alcohol concentration has yet to be developed.

A limited number of studies have investigated the relationships between BAC and skin alcohol concentration. A preliminary study performed on rats found a strong correlation between BAC and skin alcohol concentration. The rats were given a bolus injection of an ethanol/saline solution while under anesthesia. After the rats regained consciousness, measurements were made using an alcohol vapor sensor over the rats' unshaved abdomen as well as measurements made from blood drawn from the tail vein. The two measurements were plotted on the same graph and show the drop of ethanol concentration in the blood versus time with good correlation between the two sets of data ($r = 0.99$) (Giles et al, 1987).

Comparison of blood and skin alcohol concentrations on humans found a similarly high correlation. A set of healthy human test subjects were intravenously given ethanol. Alcohol vapor concentration measurements were made on the palms of the subject's hands and blood was also drawn to measure BAC. A comparison of blood alcohol concentration and skin vapor concentration showed a good correlation. An example plot is given in Figure 1-4 for one of the subjects in the study.

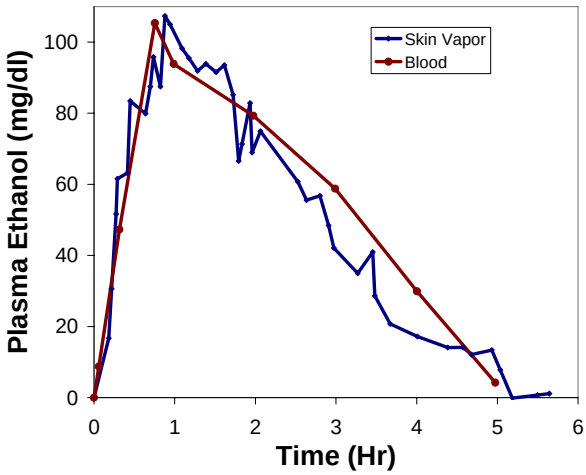

Figure 1-4. Blood and Skin Alcohol Concentration (Giles et al, 1987)

A different study compared blood alcohol concentration values obtained by breath alcohol detector to skin alcohol concentration measured by a wearable electronic transdermal alcohol sensor resembling a large watch. Comparison between transdermal sensor and the breathalyzer showed a good correlation between the data. The most significant difference noted by this study, aside from the magnitude of concentration measured, was the time lag between the peak alcohol concentration measured in the blood versus the peak alcohol concentration of the skin. This attributed to the time it takes for the ethanol to diffuse from the blood into the body's tissues (Swift, 1992).

Previous research has shown that transdermal ethanol concentration accurately follows the concentration profile of the ethanol in the blood via proportionally smaller concentrations of ethanol emitted at the surface of the skin. The largest issue with using skin measurements to detect BAC is that the alcohol does not diffuse through the skin instantly. Because of this, there can be a significant time delay between the equivalent blood and skin concentration values.

The purpose of this study is to better understand how the relationship between blood and skin alcohol concentration. Specifically, this study seeks to find what affects the lag time between equivalent blood and skin alcohol concentrations. The end goal of this research is determine if transdermal alcohol concentration measurements can be used as a reliable method to non-invasively sense a driver's BAC.

To approach this issue we have developed a computational model to predict the concentration of alcohol at the surface of the skin based on a given dose of alcohol. We have also developed prototype transdermal alcohol sensors and have taken preliminary data to assess if inexpensive alcohol sensors can be used to detect the alcohol emitted from the surface of the skin.

Chapter 2. Alcohol Metabolism and Transport Model

This chapter describes the development of a model to simulate the transport of alcohol from ingestion to excretion through the skin. The model comprises two linked component models: (1) a model of human ethanol metabolism and (2) a model of ethanol diffusion through the skin. The goal of this study is to assess the feasibility of transdermal alcohol sensing using a computational model that predicts the lag time between peak blood and skin alcohol concentrations. In particular, our objective is to determine how the lag time varies with ethanol dose, body weight and metabolic rate. We used the model as a tool to determine if transdermal alcohol sensing is appropriate for detecting driver BAC for different segments of the population and levels of intoxication.

2.1. Methods

The ethanol metabolism model consists of three well mixed compartments: the liver, the body fluids, and the stomach compartment. The second model describes ethanol diffusion through the skin. The skin is modeled as a two layer system that is exposed to the concentration of alcohol in the blood on one side and atmospheric air on the other. Since only minute amounts of ethanol are actually lost through the skin, the complete model does not reduce the total ethanol mass by the mass of ethanol excreted through the skin. Figure 2-1 shows a diagram of the system.

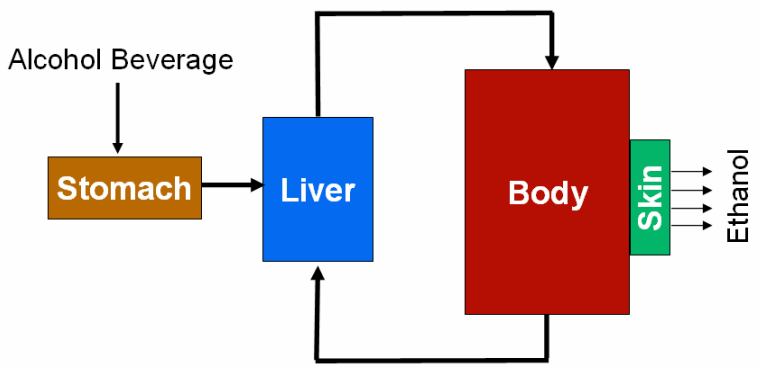

Figure 2-1. Model Diagram

2.2. Ethanol Metabolism And Blood Transport

The metabolism of ethanol has been rigorously studied both experimentally and computationally. Dose dependent BAC profiles have been well documented for specific body weight and ethnic groups (Widmark, 1932; Wilkinson, 1977) and mathematically modeled by several authors (Levitt, 1998; Umulis, 2005). After the consumption of an alcoholic drink, the ethanol in the drink is metabolized by the body via several biochemical reactions mostly occurring in the liver. Although studies have shown that other organs can metabolize alcohol to a lesser degree (Ramchandani, 2001) we chose to restrict ethanol elimination to only the liver compartment.

We modeled ethanol elimination in the liver using classical Michaelis - Menten kinetics for enzymatic reactions. The ethanol elimination rate is given in Equation 2-1.

$$\text{Ethanol Elimination Rate} = \frac{V_{max} C_{Liver}}{C_{Liver} + K_m} \tag{2-1}$$

V_{max} represents the maximum rate the liver can metabolize ethanol given in mol/min, K_m is the concentration of ethanol necessary for the liver to metabolize ethanol at half of its maximum elimination rate, given in mol/liter and C_{Liver} is the concentration of ethanol in the liver, also given in mol/liter. At lower concentrations of ethanol the rate of ethanol elimination is proportional to the concentration of ethanol in the liver, so that ethanol is eliminated faster as alcohol concentrations increase. Ethanol metabolism reaches a maximum elimination rate of V_{max} when C_{Liver} overwhelms K_m. This is shown in Figure 2-2 for low alcohol concentrations in the liver.

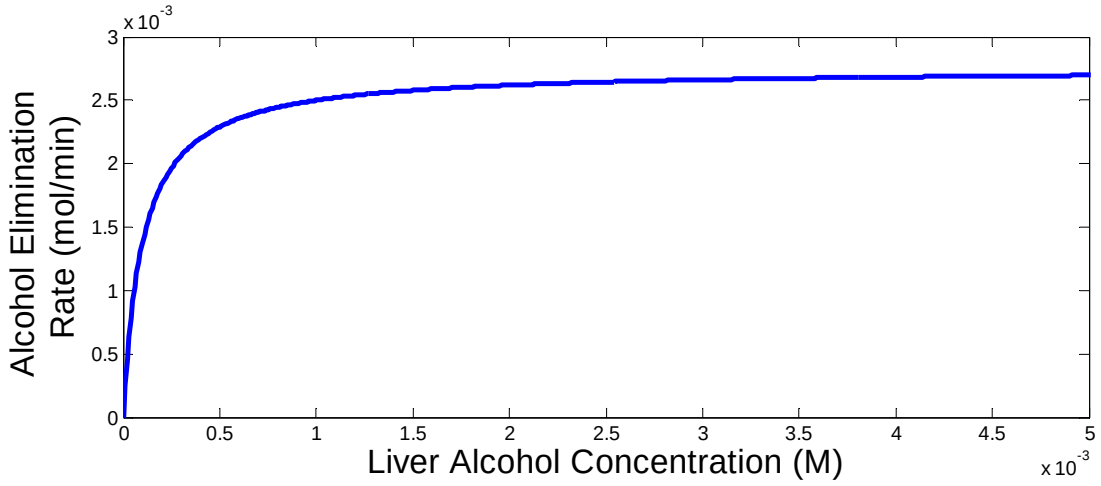

Figure 2-2. Alcohol Elimination Rate vs. Liver Alcohol Concentration (C_{Liver})

The stomach compartment was added to the model to gradually add ethanol to the body, mimicking the actual behavior of the stomach. This is representative of how alcoholic beverages are absorbed into the blood stream. Figure 2-1 shows that the stomach compartment empties into the liver simulating the transport of ethanol from the stomach to the liver via the Portal vein which connects the small intestines to the liver. In this manner the liver may eliminate some of the ethanol ingested before it enters the body compartment. The rate at which the stomach

empties is controlled by the constant k_s. Equation 2-2 describes the volumetric rate of change of the stomach contents as a function of k_s and the current fluid volume in the stomach.

$$\frac{dV_s}{dt} = -k_s V_s \tag{2-2}$$

Many values, developed both experimentally and computationally, have been suggested for k_s (Levitt, 1994, Wilkinson, 1977, Umulis, 2005). k_s was calculated based on k_{smax}, the maximum rate of emptying in min^{-1}, x, the dose of ethanol given in moles and a, a constant with units mol^{-2} as shown in Equation 2-3. Figure 2-3 is a plot showing how ks varies with alcohol dose, x.

$$k_s = \frac{k_{S\max}}{\left(1 + a(x)^2\right)} \tag{2-3}$$

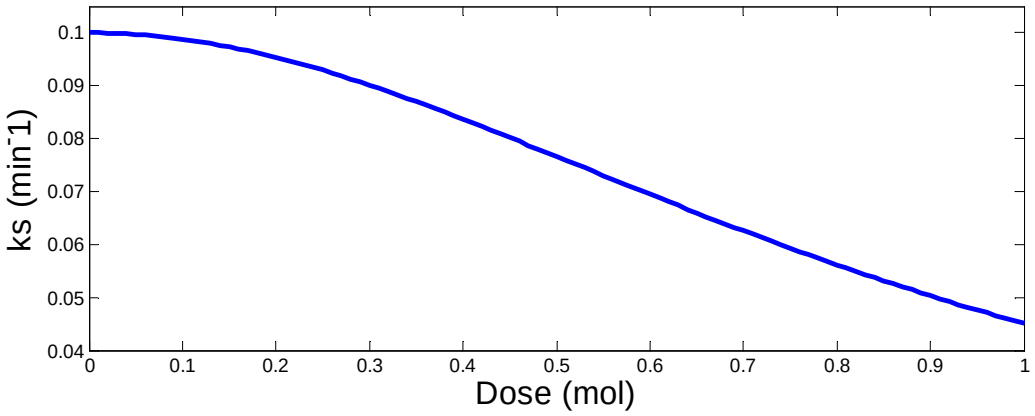

Figure 2-3. Stomach Emptying Rate vs. Alcohol Dose

Using Equations 2 and 3, the rate of stomach emptying, and thus the rate of ethanol addition to the body, is controlled by the amount of ethanol in the stomach, in moles, and the volume of the

stomach, in liters. The rate at which ethanol is added to the body is dependent largely upon the initial dose of ethanol in the stomach and the current volume of the stomach.

Mass balance equations were developed to describe the change in concentration between the liver compartment and the body compartment. Equation 2-4 describes the change in concentration of ethanol in the body compartment, where V_{Body} is the volume of the body fluids given in liters, and Q is the blood flow rate into and out of the liver, given in liters/min. It should be noted that V_{Body} represents both the blood volume and the volume of tissue fluids combined, which we took to be 60% of the total body mass (Levitt and Levitt, 1998). In this model both blood and water are considered to be well mixed since we are only concerned with the concentration of ethanol. Equation 2-5 describes the rate of concentration change in the liver. V_{Liver} is the volume of the liver, which we chose to be 0.61 liters. All concentrations are given in mol/min. The stomach emptying rate appears in the middle of this equation serving as the addition of ethanol to the liver compartment, multiplied by the concentration of ethanol in the stomach to give units of mol/min. Finally, ethanol is eliminated from the liver by the last term, as described previously, at a rate proportional to the liver ethanol concentration.

$$V_{Body}\frac{dC_{Body}}{dt} = Q\left(C_{Liver} - C_{Body}\right) \tag{2-4}$$

$$V_{Liver}\frac{dC_{Liver}}{dt} = Q\left(C_{Body} - C_{Liver}\right) + \left(k_s V_{Stomach} C_{Stomach}\right) - \frac{V_{max} C_{Liver}}{K_m + C_{Liver}} \tag{2-5}$$

Equations 2-2, 2-4 and 2-5 were solved using a stiff ordinary differential equation solver from the commercial computing package MATLAB. ODE23s was used because it gave the smoothest solution. ODE45 was used initially, but it did not produce smooth results during early development of the model resulting in oscillations in the solution.

2.2.1. Skin Model

Several models exist to describe the transport of substances across the skin both from the skin's surface to the blood and vice versa [Anderson, 2006]. Based on these models we modeled the skin as a two-layer system consisting of the epidermis and the stratum corneum, which have drastically different transport properties. A diagram is given in Figure 2-4. The concentration of ethanol in the blood, as calculated from the metabolism model, serves as the time dependent boundary condition imposed at the blood-epidermis boundary. Driven by the concentration gradient, ethanol diffuses through the epidermis and the stratum corneum to the atmospheric air boundary where a constant concentration devoid of ethanol is imposed.

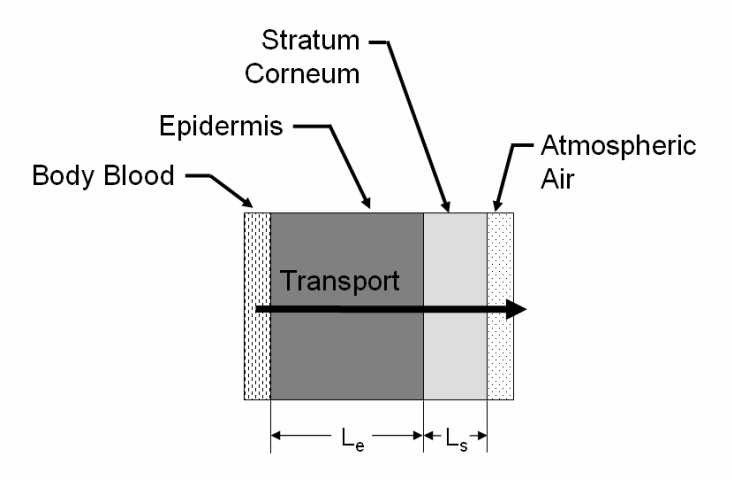

Figure 2-4. Skin Diagram

Equations 2-6 and 2-7 describe the transport of ethanol, in terms of partial pressures, across the epidermis and stratum corneum respectively. β represents ethanol solubility, D represents molecular diffusivity, A is the cross sectional area for transport and L is the linear distance for this transport; all for the medium indicated by the subscript.

$$\beta_e A L_e \frac{\partial P_e}{\partial t} = D_e \beta_e A L_e \frac{\partial^2 P_e}{\partial x^2} \qquad 0 \le x < L_e \tag{2-6}$$

$$\beta_s A L_s \frac{\partial P_s}{\partial t} = D_s \beta_s A L_s \frac{\partial^2 P_s}{\partial x^2} \qquad L_e < x \le L_e + L_s \tag{2-7}$$

At x = 0, the partial pressure of ethanol in the blood is imposed at the epidermis. This was found using Equation 2-8 which converts the concentration of alcohol in the blood to the partial pressure of alcohol in the skin. R is the universal gas constants and T is the body temperature.

$$P_1^t = BAC^t \frac{RT}{1000} \tag{2-8}$$

Similarly, at $x = L_e + L_s$ a partial pressure of zero is imposed which represents the clearing of the surface of the skin of ethanol vapor which would have accumulated there due to the diffusion process. A forward-difference approximation was implemented using MATLAB to solve Equations 2-6 and 2-7 simultaneously. Since the transport of alcohol across the skin can be modeled using diffusion in one dimension, calculation of the concentration of alcohol in both time and space can be discretely determined using the Fourier number to simplify the expression. Equations 2-9, 2-10 and 2-11 describe how the forward difference finite difference solving

method was implemented. Note that *Fo* was selected to be less than 0.5 so a stable solution could be found. Other finite difference methods can be used to solve the model.

$$P_m^{t+1} = Fo_e(P_{m+1}^t + P_{m-1}^t) + (1 - 2Fo_e)P_m^t \tag{2-9}$$

$$Fo = \frac{\alpha}{(\Delta x)^2} \tag{2-10}$$

$$\alpha = \frac{D\beta AL}{\beta AL} \Rightarrow D \tag{2-11}$$

Table 2-1 summarizes the constants used in the simulation of this model.

Table 2-1. Summary of Constants (Levitt and Levitt, 1998; Anderson and Hlastala, 2006)

Variable	Value	Description	Unit
V_{max}	2.75	Maximum Liver Metabolism Rate	mmol/minute
K_m	0.1	Concentration for 50% V_{max}	mM
K_{smax}	0.1	Maximum Stomach Emptying Rate	min^{-1}
a	1.22	Stomach Emptying Constant	mol^{-2}
Q	1.5	Liver Blood Flow	liter/minute
β_e	232	Solubility in Epidermis	ml ethanol*100 ml $medium^{-1}$*$Torr^{-1}$
β_s	211	Solubility in Stratum Corneum	ml ethanol*100 ml $medium^{-1}$*$Torr^{-1}$
D_e	5.00E-06	Molecular Diffusivity in Epidermis	cm^2/second
D_s	5.00E-10	Molecular Diffusivity in Stratum Corneum	cm^2/second
L_e	0.02	Thickness of Epidermis	cm
L_s	0.0015	Thickness of Stratum Corneum	cm
A	7.50E-02	Capillary Surface Area	cm^2
R	62360	Universal Gas Constant	Torr*cm^3*mol^{-1}*K^{-1}

2.3. Results

2.3.1. Metabolism Model Validation

Validation of the model was performed using available experimental data published from several sources. Figure 2-5 presents the BAC predicted by the model overlaid with experimental data taken from Wilkinson (1977) under the same experimental conditions. During the Wilkinson study eight health adult human subjects were dosed with the equivalent of 1, 2, 3 and 4 standard drinks after fasting for 10 hours. Blood was drawn to measure their BAC from the tip of their fingers at regular intervals. The BAC curves vs. time curves collected during this study were averaged yielding a single curve per dose of alcohol given.

Simulations were conducted for 95% ethanol doses of 15, 30, 45 and 60 ml diluted in 150 ml of fluid and compared to the average BAC curve generated from eight adult males averaging 74.6 kg in weight. Figure 2-5 shows good agreement between the model and the experimental data. Comparison of the model and experimental data using root means square (RMS) differences gave R^2 values of 0.94, 0.95, 0.94 and 0.99 for each of the doses previously mentioned. The concentration curves generated by the metabolism model were then used to drive the skin diffusion model.

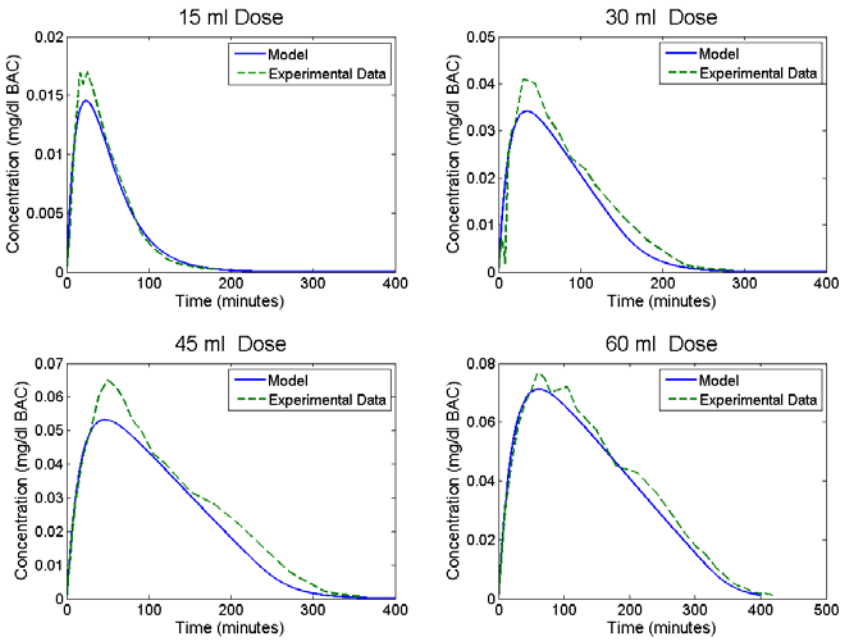

Figure 2-5. Metabolism Model Validation using Wilkinson data (1977)

Figure 2-6 shows how liver metabolism rate varies with time. Note that it quickly levels out to a value equal to V_{max} and slowly deceases around 200 minutes in proportion of the concentration of alcohol in the liver.

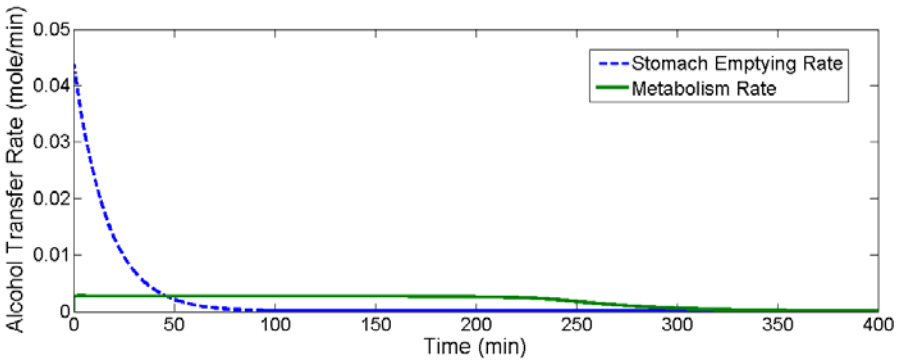

Figure 2-6. Transport and Elimination Rates in the Liver

2.3.2. Complete Model Validation

The combined metabolism-diffusion model was validated using data published by Swift [1998] in a paper describing a transdermal ethanol sensor system. The subject in the Swift study was given 0.75 ml ethanol per kg of body weight diluted 4:1 in cold orange juice. The weight of the subject was not specified in the study. We assumed a 50^{th} percentile male (78 kg). Our model input parameters were adjusted to reflect this dosage of 1.028 moles of ethanol and an initial stomach volume of 240 ml.

In the Swift study, blood alcohol concentration was carefully measured using a breath alcohol detector. The subject also wore a wrist watch style data logger/ethanol sensor that measured and recorded the concentration of ethanol at the surface of the skin during the experiment. The data logger reported the concentration as an electrical current proportional to the actual ethanol concentration present. Data was reported in microamperes, rather than in concentration. The correlation between the electrical current and actual concentration was not given. The ethanol concentration time-course behavior of the skin relative to the blood is of interest in this study; for validation purposes, model predicted transdermal alcohol concentration values were scaled to match the peak magnitude of the Swift data. Some time shifting was also required as the time zero in the Swift study was different from the time zero in our model. The results are shown in Figure 2-7 and Figure 2-8.

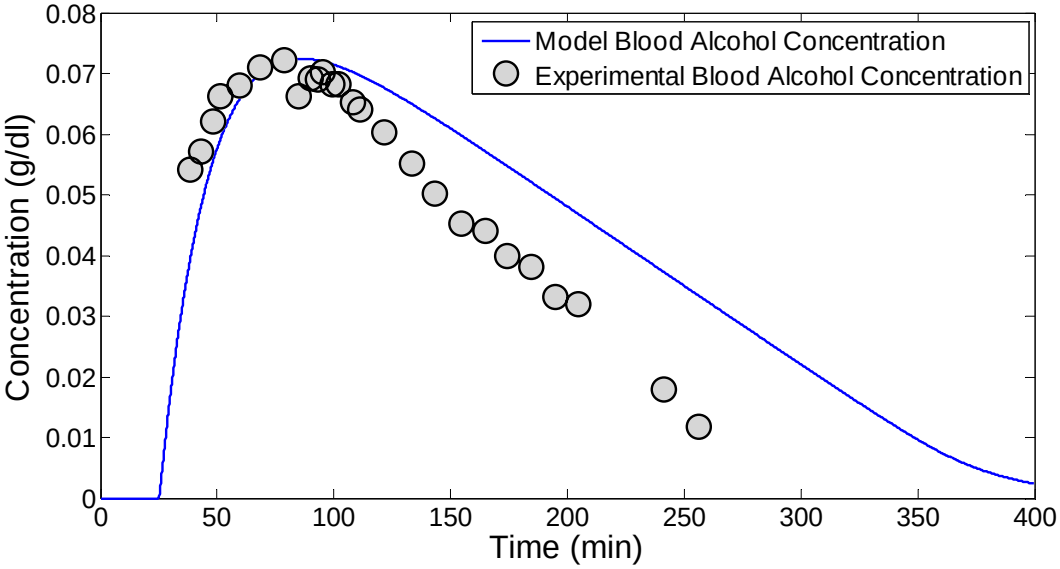

Figure 2-7. BAC Validation

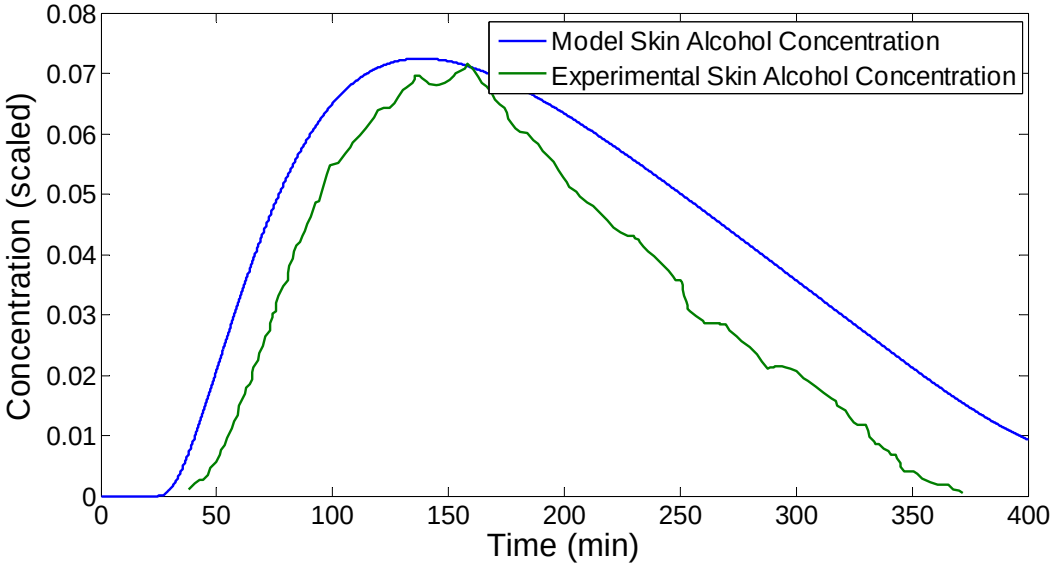

Figure 2-8. TAC Validation

The model accurately predicts when the BAC and Transdermal Alcohol Concentration (TAC) curves will peak, which we will use a registration mark to study time lag effects. The model is also able to replicate the shape of the experimentally determined BAC and TAC curves up to the point of peak TAC. Beyond peak TAC the model over predicts TAC. Comparison of the model

and experimental BAC curves RMS differences gave an R^2 value of 0.75 over the full range of data. The model and experimental TAC curves have an R^2 value of 0.66 over the full range of values and an R^2 value of 0.96 if only the first 180 minutes are considered.

2.3.3. Lag Time Effects

Using the validated model we studied the effects that body weight, metabolic rate and ethanol dose had on the peak lag time between the BAC and TAC curves.

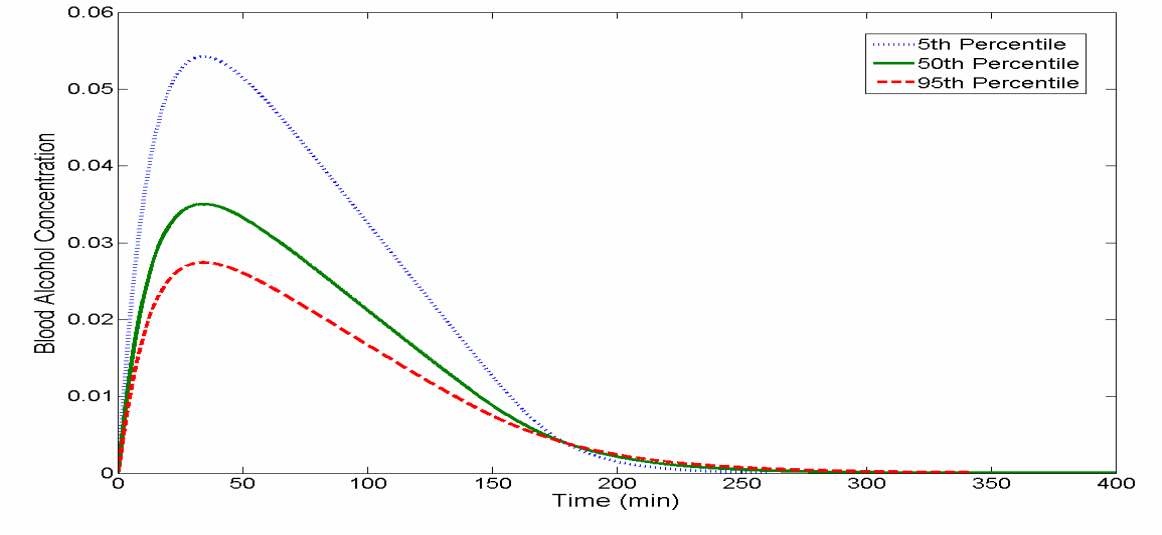

Figure 2-9. BAC curves as a Function of Body Weight

30 ml of 95% Ethanol in 150 ml Solution

To give the reader some perspective as to how BAC varies with body weight Figure 2-9 shows BAC vs. time curves for 5th (50 kg), 50th (78 kg) and 95th (100 kg) percentile body weights given the same dose of ethanol. Hereafter, a subject with a 5th, 50th or 95th percentile body weight will be referred to as a 5th, 50th or 95th percentile driver, respectively.

For a given dose, peak BAC increases as body weight decreases. Body fluid volume is proportional to body weight. When compared to 50th and 95th percentile drivers, a 5th percentile driver has a lower body fluid volume and is not able to dilute the ethanol to the same extent as the two larger drivers; this results in a higher predicted peak BAC. Additionally, all three drivers are assumed to have the same liver size and metabolize ethanol at the same maximum rate.

Our model shows that the dose of ethanol given to a driver affects the maximum BAC and time of max BAC. To show this, we held the body weight constant and varied the dose Table 2-2 shows the peak BAC values as well as the time it takes for the BAC to reach its maximum for a 50th percentile driver given 15, 30, 45 and 60 ml doses of 95% ethanol in 150 ml of solution. As dose size increases the maximum BAC increases and the time to reach peak BAC increases.

Table 2-2. Dose Effects on Peak Value and Time for 50th Percentile Driver

Dose (ml)	Peak BAC (g/dl)	Peak Time (min)
15	0.01	23.3
30	0.04	34.4
45	0.05	46.5
60	0.07	60.9

2.3.4. Lag Time Vs Body Weight And Dose

With the knowledge of how our model predicted the BAC response to different doses for different body weights, we examined how body weight affects the time lag between peak BAC and peak TAC. Skin diffusion coefficients and thickness were maintained constant for all simulations.

We first examined how the dose of ethanol given would affect the lag between the peak BAC and peak TAC. We chose dosages of 15, 30, 45 and 60 ml of 95% ethanol given in 150 ml of solution. We applied these doses to the model for 5th, 50th and 95th percentile driver body weights. The results are reported in Figure 2-10.

As dose size increases, the lag time between peak BAC and peak TAC also increases. From this plot we also see that lag time is insensitive to body weight.

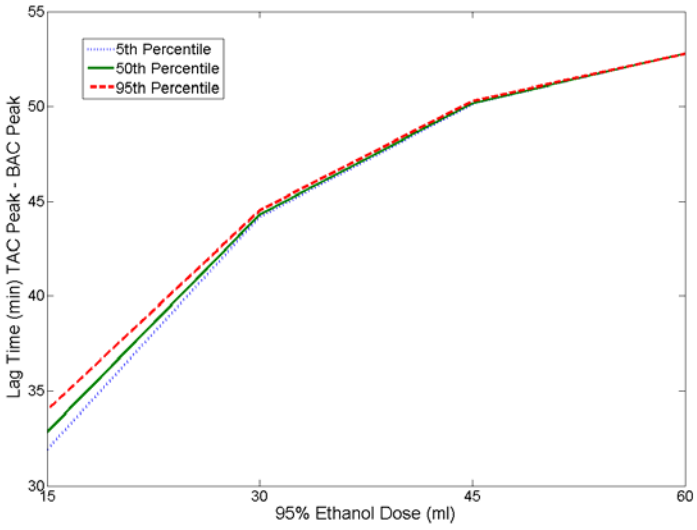

Figure 2-10. Time Lag Between peak BAC and peak TAC as a Function of Dose

2.3.5. Lag Time Vs Metabolic Rate

There is also variance in the rate at which individuals metabolize ethanol. This variance comes from a variety of sources including the individual's developed tolerance to alcohol and ethnicity.

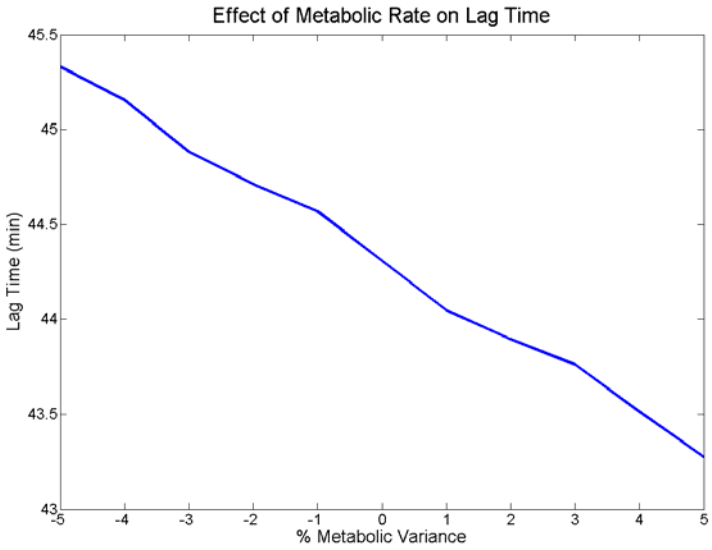

Figure 2-11. Metabolic Effects on Lag Time

We simulated the effect of different metabolic rates on a 50th percentile body consuming 30 ml of 95% ethanol diluted in 150 ml of fluid. We varied the maximum rate which the liver can metabolize ethanol, V_{max}, by +/- 5%. The results are plotted in Figure 2-11. We see that as V_{max} is varied from below nominal to above nominal the lag time decreases. Over the entire +/- 5% variance on V_{max} the time lag varied approximately 2 minutes, which equates to a total variance of 5% of the nominal lag time.

2.4. Discussion

The model presented here is capable of predicting the blood alcohol concentration in a person given a single dose of ethanol in beverage form. It also predicts the concentration of ethanol at the surface of the skin as a result of diffusion from the blood stream. Validation of the model

was performed using experimental data taken from a study performed by Swift [1992]. The model was used to estimate the time lag between peak BAC and TAC values to assess the feasibility of transdermal ethanol sensing as a method to measure real time BAC.

2.4.1. Body Weight

Our model shows that body weight has little effect on the time lag between peak BAC and TAC. Using four different doses we showed that the lag time was approximately the same for 5^{th}, 50^{th} and 95^{th} percentile drivers. This assumes that the metabolic rate and liver size is the same for all three body weights.

2.4.2. Dose

The amount of ethanol ingested had a significant effect on the lag time; as the dose increased so did the lag time. We varied the dose of ethanol given to 5^{th}, 50^{th} and 95^{th} percentile drivers and calculated the lag time between peak BAC and TAC. In our study, increasing the dose from 15 ml to 60 ml of 95% ethanol increased the lag time by approximately half an hour. As we showed previously, increasing the dose increases the peak BAC and increases the time to max BAC. However, this relationship is not linear which becomes apparent when the BAC curves are applied to the skin model. Different BAC values are imposed on the skin model's blood boundary during the same periods of time for the different doses. Since ethanol diffusion through the skin is concentration driven this affects the time it takes for each of the dose curves to cross the skin. The time differences experienced at the skin for each curve combined with the delay in peak BAC time results in an increase in the lag time as the dose is increased.

2.4.3. Metabolic Rate

We modeled differences in metabolic abilities among individuals by varying the V_{max} variable in the ethanol elimination expression by +/- 5%. This changed the rate at which ethanol was eliminated from the body. We noted that decreasing the metabolic rate increased lag time. These results are consistent with the values gathered from the dose-dependant study because decreasing the metabolic ability is similar to ingesting a larger dose of ethanol, which both result in a higher concentration of ethanol present in the body and a greater peak lag time. Similar to decreasing the ethanol dose, increasing the metabolic rate decreased the lag time. Changes in metabolic rate did not affect the lag time as significantly as changes in the dose amount. Regardless, by decreasing the metabolic rate by 5% the lag time was changed by approximately 5%.

2.5. Implications

The time lag between the blood and skin ethanol concentrations is not constant for all situations, making it difficult to develop a reliable algorithm to calculate BAC based on a TAC measurement. An ethanol measurement made at the surface of the skin could be mapped to a range of BAC values depending on the amount of alcohol consumed, as shown in the dose effect studies presented previously. Therefore, an ethanol concentration measurement made at the surface of the skin under quiescent conditions can not be equated to a real-time BAC value without additional information about how much the subject had to drink. Transdermal measurements made in this manner cannot accurately measure BAC in real-time. However, this

detection method could prove useful as a dichotomous test to sense if the driver has been drinking.

Additionally, an easy way to circumvent a transdermal measurement would be to block direct skin contact with the sensor. An intoxicated driver wearing gloves could potentially prevent the sensors for detecting any ethanol on their skin at all. A secondary sensor system would be required to ensure that the measurement is being made at the surface of the skin.

2.6. Limitations

The model used for these simulations is a simple ethanol metabolism and skin diffusion model, which has several limitations. The model was developed using metabolic rate and transport coefficients developed from a limited number of experiments performed on subjects who fall into the 50^{th} percentile driver weight class. Because of this, it is unknown how accurate our results are for the 5^{th} and 95^{th} percentile weight groups. Additionally, the model does not account for human variability in ethanol metabolism and transport; in particular, differences in gender or ethnicity. Our model also assumes that the stomach is empty when the dose of ethanol is given, which ignores the effects of a full stomach on ethanol absorption. Finally, our model uses a rudimentary mass scaling approach to generate the differences between the weight groups. The issue is examined more closely in the next chapter.

2.7. Conclusion

Transdermal sensing of the alcohol in a driver's blood is one possible way to non-invasively detect intoxicated drivers. However, the feasibility of this method suffers from the time delay required for the alcohol in the driver's blood to diffuse to the surface of the skin where it can be easily and non-invasively measured. To explore the feasibility of transdermal sensing, we developed and validated a model capable of predicting the time difference between the peak blood alcohol concentration and peak skin alcohol concentration in human subjects given a single dose of ethanol. The model and our findings are limited to the study of a single dose of ethanol; therefore our findings may not be applicable to drivers who ingest multiple drinks. We used this model to study the effects that body weight, amount of alcohol consumed and differences in ethanol metabolic rates have on the lag time between peak BAC and TAC values. We found that, for a given dose of alcohol, lag time is insensitive to body weight. However, the dose size has a significant impact on the blood-skin concentration lag. A larger dose of alcohol causes an increase in the lag time. A 15 ml dose of 95% ethanol given to all percentile drivers was found to have a lag time of approximately 33 minutes. Quadrupling the dose to 60 ml of ethanol increases the lag time to approximately 53 minutes. Finally, we examined the effect of minor variances in a person's ability to metabolize alcohol, which is representative of the differences between individuals. A 5% decrease in metabolic rate corresponds approximately to a 5% increase in time lag. Our model suggest that, due to the highly variable relationship between the BAC and TAC curves, transdermal sensing of real-time BAC using only skin surface measurements may prove to be very challenging.

Chapter 3. Effect of Gender and Body Mass on TAC Lag Time

Ethanol metabolism is a function of several factors including gender and body mass. The model described in the previous chapter was limited in its ability to differentiate between the lean body mass of males and females. For this study, lean body mass (LBM) will be considered to be the mass of the body that is capable of absorbing alcohol, i.e. the mass of the muscles and other organs that readily absorb alcohol. Adipose tissue and bone are not considered part of the lean body mass because they do not readily absorb alcohol. LBM is an important factor to consider when examining alcohol metabolism because it directly affects the maximum BAC for a given dose of alcohol. If the same amount of alcohol is given to two subjects of the same weight but different LBMs the subject with the larger LMB will have a lower BAC due to a larger available volume of tissue and fluid to dilute the alcohol.

An additional limitation of the previous model was that all subjects were considered to have the same liver size regardless of their total body weight. We assumed that ethanol metabolism only occurs in the liver at a rate proportional the concentration of ethanol in the liver. It is known that liver size varies with body size, however it was not known how liver size variation will affect the blood-skin lag time of the model. Liver sizes scaled to appropriately match body size and gender will be used in this study based on established body-liver size relationships.

This study will examine how gender and variations in liver size affect the lag time between the blood and skin alcohol concentrations using an improved model that scales LBM and liver mass to better represent males and females of different body masses.

3.1. Methods

To examine the effect of gender and scaled liver size on the transdermal transport lag of alcohol 5th, 50th and 95th percentile body weights based on the US population will be used (McDowell et al., 2005). Figure 3-1 and Figure 3-2 show weight distributions for US adult males and females.

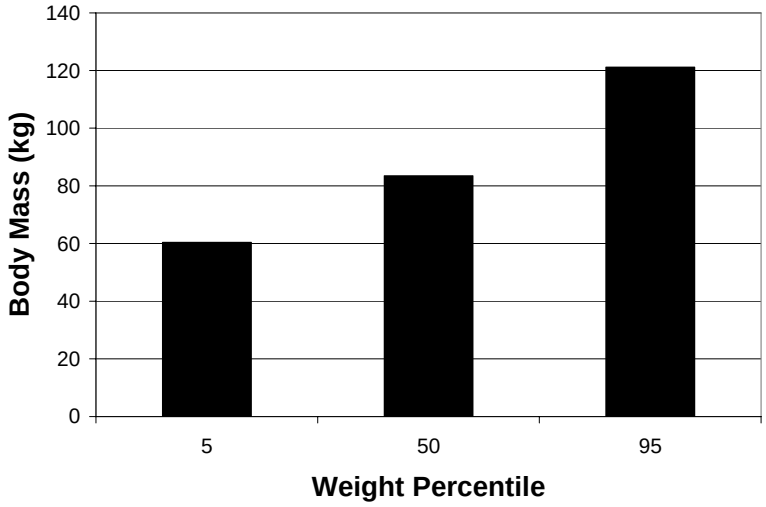

Figure 3-1. Weight Distribution by Percentile (Male)

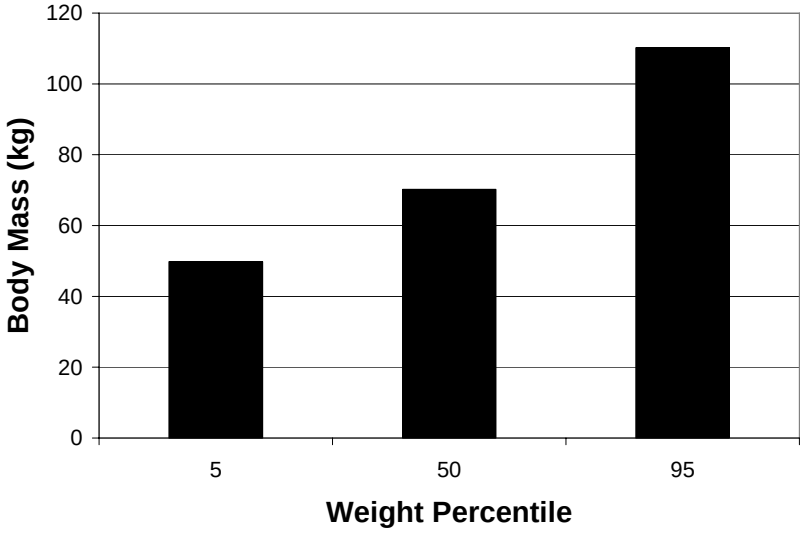

Figure 3-2. Weight Distribution by Percentile (Female)

It will be assumed that the lean body mass of males is 68% of their total body mass and 55% for females (Widmark, 1981). This is known as the Widmark Factor representing the fraction of total body mass that is alcohol soluble. Figure 3-3 and Figure 3-4 give the lean body mass for males and females for 5^{th}, 50^{th} and 95^{th} percentile body weights.

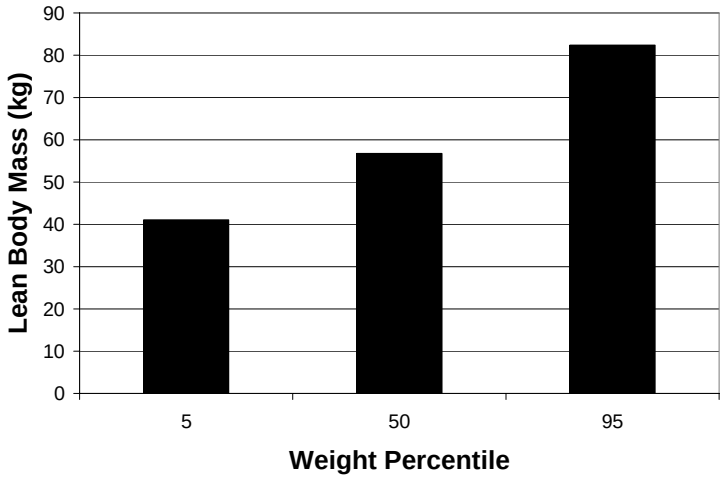

Figure 3-3. Lean Body Mass vs. Weight Percentile (Male)

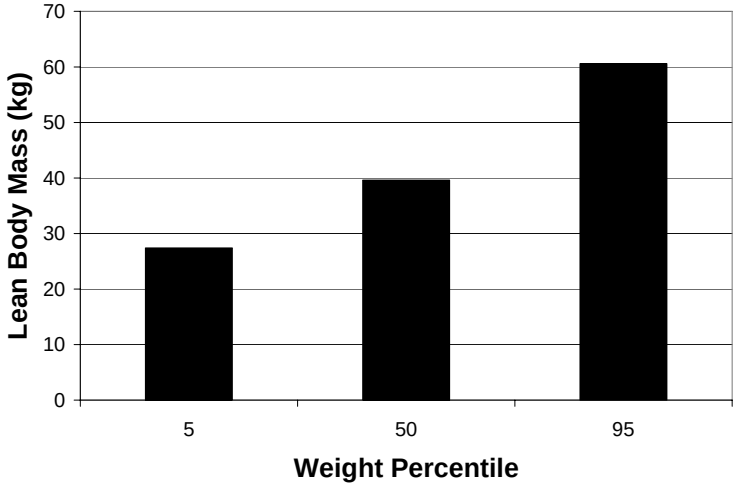

Figure 3-4. Lean Body Mass vs. Weight Percentile (Female)

Liver weight was calculated based on the relationship between body mass and gender developed by Chan et al (2006) shown in Equation 3-1. Calculated liver weights for males and females by body weights are given in Figure 3-5.

$$M_{Liver} = 218 + M_{Body} \cdot 12.3 + G \cdot 51 \qquad (3\text{-}1)$$

Gender	*G*
Male	1
Female	0

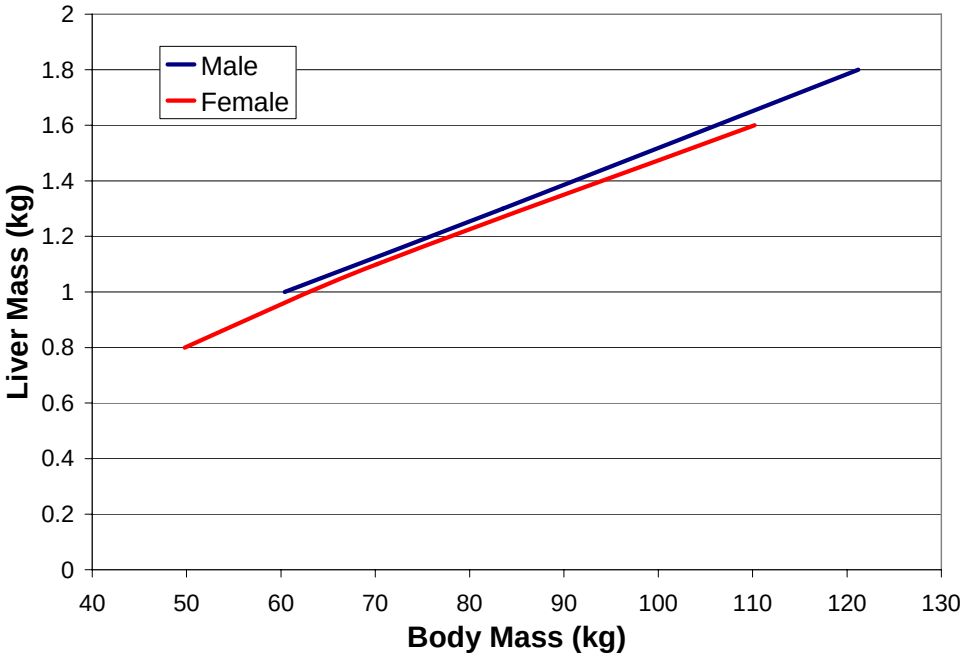

Figure 3-5. Liver Size by Weight and Gender

A summary of the values used in this analysis is given in Table 3-1.

Table 3-1. Summary of Model Input Variables

	Weight Percentile					
	5th		50th		95th	
	Male	Female	Male	Female	Male	Female
Body Mass (kg)	60.4	49.8	83.5	70.2	121.2	110.2
Lean Body Mass (kg)	41.1	27.4	56.8	38.6	82.4	60.6
Liver Weight (kg)	1.0	0.8	1.3	1.1	1.8	1.6

The metabolism model and transdermal transport model were solved using MATLAB. A stiff ordinary differential equation solver was used for the metabolism model and a forward finite difference approximation was used to solve the skin diffusion model.

3.2. Results

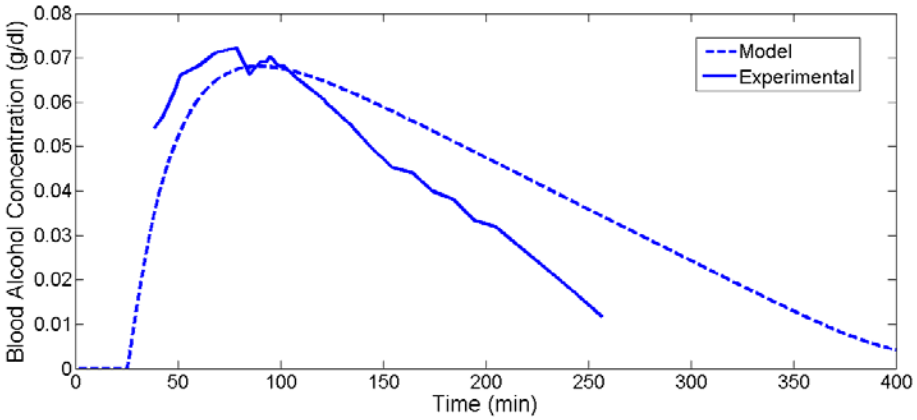

Figure 3-6. Model Validation (BAC)

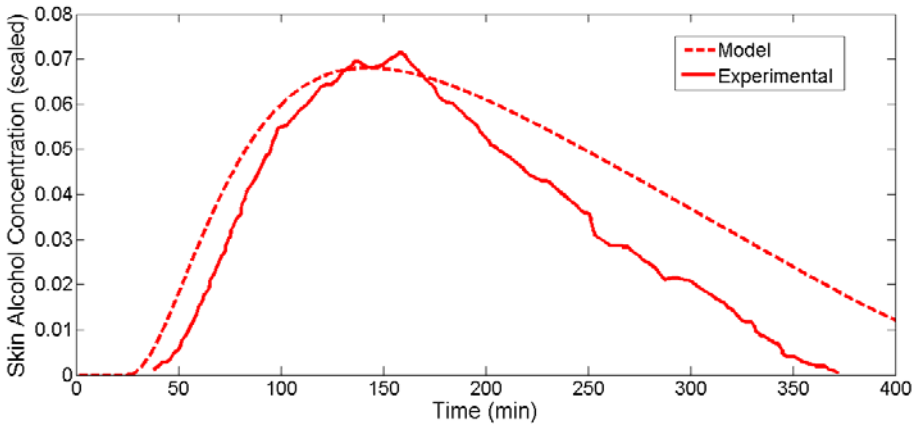

Figure 3-7. Model Validation (TAC)

Simulations were run using the values given in Table 3-1 for 15, 30, 45 and 60 ml doses of 95% alcohol diluted in 150 ml of solution. Figure 3-8, Figure 3-9 and Figure 3-10 show a comparison of maximum BAC for the original model and the new model employing mass scaling.

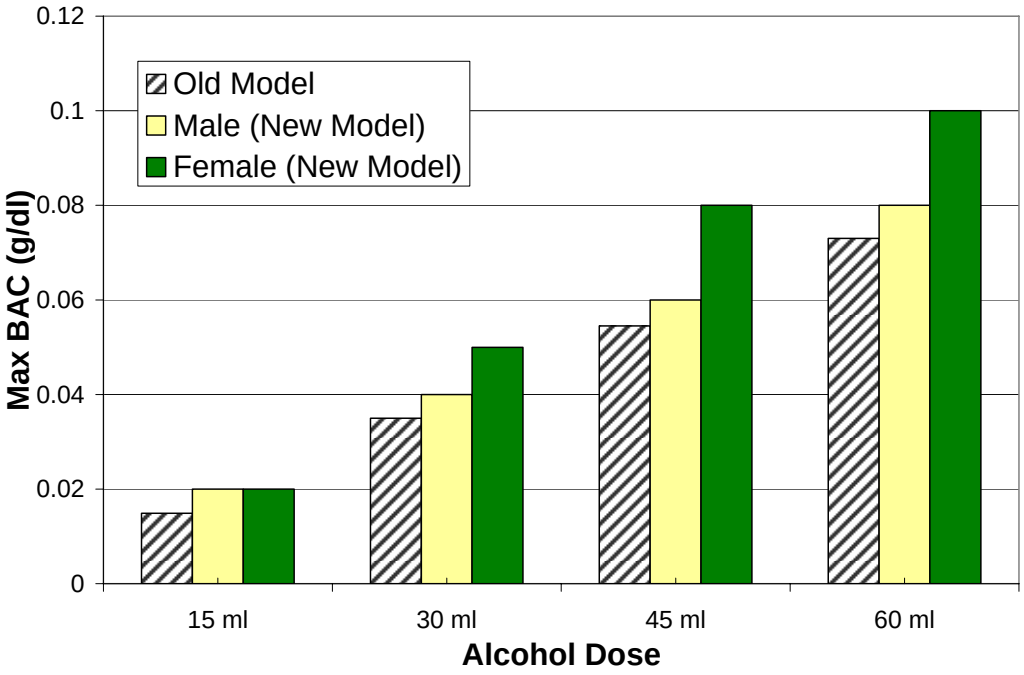

Figure 3-8. Comparison of Maximum BAC for 5th Percentile Humans

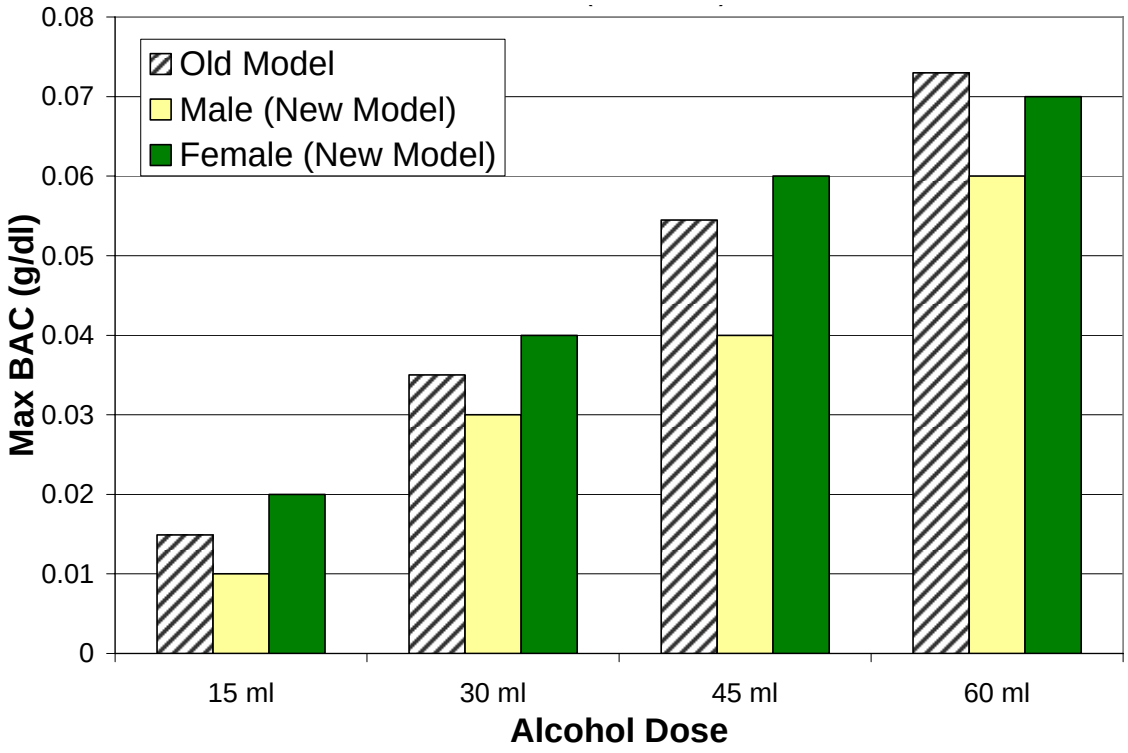

Figure 3-9. Comparison of Maximum BAC for 50th Percentile Humans

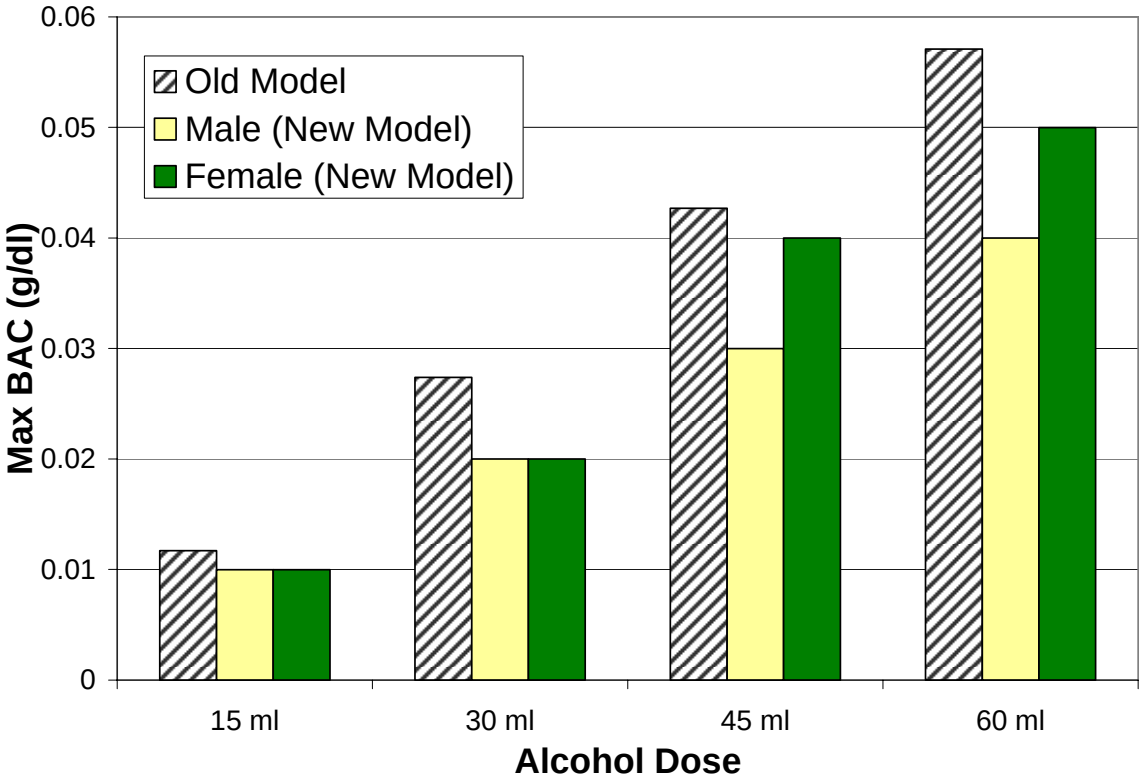

Figure 3-10. Comparison of Maximum BAC for 95th Percentile Humans

Figure 3-11, Figure 3-12 and Figure 3-13 compare the old and new model results for transdermal lag time for 5th, 50th and 95th percentile males and females.

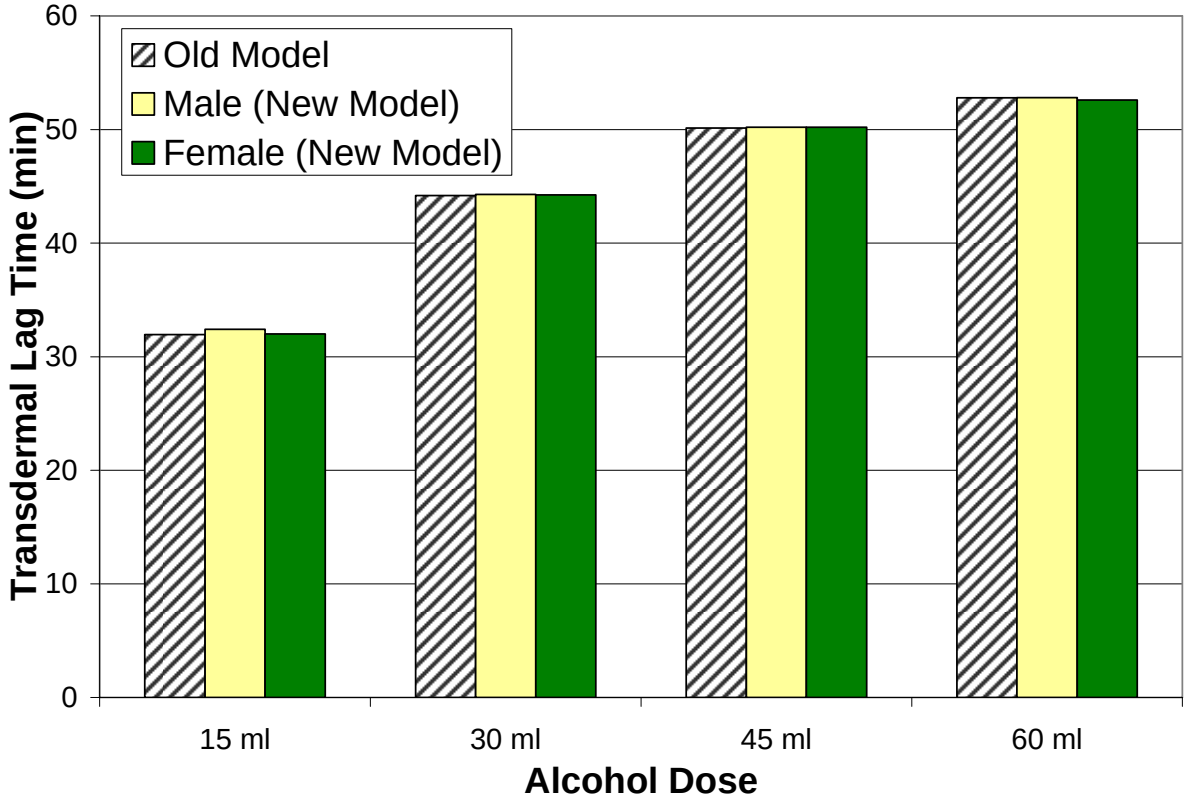

Figure 3-11. Comparison of BAC-TAC Peak lag for 5th Percentile Humans

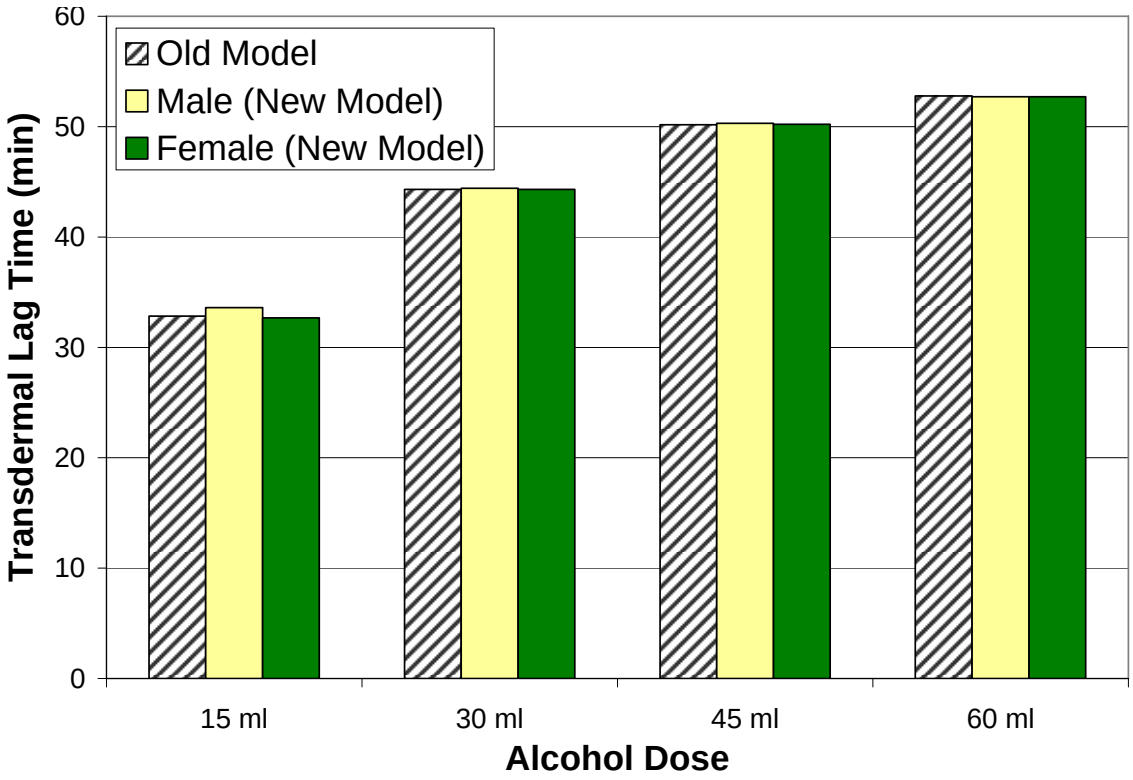

Figure 3-12. Comparison of BAC-TAC Peak lag for 50th Percentile Humans

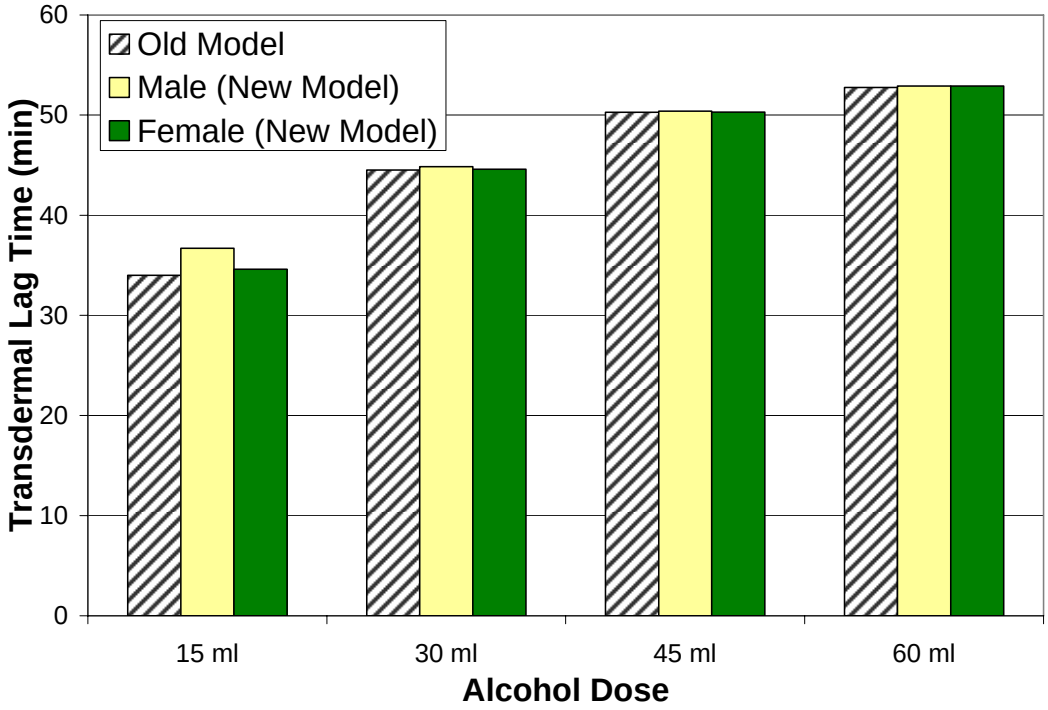

Figure 3-13. Comparison of BAC-TAC Peak lag for 95th Percentile Humans

Figure 3-8, Figure 3-9, and Figure 3-10 show that the original model under predicted maximum BAC for 5th percentile males and females, over predicted 50th percentile males and under predicted 50th percentile females and over predicted 95th percentile males and females. The trends apparent in the new model match those of the old model: as dose increases maximum BAC and transdermal lag increase. Additionally, the amount of time lag for each weight and dose case is insensitive to the model used.

3.3. Discussion

3.3.1. Effect of Gender on Transdermal Lag

The variations in male and female LBM were incorporated into the model effectively reducing the amount of alcohol soluble body mass available to dilute ingested alcohol in females when compared to a male of the same body weight. In addition, males were modeled to have larger livers than females of the same body weight; effectively increasing the concentration of alcohol in the liver for females when compared to males of the same weight. Examination of Figure 3-8, Figure 3-9 and Figure 3-10show that females will have higher maximum BACs after consumption of the same dose as males in the same weight percentile. Inspection of Figure 3-11, Figure 3-12 and Figure 3-13 show that transdermal concentration lag is insensitive to gender. For a given dose and body mass both genders had approximately the same lag time. Only at low doses of alcohol does variance in lag time within a gender/weight group become apparent.

3.3.2. Effect of Body Weight and Liver Scaling on Transdermal Lag

Figure 3-8, Figure 3-9 and Figure 3-10 show that as body weight increases the maximum observed BAC decreases for a given dose of alcohol. An increase in body weight increases LBM with respect to gender allowing alcohol to be diluted to a greater extent in a larger person than in a small person. This results in a decrease in max BAC. Figure 3-11, Figure 3-12 and Figure 3-13 show that for a given dose of alcohol, transdermal lag is body weight insensitive. The blood-skin peak lag time for all body weights for a given dose of alcohol were approximately the same.

3.3.3. Effect of Body Weight, Lean Body Mass and Liver Size on Metabolism Time

Scaling the liver and LBM size has little effect on alcohol metabolic rate. This is best explained in Figure 2-6 which shows mass flow rates of alcohol into the liver. The size of the liver directly affects the concentration; larger livers will have lower alcohol concentrations when compared to smaller livers for the same dose. Alcohol elimination rate is governed by the concentration of alcohol in the liver but limited by V_{max}. The 'Metabolism Rate' curve in Figure 2-6 quickly reaches a plateau equal to the value of V_{max} and remains at this level for most of the simulation. For all simulations the alcohol metabolism rate quickly reaches V_{max}. Changes in the liver size only affect the alcohol metabolism rate at the end of the simulations when the concentration in the liver drops low enough to not overwhelm the K_m term of Equation 3-1. Men and women of all weights reach their maximum and minimum peak BACs at nearly the same time for a given dose of alcohol explaining why body weight and gender have no effect metabolism time or blood-skin lag.

3.3.4. Limitations

The model was validated using data from a 50th percentile male given a single does of alcohol; therefore the results may not be applicable for other body weights or genders. All subjects were taken to have the same maximum metabolic rate, stomach empting constant and skin diffusion coefficient which may not accurately represent the actual population. In addition, the model does not reduce amount of alcohol in the body by the amount predicted to leave the skin. The model also does not account for alcohol lost through the breath, estimated to be 0.7% of the total dose, or alcohol excreted in the urine, estimated to be 0.3% of the total dose (Ramchandani et al., 2001). Since such small fractions of alcohol are lost through the breath and urine, they were not included as elimination paths in the model; however their absence may explain why the experimental data shows a faster elimination rate when compared to the model after the curve peaks.

3.4. Conclusions

This study examined how gender and body weight affect blood-skin concentration lag in humans after oral ingestion of alcohol using an improved validated computation model. It was found that body mass and gender do not significantly affect the time lag between peak blood and skin alcohol concentrations. This is because body mass and gender do not significantly affect metabolic time resulting in similar BAC peak times. When applied to the skin diffusion model, virtually no change in peak lag was noted.

Chapter 4. Development of a Transdermal Ethanol Sensor

Little experimental data is available in the literature concerning the relationship between BAC and skin alcohol concentration. The data that is available does not describe how the transdermal lag varies between individuals, with alcohol dose or fed/fasting condition. In addition this lack of experimental data makes the validation of our computational model challenging. The goal of this study was threefold: (1) design, build and test an inexpensive transdermal alcohol vapor sensing package, (2) to collect BAC and TAC data to determine if inexpensive sensors are suitable to measure the concentration of alcohol emitted from the skin, and (3) to collect coupled BAC-TAC data from human volunteers to validate the computational model. This chapter will describe the development of a transdermal alcohol vapor sensor package; human subject testing will be discussed in the following chapter.

4.1. Development of a Prototype Transdermal Alcohol Sensor

Off-the-shelf transdermal alcohol sensors are not readily available for research purposes. Professional quality breath alcohol detectors use fuel cell sensors to measure the concentration of alcohol in the breath sample, however inexpensive consumer level breath alcohol detectors use a semiconductor based sensor to measure breath alcohol concentration. This type of sensor is considerably less expensive than its fuel cell alternative. In 2008, the cost of a semiconductor solvent vapor sensor was approximately $15 while a fuel cell alcohol sensor costs $110 (Figaro USA, Guth Labs). Semiconductor based sensors were also used in previous transdermal ethanol sensing experiments with positive results (Giles et al., 1987). Semiconductor sensors have the

advantage of being inexpensive, small and easily implemented; making them an appealing choice for widespread use in an inexpensive intoxicated driver detection system.

Figure 4-1. TGS 2620 Solvent Vapor Sensor

Semiconductor based volatile gas sensors typically use tin dioxide as the sensing material. An integrated heater heats the SnO_2 crystal to a manufacturer determined temperature where it becomes reactive with volatile gases, including ethanol alcohol present in the atmosphere. The concentration of gas present changes the electrical conductance of the SnO_2 crystal. These changes can be detected when the sensor is integrated into a measuring circuit (Figaro, 2003).

The change in conductance of the sensor in the presence of alcohol can be used to measure the concentration of alcohol by implementing a voltage divider circuit as shown in Figure 4-2. The electrical properties of the detector require that the sensor be heated via an internal heater.

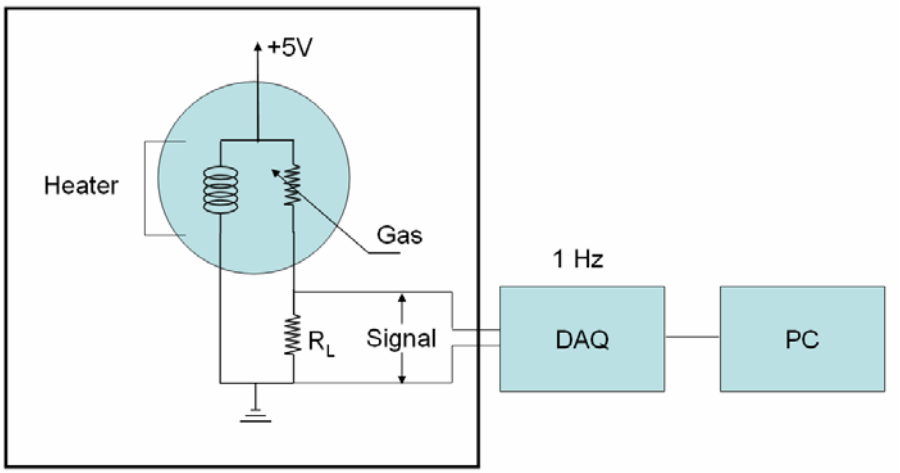

Figure 4-2. Transdermal Ethanol Sensor Block Diagram

Four different semiconductor based sensors candidates were evaluated before one was selected for use in the transdermal alcohol sensor package. The candidate sensors and their respective manufactures are given in Table 4-1.

Table 4-1. Candidate Semiconductor Based Alcohol Sensors

Manufacturer	Model	Diameter (mm)
HanWei	MR513	12
HanWei	MQ-3	20
Figaro	TGS 822	17
Figaro	TGS 2620	9.2

The sensors were installed on a custom printed circuit board and wired so that their voltage signals could be measured with an embedded PIC16F648A microcontroller.

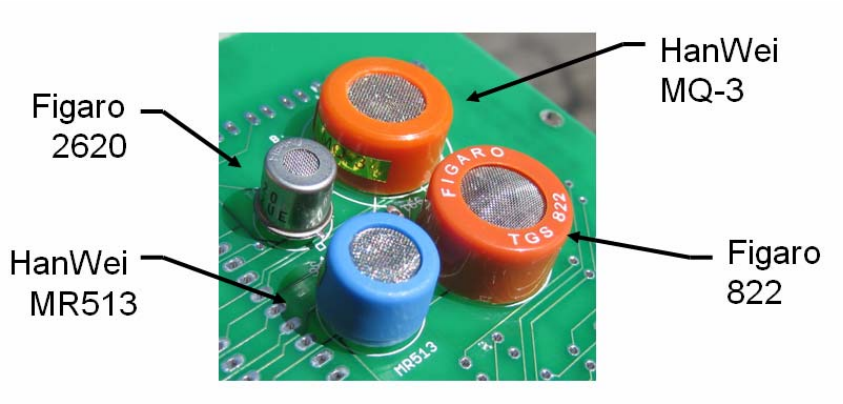

Figure 4-3. Semiconductor Based Alcohol Sensor Evaluation Board Assembly

The sensors were then exposed to alcohol vapor and their voltage responses were recorded. Isopropyl alcohol and vodka at room temperature were used to generate an alcohol vapor. Figure 4-4 presents a diagram of the test setup.

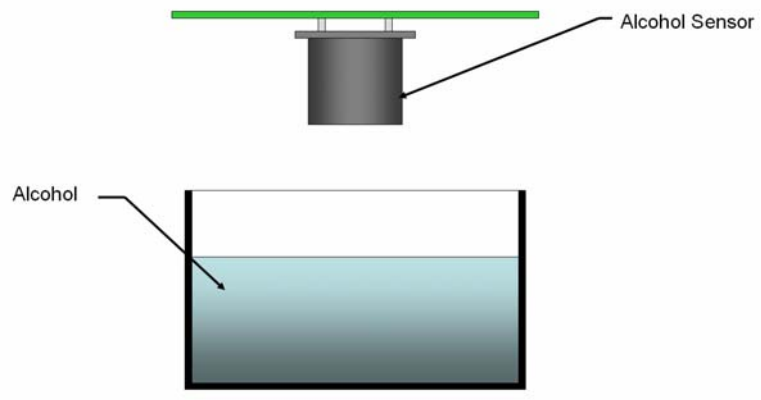

Figure 4-4. Sensor Evaluation Setup

The sensors were evaluated on their response time, size, easy of integration and cost. Figure 4-5 presents the voltage signal response of the Figaro TG 822 and Figaro TGS 2620 solvent vapor sensors.

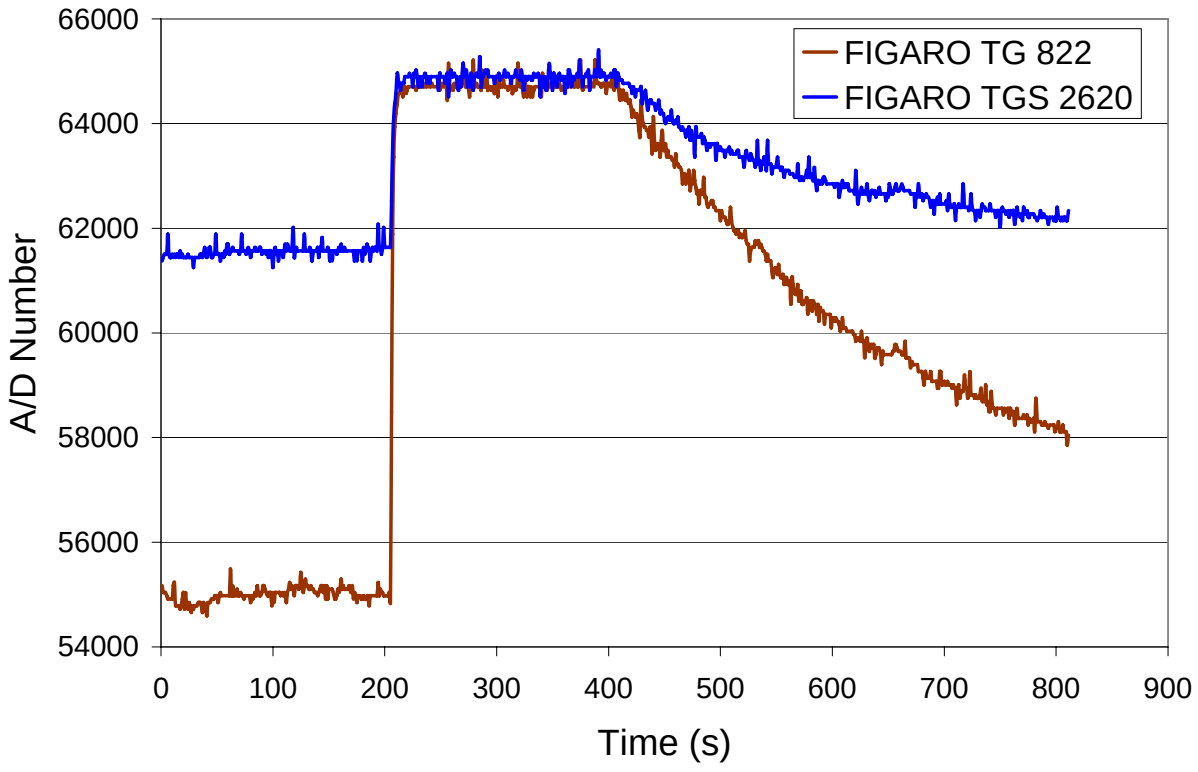

Figure 4-5. Candidate Sensor Response to Alcohol Vapor

Despite closely following the manufacturer's wiring diagram when designing the printed circuit board the HanWei MR513 and the HanWei MQ-3 vapor sensors were never able to produce a readable signal, so they were not considered for use in the prototype. Figure 4-5 shows a sharp increase in the voltage for both the TG 822 and TGS 2620 sensors. Both sensors respond to the stimulus in less than a second.

The TGS 2620 solvent vapor sensor was selected for use in the transdermal ethanol sensors developed here (Figaro USA, Inc Arlington Heights, IL). This sensor had the smallest footprint

and had fewer leads to connect when compared to the TG 822, which is the predecessor to the TGS 2620.

A custom printed circuit board was developed to power the sensors. A complete electrical schematic and printer circuit board trace diagram are included in Appendix B. Each circuit board had the capacity to carry two separate TGS 2620 sensors so that redundant channels could be sampled at the same place on the body. The signal from each sensor was connected to a National Instruments NI 9205 32 channel A/D data acquisition module and sampled at 1 Hz. By sampling the alcohol concentration with two sensors in the same location insight into the repeatability and accuracy of the sensors could be determined. An example electrical assembly is shown in Figure 4-6.

Figure 4-6. Ethanol Vapor Sensors on PCB

A custom housing was designed and fabricated from ABS plastic using a fusion deposition modeler (FDM) to contain the ethanol vapor sensors and allow for easy attachment to the body.

Figure 4-7 is an exploded view showing the top and bottom of the custom housing as well as the custom printed circuit board that the alcohol sensors are mounted to.

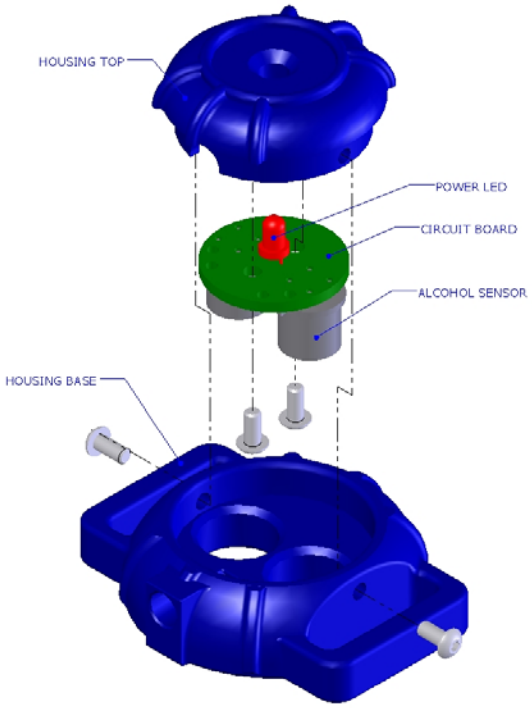

Figure 4-7. Exploded Diagram of Complete Transdermal Alcohol Sensor

Velcro straps were attached to each sensor to allow it securely attach to most body parts. An example is shown in Figure 4-8.

Figure 4-8. Alcohol Sensor Bracelet

Prior to use each sensor package was tested to ensure that it would respond to ethanol vapor. This was accomplished by placing each bracelet in the air space above a small amount of vodka. The sensors were not formally calibrated because only the relative peak was of interest for this study. However, future studies should attempt to calibrate the sensors prior to use so that the spatial distribution of alcohol concentrations can be quantified. Previous research has reported skin alcohol concentration in milliamperes (Swift, 1998).

4.2. Sensor Response Tests

A few bench test were performed with the sensors prior to use on humans. Figure 4-9 shows the sensor voltage response to open air conditions. The data recording started at the same time the sensors were initially powered up resulting in the initial decay of voltage around 0 minutes. Also of note is the dip in signal just after 100 minutes and 175 minutes. This dip was clear in all sensor channels but not in the voltage reference channel. The most likely cause of this anomaly is someone walking into the room where the bench test was being conducted which disturbed the air, changing the concentration of voltage gas near the sensor.

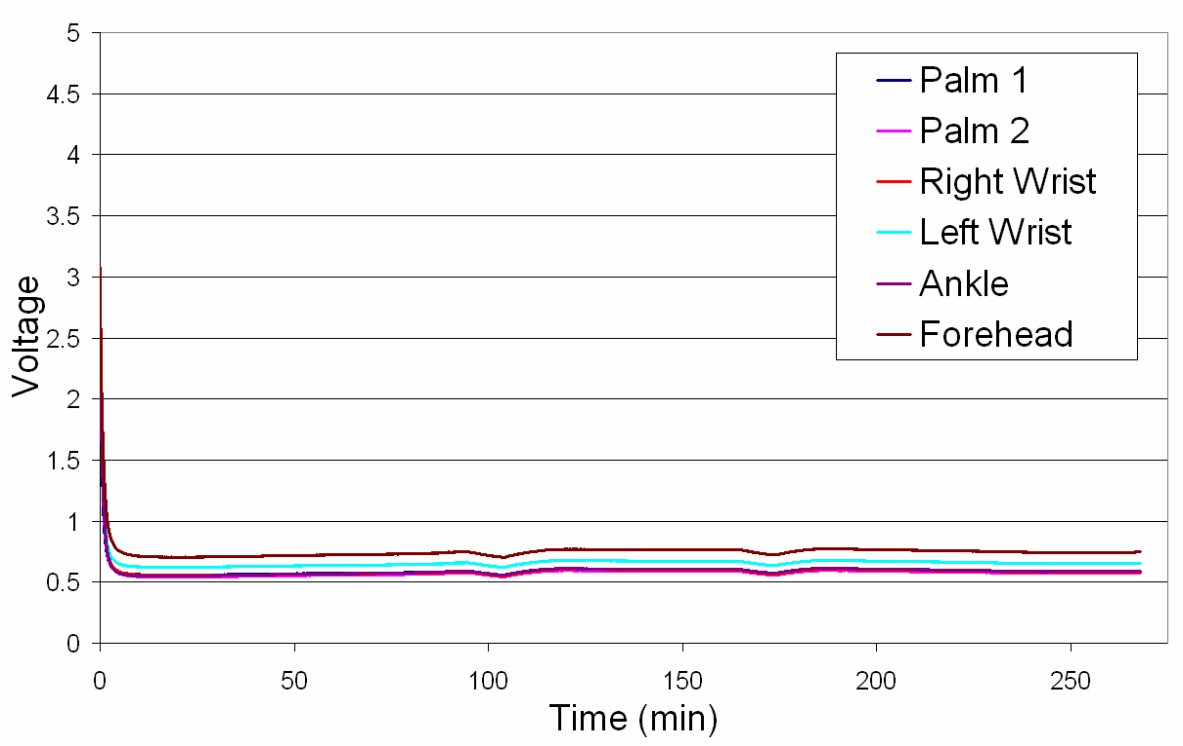

Figure 4-9. Sensor Array Response to Open Air

Figure 4-10 shows the sensor response when exposed to the vapor above a small amount of vodka mixed with water. The sensors were approximately 3 inches above the surface of the solution. The data is considerably nosier than the data presented in Figure 4-9. Not that the sensors were not exposed to the vapor until 5 minutes after data collection began, as shown by the increase in signal value around that time. Dips in the signal are all present in this data around 60 minutes and 125 minutes.

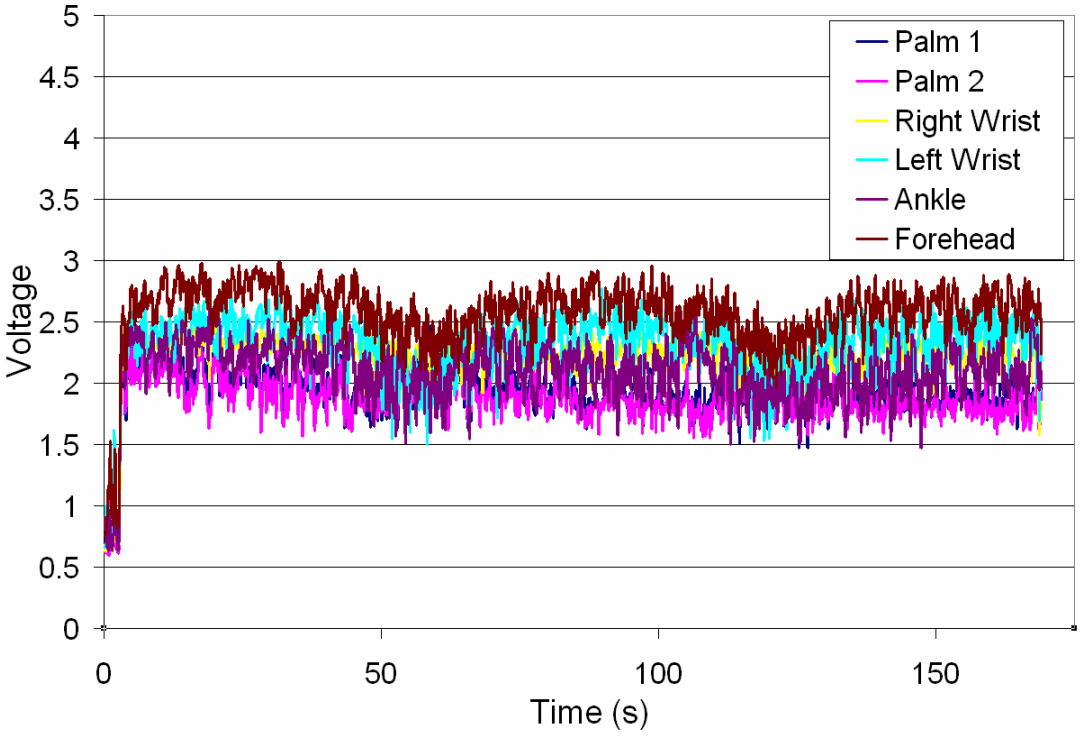

Figure 4-10. Sensor Array Response to Dilute Alcohol Vapor

4.3. Conclusion

A low cost commercially available solvent vapor sensor has been integrated into a wrist watch style sensor package designed to measure the concentration of alcohol at the surface of the skin. The vapor sensor has been show to be sensitive to different types and concentrations of alcohol in the laboratory. The housing, PCB and data acquisition software were all developed at Virginia Tech. Several bench tests were conducted to check the sensor package's performance over a few hours and found that the system can remain sensitive over a 4 hour period.

Chapter 5. Pilot BAC vs. TAC Experiments

The goal of this experiment was to collect BAC and skin alcohol concentration data after oral consumption of an alcohol beverage. This data will be compared to the results of the computational model described previously. A professional grade breath alcohol detector was use as a surrogate for direct blood alcohol concentration measurements. The transdermal alcohol sensors described in the previous chapter were used to collected skin alcohol concentration measurements.

5.1. Experimental Design

To allow comparison with published BAC results, the design of the experiment was based on a study performed by Wilkinson (1977). Three healthy adult human volunteers were given varying doses of alcohol diluted in cold juice after fasting for 10 hours and abstaining from alcohol for 3 days prior to the experiment. The subjects were also asked not to use any alcohol containing toiletries, e.g. aftershave, perfume, hand sanitizer, for 10 hours prior to the experiment to ensure there would be no inference with the transdermal ethanol sensor. The subjects were given progressively more concentrated doses of alcohol starting with one standard drink at the first session and ending the test series with three standard drinks. Table 5-1 presents the equivalent doses given to each subject. Randomization of dose order was not necessary as this was a purely physiologic response study.

Table 5-1. Dose Equivalents

Dose (Standard Drinks)	Volume of 80 Proof Vodka (mL)	Dose (moles of EtOH)	Total Drink Volume (mL)
1	44.4	0.3	473
2	88.8	0.6	473
3	133.2	0.9	473

5.2. Protection of Human Subjects

IRB approval was acquired prior to performing human testing (Virginia Tech IRB# 08-100). The IRB certificates are presenting in Appendix A. Fliers were posted on campus and an ad was placed in the Collegiate Times, Virginia Tech's student newspaper, advertising the study. Potential subjects contacted the investigators via email or telephone to set up a phone screening session. After a brief description of the purpose, experimental protocol, and the time commitment of the study, potential subjects were asked for verbal consent. It was emphasized that they could change their mind and opt out of the experiment at any time without penalty. If verbal consent was given the potential subjects were screened for inclusion criteria. If they meet the inclusion requirements arrangements were made to have the written consent form delivered to them. At this time the subject were scheduled for their first experiment session, allowing at least 24 hours between when the informed consent form was delivered to the subject and the experiment. Subjects were paid after each session for their participation in the study.

Utmost care was taken to protect the personal information of each subject. Data codes were use so that the data collected from the subject was not directly linked to their name or contact information.

5.2.1. **Inclusion Criteria**

All subjects were 21 years or older in age as confirmed by two forms of photo identification. Subjects were preferably between +/- 20% of the 50th percentile weight for their gender (McDowell, 2005). Moderate drinkers were sought for this study, consuming between 2 - 14 standard drinks a week for males and between 1 and 7 standard drinks a week for females on average. This was to ensure that the subjects who participated in this study consume alcohol on a regular basis and were familiar with the physiologic effects it can cause. Additionally, the subjects could not be alcoholics or currently pregnant. Females of reproductive age were required to take a home pregnancy test prior to acceptance to the study. Subjects who were currently taking any prescription medications not were included in the study. This excludes birth control medication as the literature shows this does not affect ethanol metabolism.

5.3. Experimental Protocol

Each session was conducted privately. The subjects' weight, percent body fat and percent body water were measured at the start of the first session using an electronic body fat scale (Taylor, Las Cruces, NM). At the beginning of each session the subject was seated in a comfortable chair. Transdermal ethanol sensors were placed on up to seven locations on the subject's body. These locations included the forehead, neck, left wrist, right wrist, palm, left ankle and right ankle. Figure 5-1 shows the location of the transdermal ethanol sensors during a typical experiment. Note that the person in Figure 5-1 is only modeling the sensors, and was not a subject in the study.

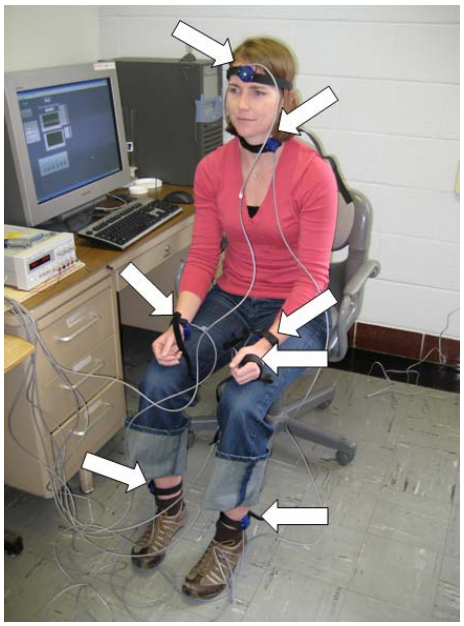

Figure 5-1. Transdermal Ethanol Sensor Locations

A baseline breath alcohol measurement was taken at the beginning of the session and five minutes of baseline skin alcohol concentration measurements were made before the subject was dosed with alcohol. The subjects were asked to drink the solution of ethanol and juice as quickly as they comfortably could. After the subject finished the drink they were asked to wash their mouth out with water to clear the alcohol absorbed by the tissues in their mouth. If this step was skipped, unrealistically high BAC readings were obtained from the breath alcohol detector, as the alcohol present in the mouth affected the results. BAC measurements, via the breath alcohol detector, were made every five minutes. The transdermal alcohol sensors were sampled at 1 Hz during the entire experiment. After two hours had elapsed the subjects were permitted to eat food. The two hour wait period was necessary to ensure that nothing slowed the emptying of the stomach. The session was concluded after four consecutive BAC readings of 0.000, or after the subject had two consecutive readings below 0.02.

5.4. Subject Pool

Table 5-2 summarizes the subject pool.

Table 5-2. Subject Pool

Subject	Age	Weight (lbf)	Body Fat (%)	Body Water (%)	Gender
1	23	187.2	13.3	57.8	Male
4	22	168.4	15.0	57.0	Male
6	27	162.8	14.9	58.2	Male

Subjects 1 and 6 completed all three sessions, subject 4 was only able to complete one session.

Due to the palatability of the alcohol/juice solution it was not possible for all subjects to completely finish the drink within the first five minutes of the session for all doses given. Table 5-3 presents approximate the time it took each subject to completely finish the dose of alcohol given for each session.

Table 5-3. Time to Finish Drink

Subject	Dose (Standard Drinks)	Time to get BAC > 0 (min)
1	1	5
	2	5
	3	10
4	1	5
6	1	10
	2	18
	3	25

Generally speaking, as the dose of alcohol given increases so does the time needed to completely finish the beverage. This represents a significant deviation from how the computational model handles the dosing of alcohol. The model assumes that all of the alcohol that is consumed starts in the stomach at time = 0. Gradually consuming the alcoholic beverage over the course of as

much as 25 minutes could have a significant effect on the stomach emptying rate which effects the blood alcohol concentration.

5.5. Experimental Results – BAC

Model simulations were run for each subject individually simulating the dosing of 1, 2 and 3 standard drinks. The model parameters were adjusted to reflect the physical attributes of each subject. Specifically, the subject's weight was used as the total weight in the simulation and the percent body water was used as the Widmark factor. The experimental BAC is compared to the model predicted BAC for each case presented in Figure 5-2, Figure 5-3, Figure 5-4 for subjects 001, 004, and 006 respectively.

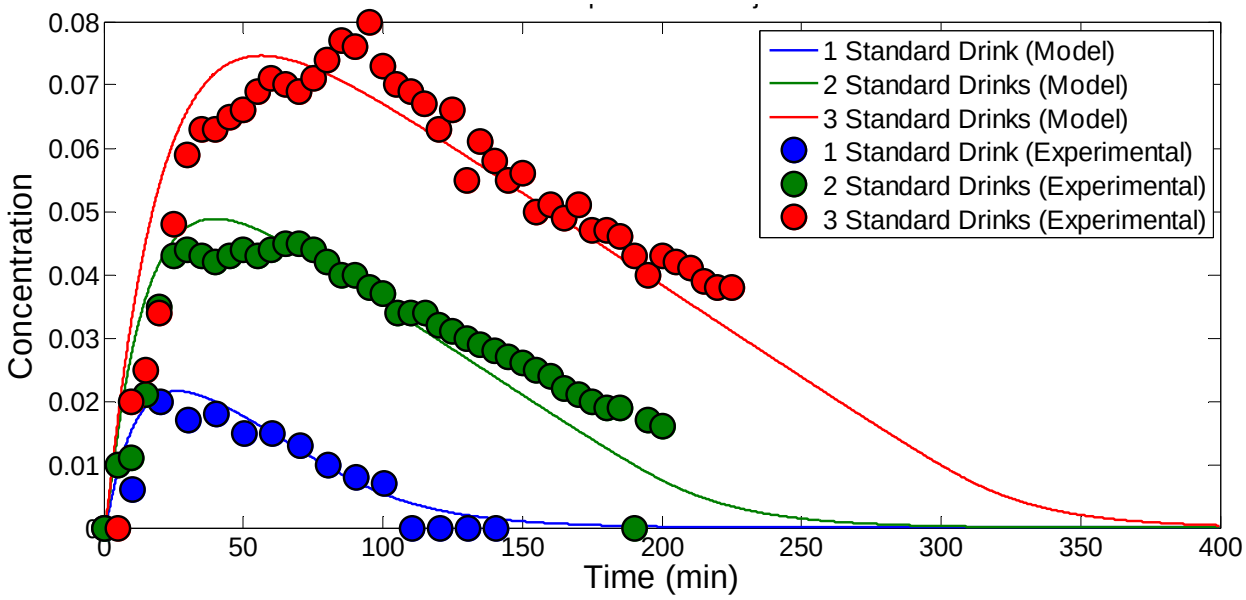

Figure 5-2. BAC Response for Subject 001

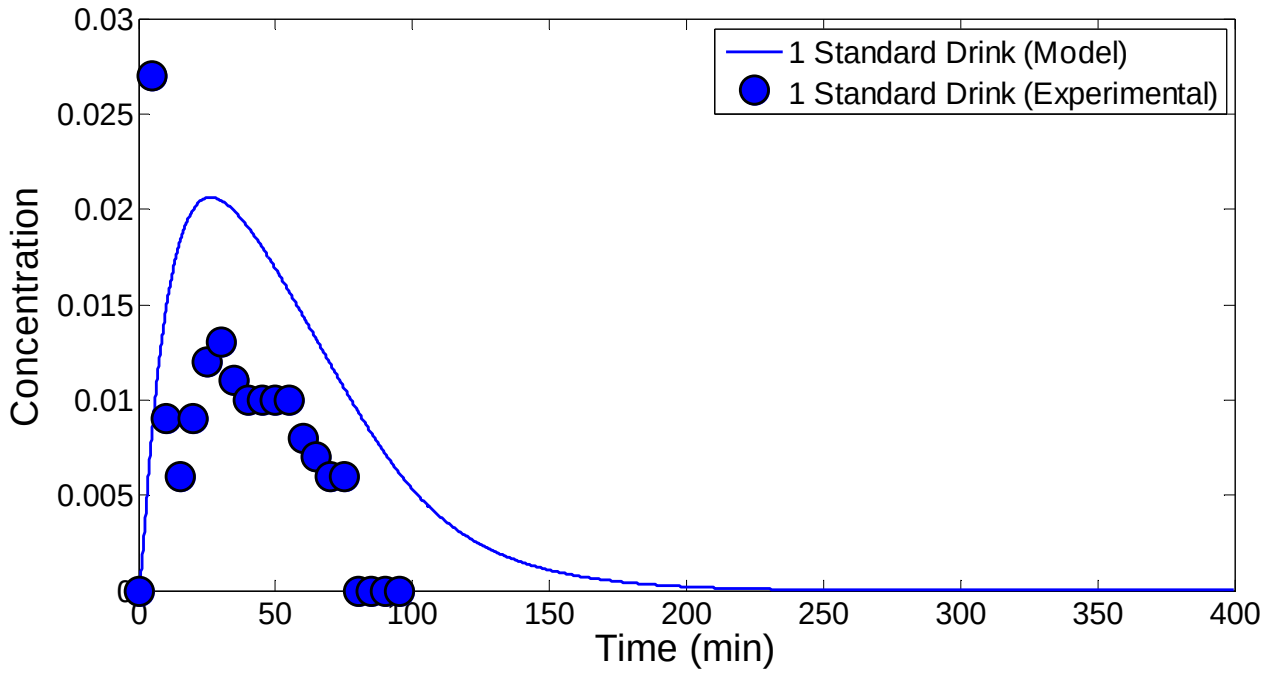

Figure 5-3. BAC Response for Subject 004

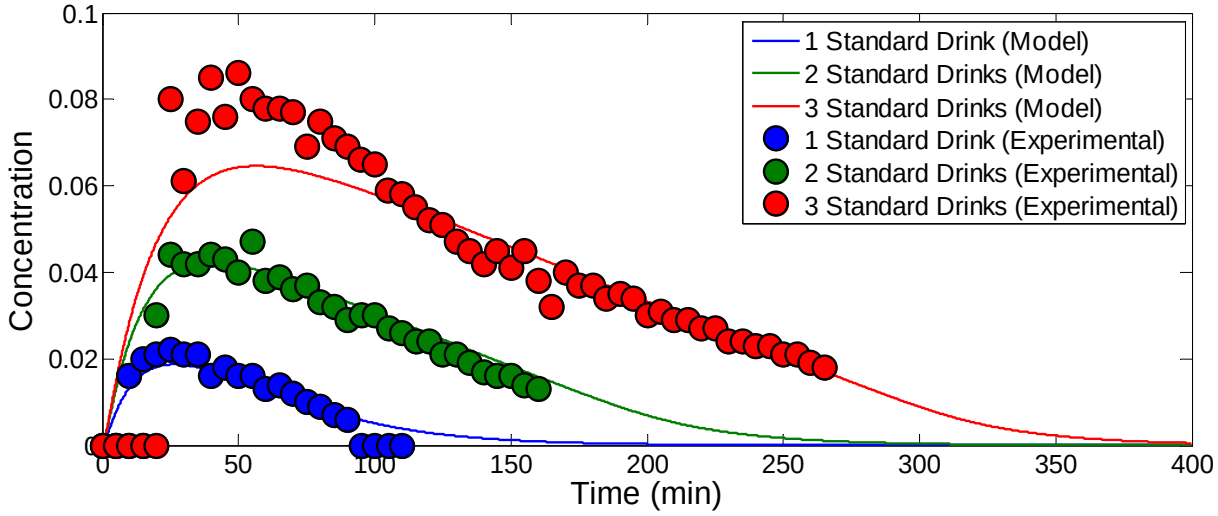

Figure 5-4. BAC Response for Subject 006

The model and experimental data for all doses given to subjects 001 and 006 agreed very well with each other. Specifically, the doses of 1 and 2 standard drinks agreed better than the dose of 3 standard drinks. The experimental data collected for subject 004 did not agree very well with the model predicted BAC response curve. It is possible that the subject can metabolize ethanol

at a higher than normal rate or that the subject was not entirely truthful about fasting for 10 hours prior to the experiment. Both cases would result in a lower than predicted BAC. Additionally, some of the data scatter observed at the 3 drink dose could be due to the extended period of time required to consume the drink. This affects the stomach emptying rate which in turn affects the ethanol metabolism rate.

5.6. Experimental Results - TAC

Analysis of the skin alcohol concentration data was not as straightforward. The data collected from the TAC sensors was recorded as a voltage. The voltage data was processed so that the average of the first 5 minutes of data is used as a baseline, and the remainder of the data set was normalized to this average. That data is then filtered using a 2-pole Butterworth filter with a 0.008 Hz cut off frequency and scaled so that the maximum skin alcohol concentration value is equal to the maximum BAC value for each session; this allows easier comparison of the two curves. Figure 5-5 presents BAC and scaled TAC data taken from subject 006. The TAC data was taken from the subject's left palm.

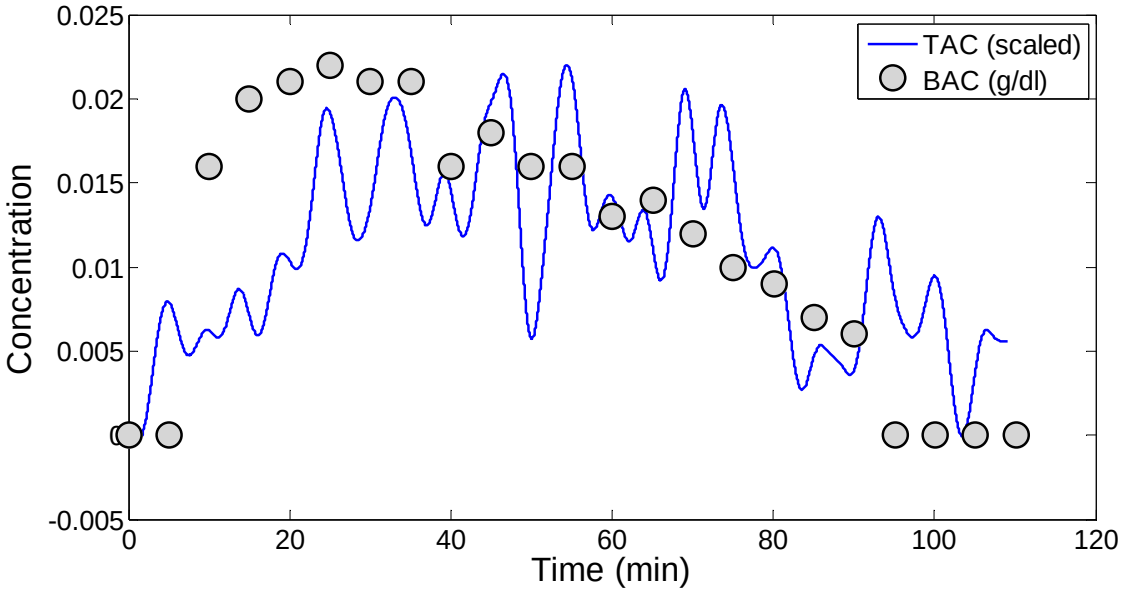

Figure 5-5. BAC and TAC values of the Palm, Subject 006, Palm 1

A considerable amount of noise is present in the TAC data, even after filtering. However, an overall parabolic trend is apparent in the data. Qualitative observance of the data shows a gradual increase in values that peak around 50 minutes and then gradually descend. All of the TAC data collected is included in Appendix C.

Due to the high signal to noise ratio present in the data, it is difficult to determine if trends apparent in the data are actual alcohol concentration measurements or if they are anomalies that fit the expected trends suggested by the model. Indirect proof that the sensors are detecting and responding to the concentration of alcohol at the surface of the skin comes from an experimental session when the subject removed the sensors during the experiment. Figure 5-6 presents the recorded TAC curve from subject 006 after the consumption of 2 standard drinks; the forehead 2 channel is shown. Approximately 2 hours into the session the subject needed to use the bathroom which required the removal of all of the sensors for a brief period of time. A sharp dip in the signal can be seen between the 115 and 125 minute time marks, indicated on the plot,

reflecting the sensor response to removal from the skin. After the sensor was reattached to the subject the signal rebounds to a value close to the value measured prior to the removal. The TAC values continue to decay along the linear trend apparent prior to removal. The dip and rebound of the signal around the 120 minute time mark is apparent to some extent in all of the channels sampled during that session.

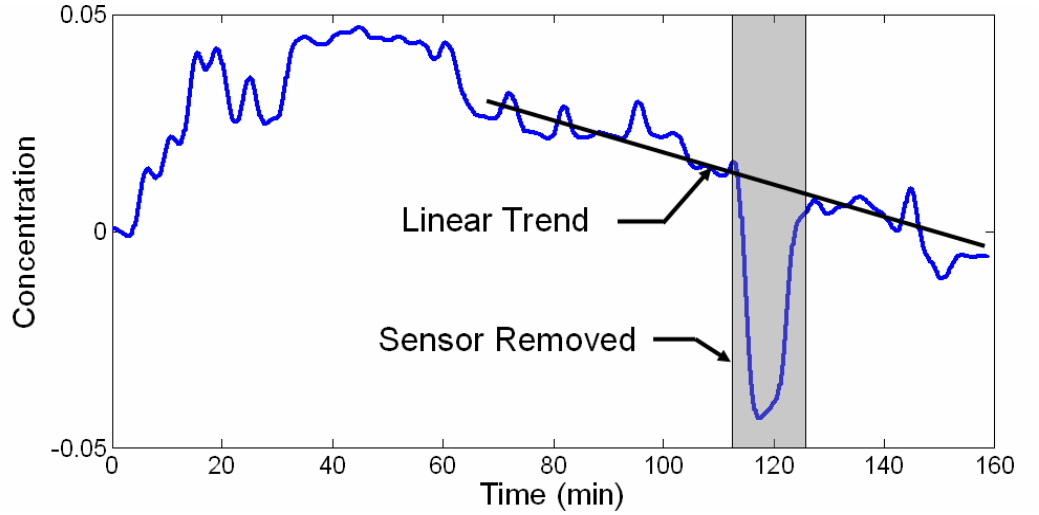

Figure 5-6. Subject 006, 2 drinks, Forehead 2 Sensor

The dip and rebound of the signal after removal provides strong evidence that some data reflecting the transdermal emission of alcohol is being collected.

5.7. Comparison of Experimental Data to Model Predictions

The next stage in analysis was to compare the collected TAC data to the curve predicted by the model to see if there is a correlation. Model simulations were run matching the dose, body weight and percent body water of the subjects. Subject 006 was used because the data collected from this subject appeared to be the cleanest. Predicted TAC curves vs. measured TAC values

were plotted with each other for the Palm and Left Wrist locations in Figure 5-7, Figure 5-8, Figure 5-9, Figure 5-10, Figure 5-11 and Figure 5-12.

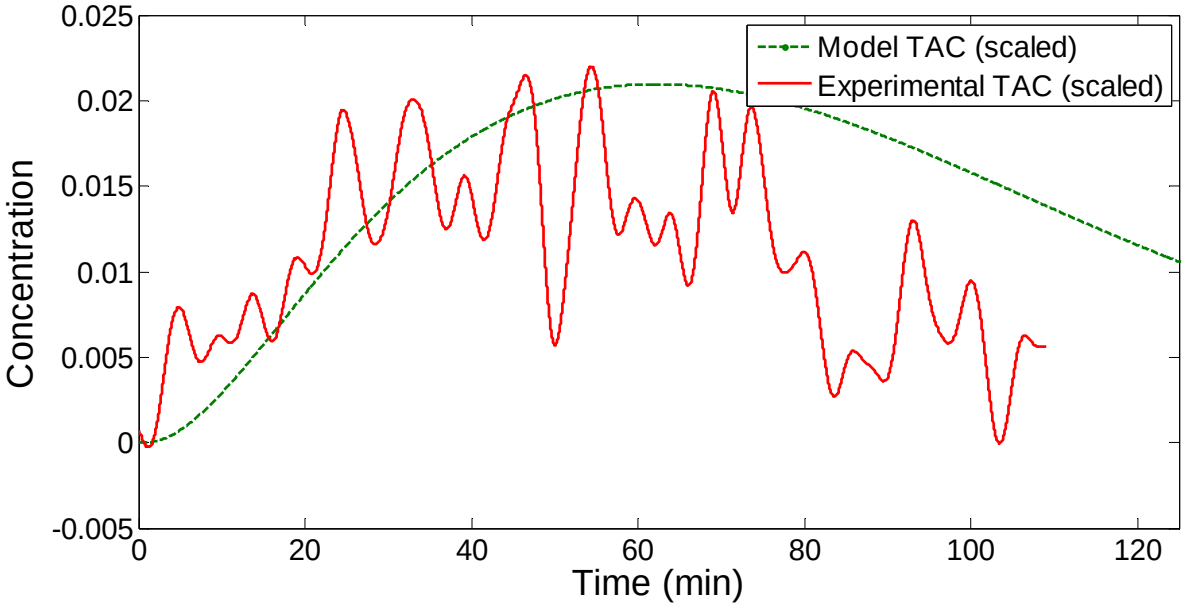

Figure 5-7. Subject 006 Model and Experimental TAC Comparison, 1 Drink, Palm 1

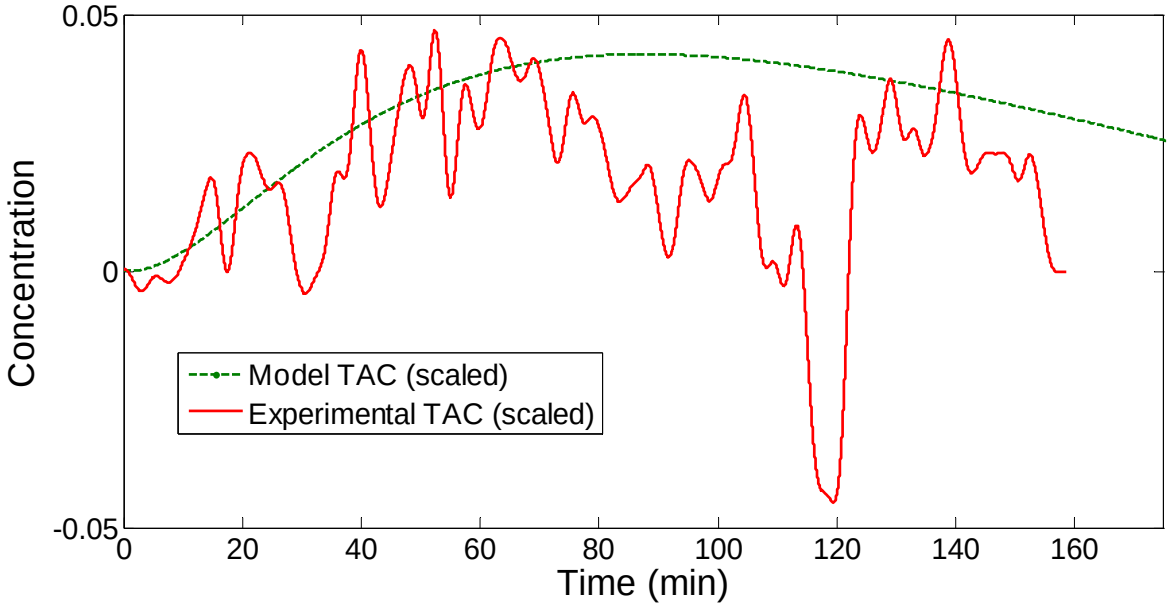

Figure 5-8. Subject 006 Model and Experimental TAC Comparison, 2 Drinks, Palm 1

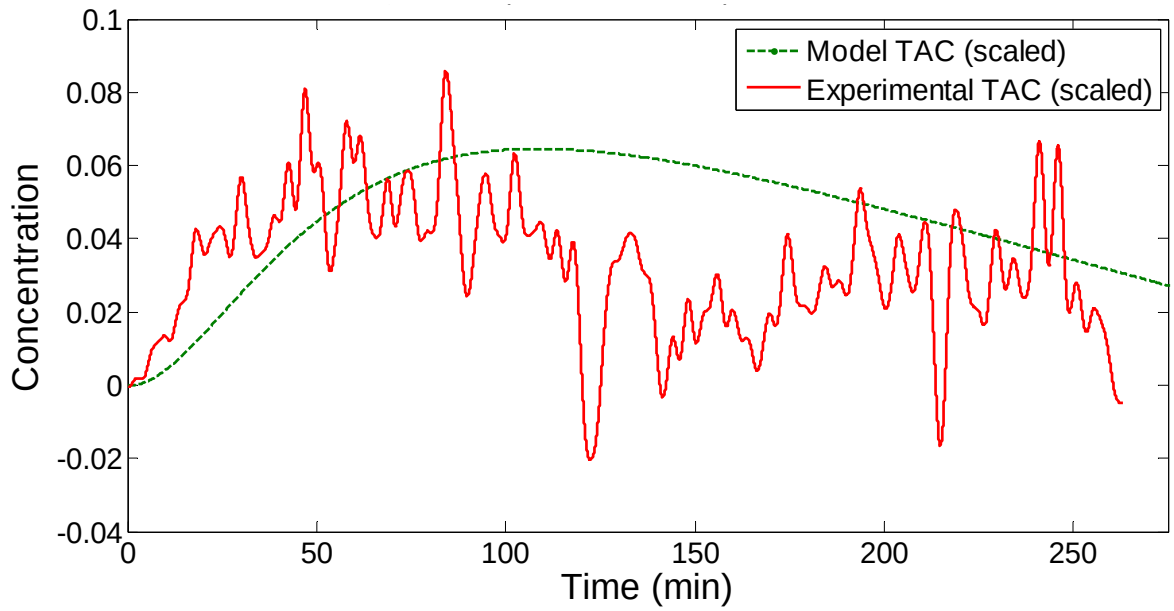

Figure 5-9. Subject 006 Model and Experimental TAC Comparison, 3 Drinks, Palm 1

There appears to be no strong correlation between the model predicted and experimentally measured TAC values for the palm. While the experimental data curves for 1 and 2 standard drinks shown in Figure 5-7 and Figure 5-8 appear to have a slight parabolic shape, the experimental curve for 3 standard drinks given in Figure 5-9 does not.

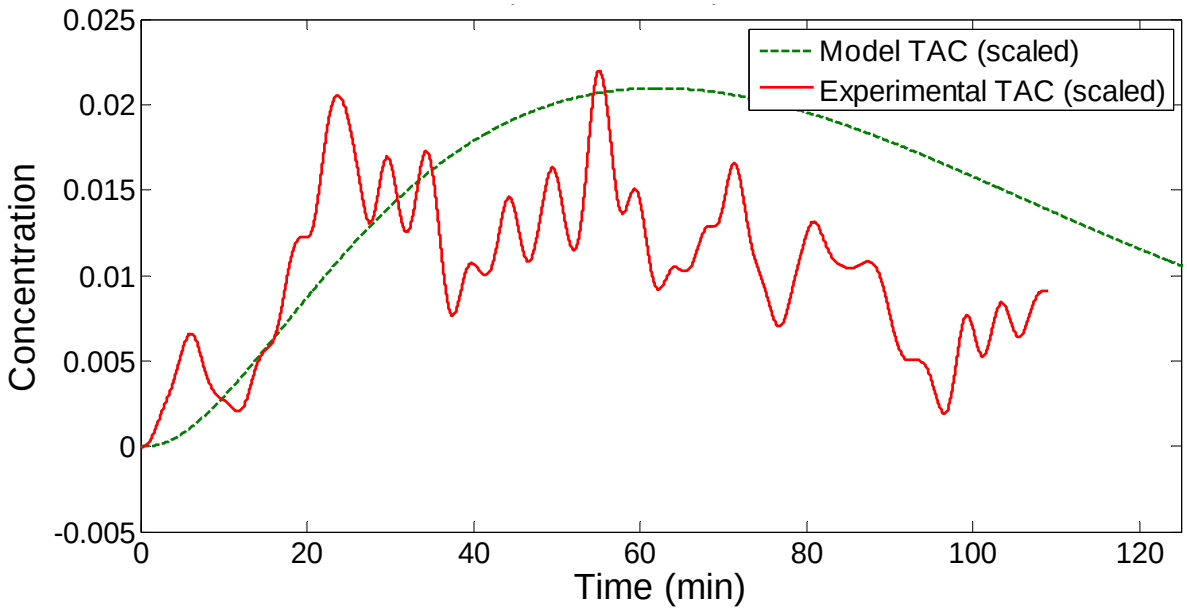

Figure 5-10. Subject 006 Model and Experimental TAC Comparison, 1 Drink, Left Wrist

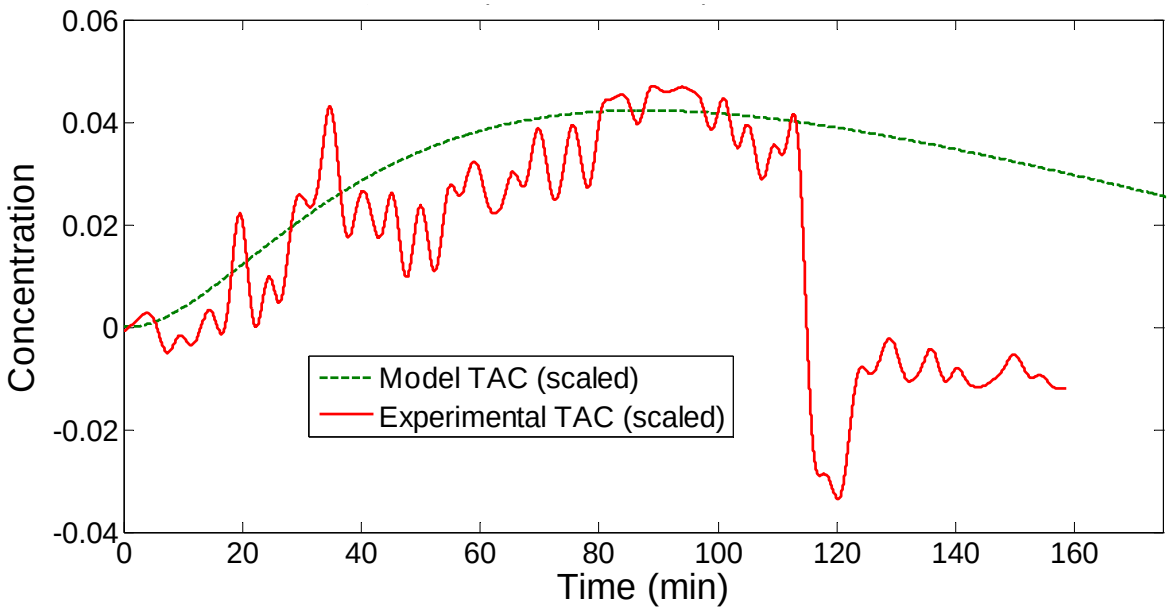

Figure 5-11. Subject 006 Model and Experimental TAC Comparison, 2 Drinks, Left Wrist

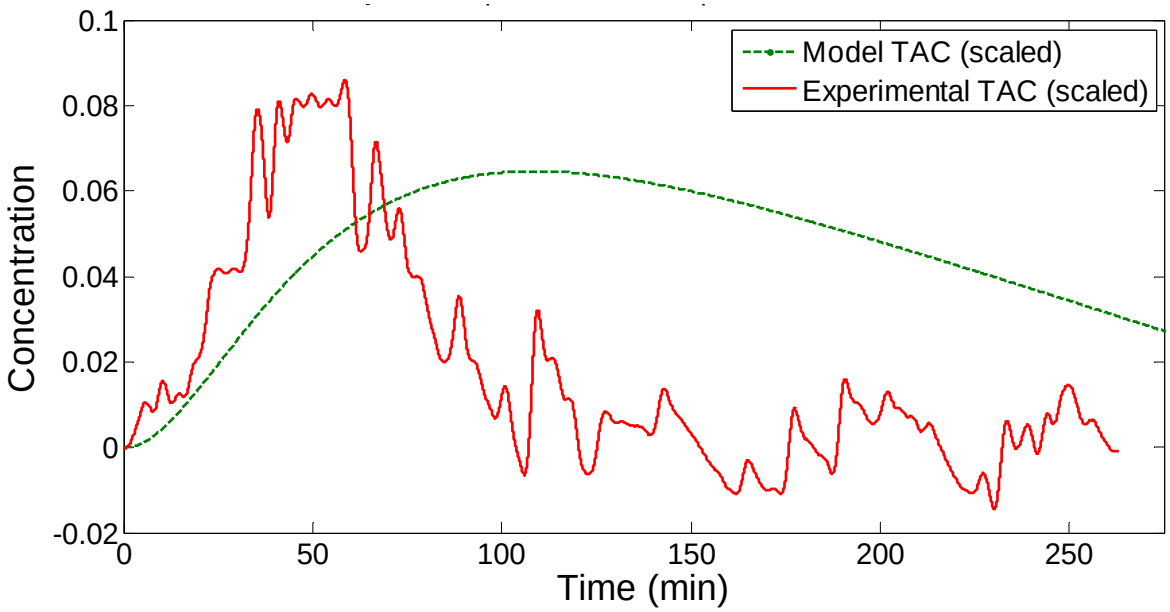

Figure 5-12. Subject 006 Model and Experimental TAC Comparison, 3 Drinks, Left Wrist

The experimental curves for 1, 2 and 3 standard drinks taken at the left wrist all show a parabolic shape, as shown in Figure 5-10, Figure 5-11 and Figure 5-12. In general, the time peaks poorly match the predicted time of peak calculated by the model. However, Figure 5-11 shows

exceptional agreement between the experimental and model predicted TAC up until the time when the sensors were removed for a bathroom break.

5.8. Comparison of Redundant Channels

A comparison of the redundant channels sampled at the same location on the body show very similar trends for all channels sampled. Figure 5-13, Figure 5-14, Figure 5-15, Figure 5-16, Figure 5-17, Figure 5-18, Figure 5-19, Figure 5-20, Figure 5-21, Figure 5-22 and Figure 5-23 show the redundant channels from the palm, forehead and neck for subjects 001 and 006. Redundant channels for the neck and forehead sensors were not added to the experiment until late in Subject 001's sessions, therefore these channels are absent from this analysis.

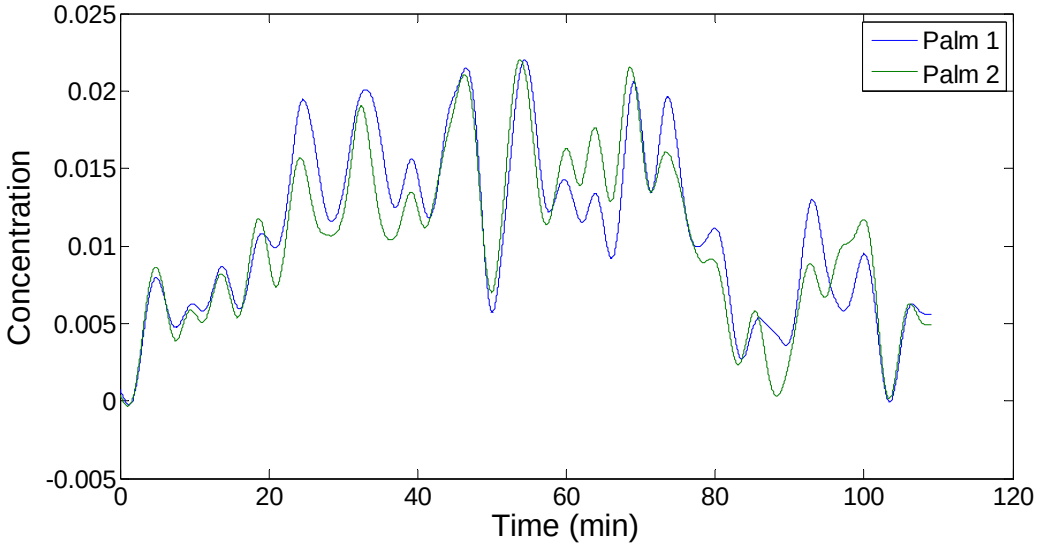

Figure 5-13. Subject 006, 1 Drink, Palm Redundant Sensors

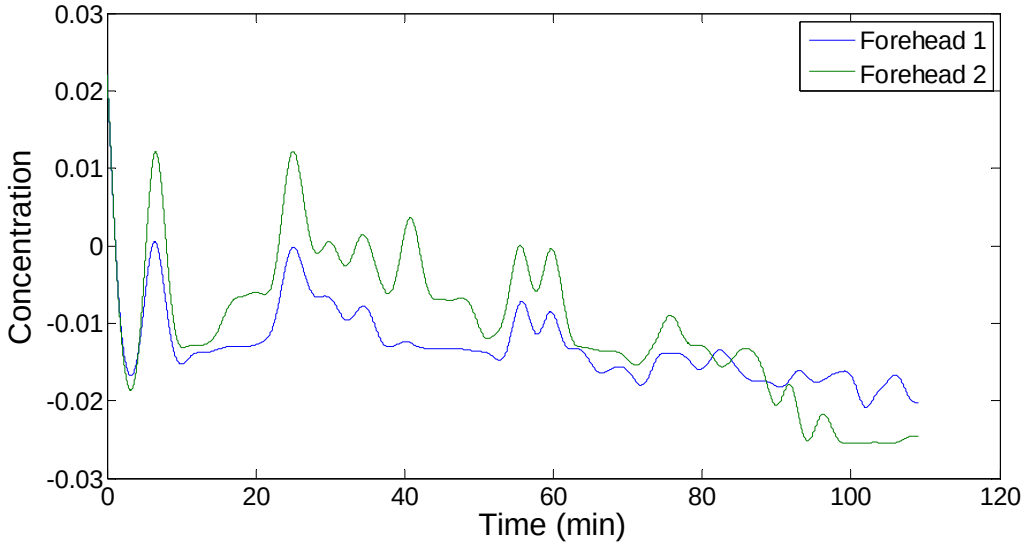

Figure 5-14. Subject 006, 1 Drink, Forehead Redundant Sensors

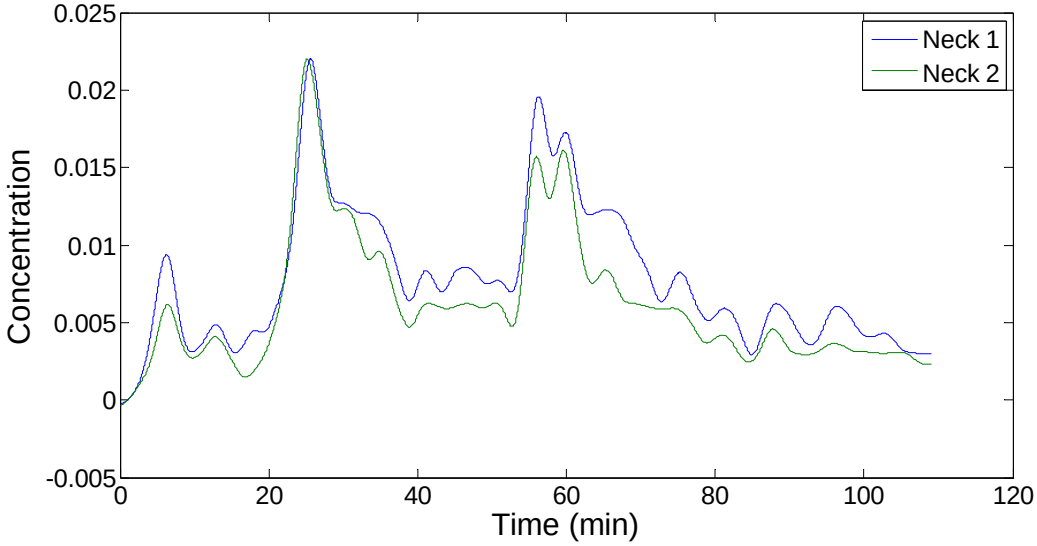

Figure 5-15. Subject 006, 1 Drink, Neck Redundant Sensors

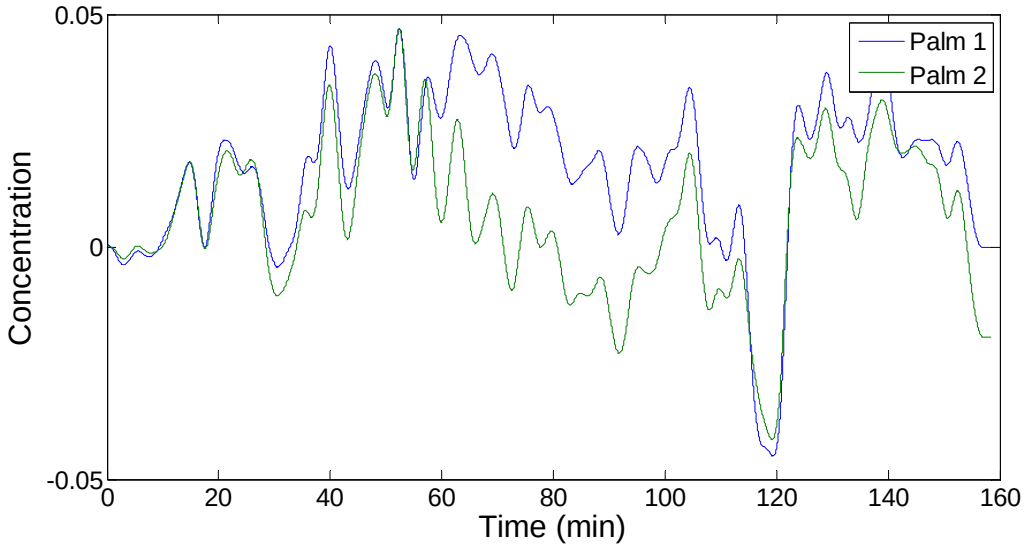

Figure 5-16. Subject 006, 2 Drinks, Palm Redundant Sensors

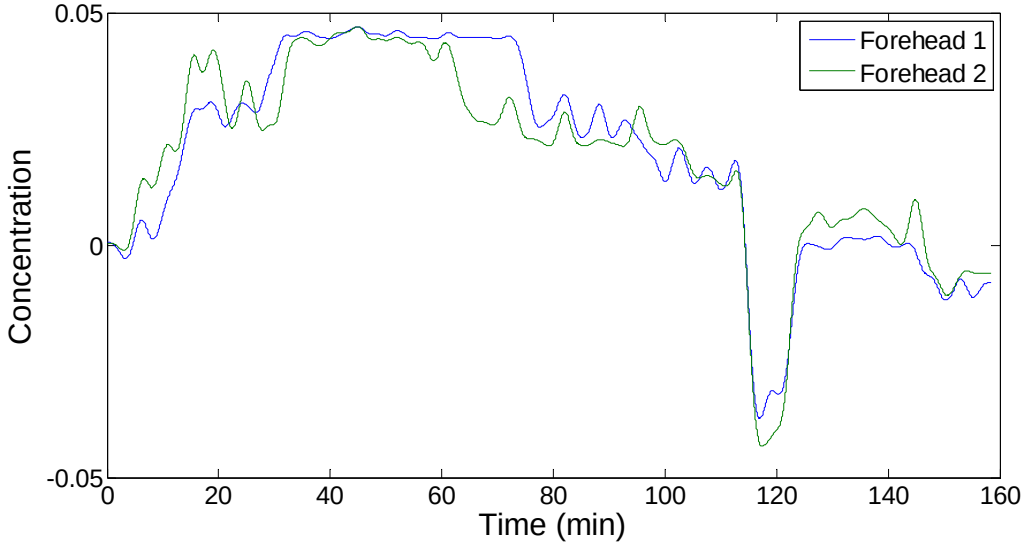

Figure 5-17. Subject 006, 2 Drinks, Forehead Redundant Sensors

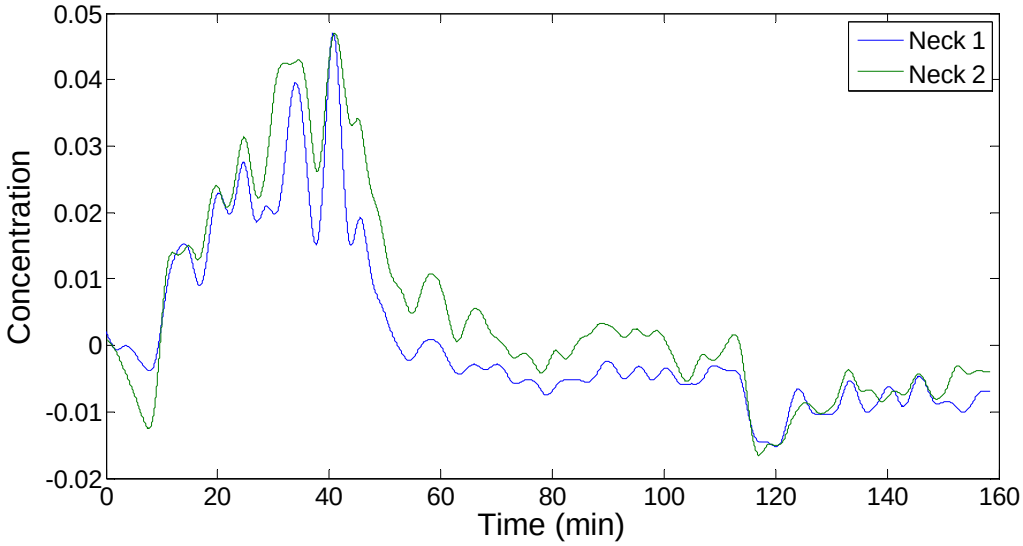

Figure 5-18. Subject 006, 2 Drinks, Neck Redundant Sensors

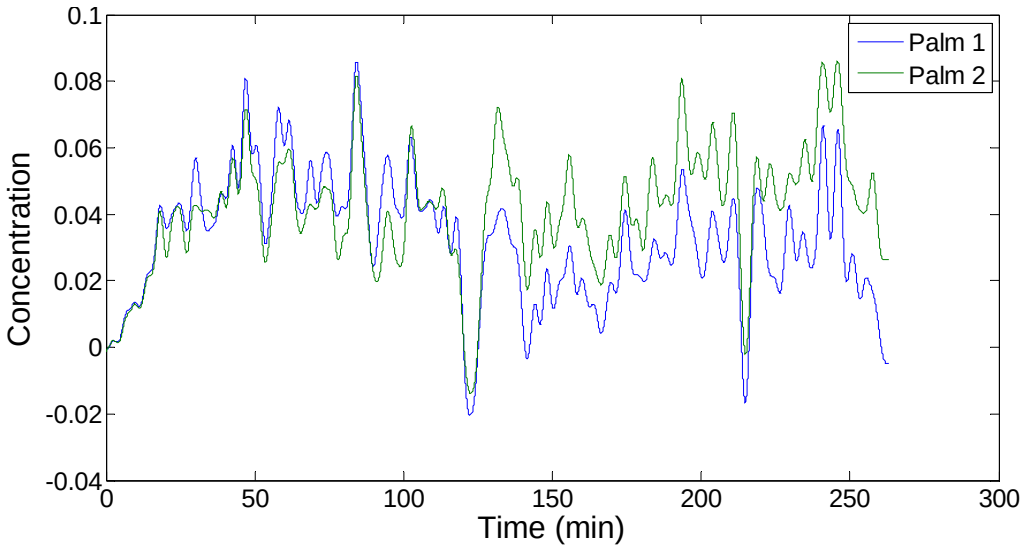

Figure 5-19. Subject 006, 3 Drinks, Palm Redundant Sensors

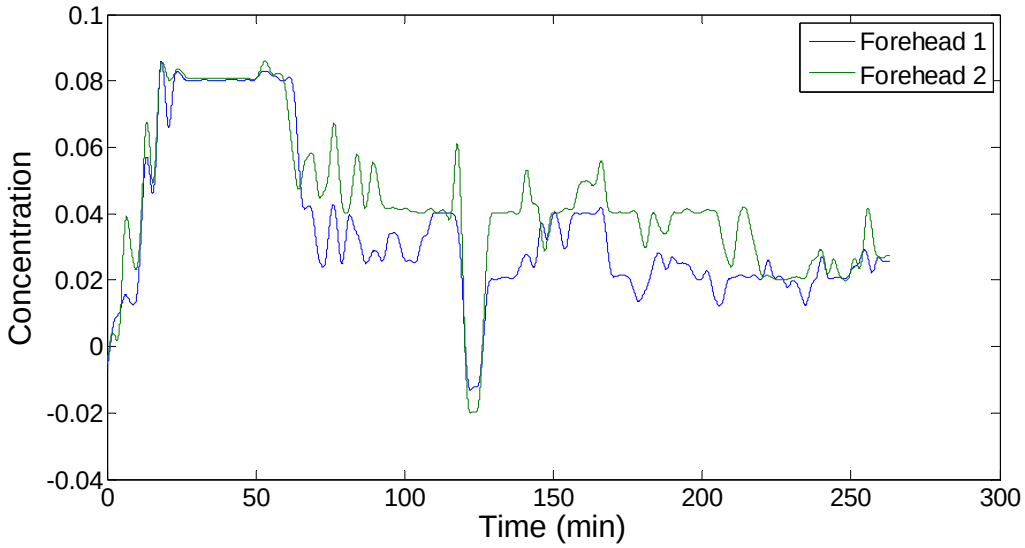

Figure 5-20. Subject 006, 3 Drinks, Forehead Redundant Sensors

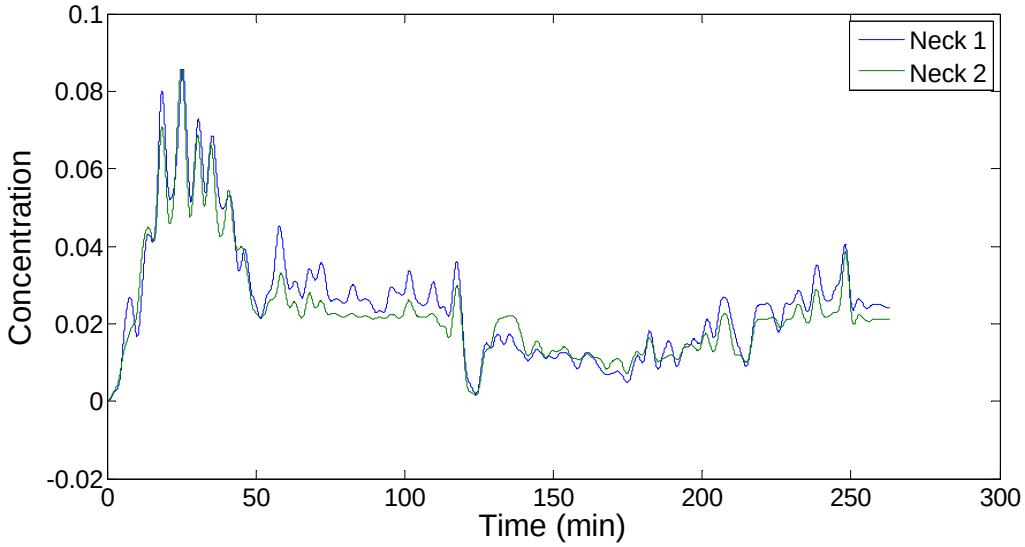

Figure 5-21. Subject 006, 3 Drinks, Neck Redundant Sensors

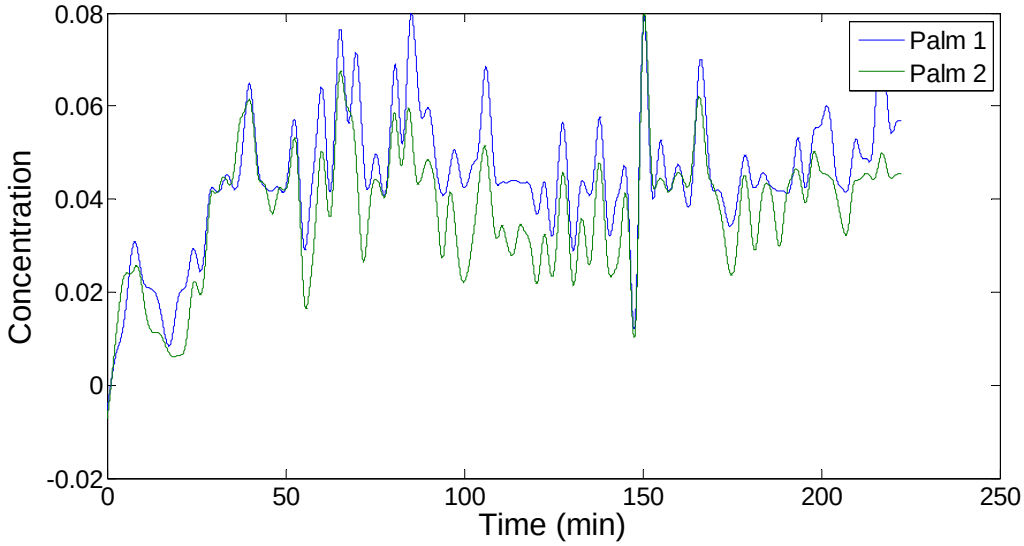

Figure 5-22. Subject 001, 3 Drinks, Palm Redundant Sensors

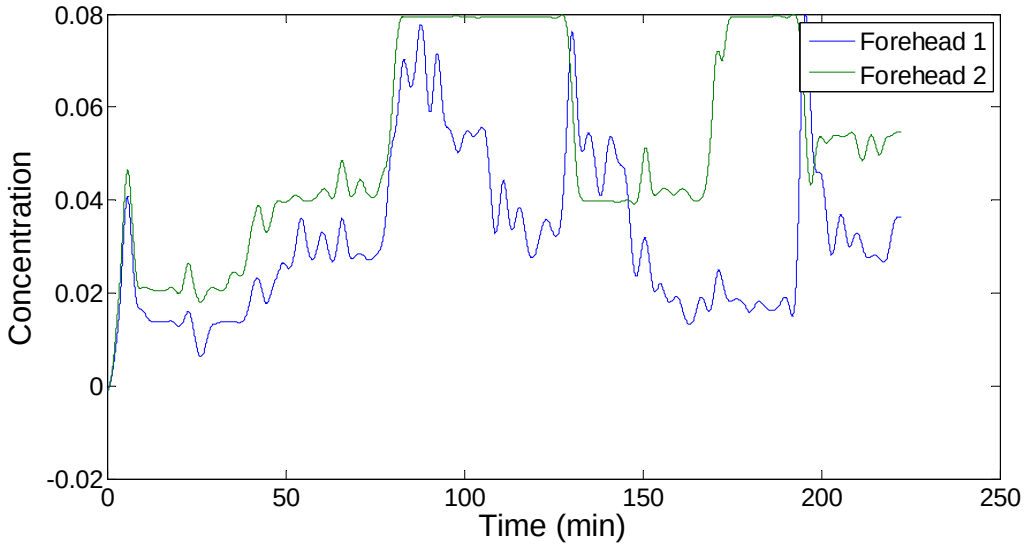

Figure 5-23. Subject 001, 3 Drinks, Forehead Redundant Sensors

The redundant channels agree very well for most cases. In a few cases the signal curves were offset from each other but still followed the same trend, as shown in Figure 5-16 and Figure 5-17. Visually, Figure 5-23 shows the worst agreement between the redundant sensors. The good agreement between the redundant sensor channels suggests that the transdermal sensors are actually capturing the concentration of alcohol emitted from the skin and not random noise. If

the sensors were reporting random noise then there would most likely be a poor correlation between the two redundant channels.

5.9. Signal Response

For most cases the transdermal alcohol signal change during the session was on the order of 1 volt DC. This is the unfiltered sensor response taken thought the entire session. Table 5-4 presents the maximum, minimum and change in voltage values for each sensor for all three sessions completely by subject 006.

Table 5-4. Subject 6 Raw Sensor Data Summary

Dose (Std. Drinks)	Voltage	Palm 1	Palm 2	Forehead 1	Forehead 2	Neck 1	Neck 2	Left Wrist	Right Wrist	Left Ankle	Right Ankle	Average
1	**Min**	0.7911	0.7354	0.9260	1.5466	0.8873	0.7802	1.0100	0.2980	0.4383	0.8912	
	Max	1.6609	1.6501	1.2665	1.8195	1.6018	1.8642	1.7508	1.1526	1.6241	1.5583	
	Δ	0.8698	0.9147	0.3404	0.2729	0.7145	1.0840	0.7408	0.8546	1.1858	0.6671	**0.7645**
2	**Min**	1.5683	1.0390	1.7164	2.4146	0.9379	0.9402	1.6447	1.3420	1.1150	1.0383	
	Max	2.1243	1.9944	2.2510	3.1630	2.4777	2.2888	2.0500	1.8481	2.0756	2.2695	
	Δ	0.5559	0.9554	0.5346	0.7484	1.5398	1.3486	0.4052	0.5062	0.9606	1.2311	**0.8786**
3	**Min**	1.4895	1.3374	1.4714	2.5710	1.0561	1.0245	1.2863	1.2641	0.8376	1.0898	
	Max	2.2541	2.2578	2.7793	3.6312	2.1917	2.3118	2.3049	1.7928	1.3937	1.8010	
	Δ	0.7646	0.9204	1.3080	1.0602	1.1356	1.2873	1.0186	0.5286	0.5561	0.7113	**0.9291**

Inspection of the table shows that while there is variation between the sensors in general the change in voltage increases as the dose increases. The transdermal sensors respond to greater concentrations of alcohol by producing greater signal values. The increase in the change in voltage as the dose of a alcohol given increases is constant with the expectation that as more alcohol is consumed more alcohol is emitted from the skin. This also strengthens the argument that the sensors are measuring the small concentration of alcohol emitted from the surface of the skin.

The small amount of pilot data collected do not show strong agreement between the model and experimental data when comparing the concentration time-course trends. It has also been possible to observe the expected parabolic alcohol concentration curve on the surface of the skin that both the model and previous research suggest for a limited number of curves. The curves where the sensors were removed from the subject during the experimental suggest that it is possible to sense the minute amount of alcohol emitted from the skin with a low cost solvent vapor sensor. Additionally, it was found that as the does of alcohol given increases so does the average change in TAC signal, suggesting that greater concentrations of alcohol are emitted from the skin as the more alcohol is consumed. While this study has failed to show significant correlation between the developed model and the collected data it is believed that modification to the transdermal sensors will yield more useable data.

5.10. Sensor Improvement

Based on observation, the factor believed to most significantly contribute to the noise incurred while collecting data is the air gap between the surface of the skin and the TGS 2620 solvent vapor sensor. The TGS 2620 sensors are designed to detect the concentration of volatile gases in air. When the housing was designed a gap separating the sensor from the bottom of the housing was included so that the vapor sensors would not directly contact the skin. However, in some cases the face of the gas sensors are flush with bottom of the housing due to assembly issues, resulting in direct contact with the skin. When there is no gap, the ethanol vapor emitted from the surface of the skin is not trapped in the air pocket that the air gap would normally allow. As a result any movement by the subject during the study would result a disturbance of the ethanol

vapor present at the sensing element. Figure 5-24 shows a cross section view of the sensor housing highlighting the intended air gap.

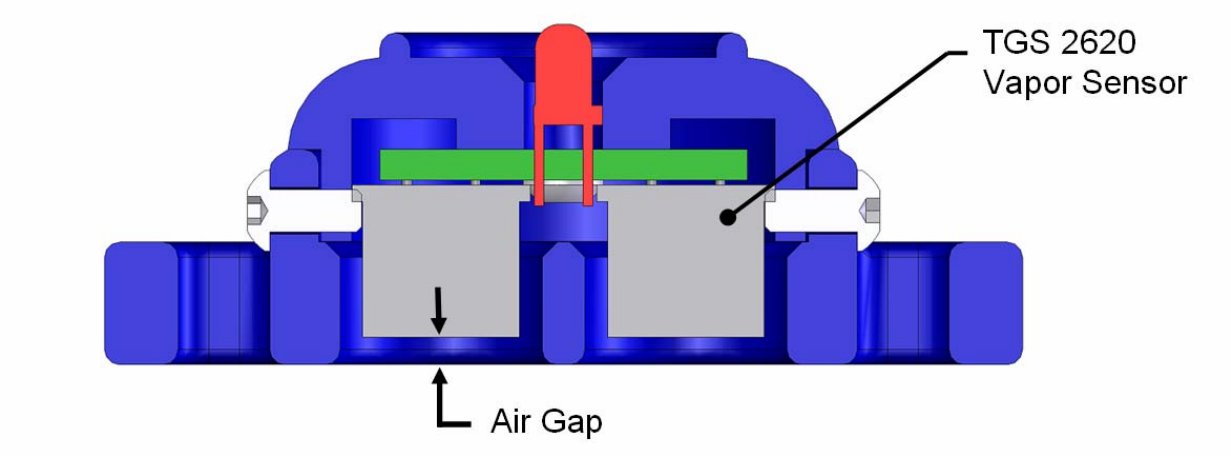

Figure 5-24. TAC Sensor Housing Cross Section

If the air gap were increased the pocket of gas directly above the skin would act like buffer, theoretically reducing the noise present using the current sensors. Additionally, this would increase the comfort to the subject as the sensors get warm during use.

The use of wireless transdermal ethanol sensors would make execution of the study considerably easier. Currently, wires run from the subject to the data acquisition equipment making the set up cumbersome to use. Additionally, as discussed previously, when the subject has to use the bathroom the sensors must be removed resulting in data lost. This would not be necessary if the sensors were wireless. An ideal system would sample and record the voltage output of the vapor sensor and store it on onboard memory during the study. The data can be downloaded after the session is over. A wireless radio connection can be used to synchronize all of the sensors at the start of the study and then be powered down to save battery power during the study.

A fuel cell sensor could also be used to replace the TGS 2620 sensor currently used. However, the fuel cell sensor is more expensive and may detract from the appeal of the design of a low-cost transdermal ethanol sensor.

5.11. Conclusions

Experimental data is needed to enhance our understanding of how alcohol is emitted from the surface of the skin after oral consumption. A limited amount of data is available in the literature; however it is incomplete and does not show how transdermal lag varies with body weight, dose or gender. A custom transdermal ethanol sensor was developed and tested to see how well it could detect ethanol emitted from the surface of the skin. A small pilot study was designed and performed on human subjects to asses how well inexpensive ethanol sensors could detect small amounts of alcohol.

The transdermal ethanol sensor package developed uses a TGS 2620 solvent vapor sensor to detect the concentration of ethanol in the air above the skin. This sensor has been shown to detect the presence of alcohol, however the data acquired from it is noisy and inconclusive. We believe that a larger air gap between the sensor and the surface of the skin may correct this problem in future studies.

A testing protocol for human subjects has been developed and approved by the IRB of Virginia Tech. This protocol allows the data collection of both breath alcohol concentrations and TAC measurements after the oral administration of different doses of alcohol. Three subjects were used in the pilot study to determine if the transdermal ethanol sensors could successfully detect the concentration of alcohol at the surface of their skin. It was shown that these sensors could

detect a small concentration of alcohol, however the noise introduced by the movement of the subject and subsequent disturbance of the vapor near the sensor made it difficult to draw conclusions from the data.

Despite the noise it was found that as the dose of alcohol given increases so does the average voltage change measured by the TAC sensors. As the sensors produce greater voltages as the concentration of alcohol increases, it can be inferred that the sensors are detecting a small amount of alcohol at the surface of the skin and that this concentration increases as more alcohol is consumed. Additionally, inspection of the redundant channels suggests that the noise present on the TAC curves is not random. For almost all cases the redundant sensors agreed very well, suggesting that both sensors were measuring the same concentration of ethanol.

Several improvements have been suggested to increase the validity of the data. The most important suggested improvement would be to increase the size of the air gap, which would increase the size of the sample chamber. This theoretically would have the effect of reducing the noise collected by the sensor.

Chapter 6. Conclusions

Transdermal sensing of the alcohol in a driver's blood is one possible way to non-invasively detect intoxicated drivers. However, the feasibility of this method suffers from the time delay required for the alcohol in the driver's blood to diffuse to the surface of the skin where it can be easily and non-invasively measured. To explore the feasibility of transdermal sensing, we developed and validated a model capable of predicting the time difference between the peak blood alcohol concentration and peak skin alcohol concentration in human subjects given a single dose of ethanol. The model scaled lean body mass and liver size to reflect the differences between males and female for three weight groups of the population.

We used this model to study the effects that body weight, gender, the amount of alcohol consumed and differences in ethanol metabolic rates have on the lag time between peak BAC and TAC values. We found that, for a given dose of alcohol, lag time is insensitive to body weight. However, the dose size has a significant impact on the blood-skin concentration lag. A larger dose of alcohol causes an increase in the lag time. A 15 ml dose of 95% ethanol given to all percentile drivers was found to have a lag time of approximately 33 minutes. Quadrupling the dose to 60 ml of ethanol increases the lag time to approximately 53 minutes. Finally, we examined the effect of minor variances in a person's ability to metabolize alcohol, which is representative of the differences between individuals. A 5% decrease in metabolic rate corresponds approximately to a 5% increase in time lag. Our model suggest that, due to the highly variable relationship between the BAC and TAC curves, transdermal sensing of real-time BAC using only skin surface measurements may prove to be very challenging. The model and

our findings are limited to the study of a single dose of ethanol; therefore our findings may not be applicable to drivers who ingest multiple drinks.

To validate the model and further explore the use of transdermal sensing, custom transdermal ethanol sensors were developed to measure the concentration of alcohol emitted from the surface of the skin. These sensors were designed to attach to the body and used commercially available solvent vapor sensors to detect the presence of alcohol. The sensors were shown to be sensitive to ethanol vapor during bench scale tests.

IRB approval was obtained to perform human subject testing using the transdermal alcohol sensors. The experiment was designed to collect blood and skin alcohol concentration data after oral consumption of alcohol. A professional grade breath alcohol detector was used to measure the subjects' breath alcohol concentrations and the prototype sensors were used to measure skin alcohol concentrations. Pilot data was collected from three health adult males were tested for alcohol doses ranging from 1 to 3 standard drinks.

Analysis of the data found that the collected BAC data agreed very well with the model prediction once the model was adjusted for the subject's body weight and percent water. The model agreed better with the experimental data at lower doses than at higher doses of alcohol, partly due to the increased time it took the subjects to drink larger amounts of alcohol.

The TAC data was too noisy to draw any conclusions concerning how well it matched the model predicted TAC. However it was shown that the average change in voltage of the TAC sensors increases as the dose of alcohol increases which is consistent with the expected results.

Additionally, when the sensors were removed and then reattached during the session in one case the signal rebounded to its original value. It is believe that the signal to noise ratio is too small using the current setup to accurate measure the concentration of ethanol at the surface of the skin. Suggested improvements to the sensors aim to increase the air gap between the sensing element and the skin which is expected to help buffer the alcohol emitted from the skin so more constant measurements can be made.

It is the conclusion of this study that it will be difficult to implement a transdermal bases sensing system into the US automotive fleet due to the dose variant time lag associated with the diffusion of alcohol across the skin. This time lag will make it very difficult to estimate the blood alcohol concentration of a driver based solely on a transdermal alcohol concentration measurement. However, transdermal alcohol sensing might be useful as a dichotomous test to determine if any alcohol has been consumed. This could be used as a 'first pass' test to determine whether or not a more accurate, and invasive, secondary test needs to be performed prior to start the vehicle. An example of a more accurate test could be a breath alcohol detector, which are used in current ignition interlock systems. This would prevent the driver from having to perform BAC checks every time the vehicle is started by limiting the requirement of these checks only to when the system suspects that alcohol may have been consumed.

Table 6-1 summarized the contribution to the literature this thesis has added.

Table 6-1. Contribution to Literature

Major Chapter	Paper Title	Conference/Year
2	Feasibility Of Transdermal Ethanol Sensing For The Detection Of Intoxicated Drivers	Association for the Advancement of Automotive Medicine, 2007
3	Modeling Of Transdermal Transport Of Alcohol: Effect Of Body Mass And Gender	45th International ISA Biomedical Sciences Instrumentation Symposium, 2008
4	Assessment Of Dermal Ethanol Emission Sensors: Experimental Design	44th International ISA Biomedical Sciences Instrumentation Symposium, 2007

Chapter 7. References

Anderson JC, and Hlastala MP. The Kinetics of Transdermal Ethanol Exchange. J Appl Physiol 100: 649-655; 2005.

Chan SC, Liu CL, Lo CM, Lam BK, Lee EW, Wong Y, Fan ST. "Estimating liver weight of adults by body weight and gender" World J Gastroenterol. 12(14): (2006) 2217-222

Figaro, "General Information for TGS Sensors." 2003. 4 Dec. 2004 <http://www.figarosensor.com/>.

Giles HG, Maggiorini S, Ranaud GE, Thiessen JJ, Vidins EI, Compton KV, Saldivia V, Orrego H, Israel Y. Ethanol Vapor above Skin: Determination by a Gas Sensor Instrument and Relationship with Plasma Concentration. Alcohol Clin Exp Res 11: 249-253; 1987.

IIHS, Status Report, Insurance Institute for Highway Safety. 41(7): 2006

Jones AW and Andersson L. Comparision of ethanol concentrations in venous blood and end-expired breath during a controlled drinking study. Forensic Sci Int 132: 18-25; 2003

Levitt MD and Levitt DG. Use of a Two-Compartment Model to Assess the Pharmacokinetics of Human Ethanol Metabolism. Alcohol Clin Exp Res 22(8): 1680-1688; 1998.

McDowell MA, Fryar CD, Hirsch R, Ogden CL. "Anthropometric reference data for children and adults: U.S. population, 1999–2002." Advance data from vital and health statistics; no 361. Hyattsville, MD: National Center for Health Statistics. (2005)

Moyse M. MADD Announces National Campaign to Eliminate Drunk Driving. Mothers Against Drunk Driving. 20 Nov. 2006. 16 Mar. 2006 <http://www.madd.org>; 2006.

NHTSA, Traffic Safety Facts 2005, National Traffic Safety Administration, U.S. Department of Transportation, Washington, DC, Report No. DOT HS 810 616; 2006.

NIAAA, Alcohol Alert No 35. National Institute on Alcohol Abuse and Alcoholism. National Institutes of Health. PH 351; 1994

Phillips M, Greenberg J, Andrzejewski. Evaluation of the Alcopatch, a Transdermal Dosimeter for Monitoring Alcohol Consumption. Alcohol Clin Exp Res 19(6): 1547-1549; 1995.

Pollard, JK., Nadler ED, and Stearns MD. Review of Technology to Prevent Alcohol-Impaired Crashes. DOT HS 810 827. NHTSA, 2007.

Ramchandani VA, Bosron WF, Li TK. Research advances in ethanol metabolism. Pathol Biol 49: 676-682; 2001.

Swift RM, Martin CS, Swette L, et al. Studies on a Wearable, Electronic, Transdermal Alcohol Sensor. Alcohol Clin Exp Res 16(4): 721-725; 1992.

Umulis DM, Gurmen NM, Singh P, Fogler HS, 2005. A Physiologically Based Model for Ethanol and Acetaldehyde Metabolism in Human Beings. Alcohol 35: 3-12; 2005.

Widmark EP. Principles and Applications of Medicolegal Alcohol Determination. Davis: Biomedical Publications; 1981.

Wilkinson PK, Sedman AJ, Sakmar E. Pharmacokinetics of Ethanol After Oral Administration in the Fasting State. J Pharmacokinet Biopharm 5(3): 207-224; 1977.

Wilschut A, ten Berge WF, Robinson PJ, McKone TE. Estimating Skin Permeation. The Validation of Five Mathematical Skin Permeation Models. Chemosphere 30: 1275-1296; 1995.

Adapated from **"**Skin layers" U.S. National Library of Medicine, http://www.nlm.nih.gov/medlineplus/ency/images/ency/fullsize/8912.jpg

Appendix A. IRB Documents

1. IRB Expedited Approval (IRB# 08-100)
2. IRB Amendment 1 Approval (IRB# 08-100)

VirginiaTech

Office of Research Compliance
Institutional Review Board
2000 Kraft Drive, Suite 2000 (0497)
Blacksburg, Virginia 24061
540/231-4991 Fax 540/231-0959
e-mail moored@vt.edu
www.irb.vt.edu
FWA00000572(expires 1/20/2010)
IRB # is IRB00000667

DATE: February 25, 2008

MEMORANDUM

TO: Clay Gabler
Gregory Webster

Approval date: 2/25/2008
Continuing Review Due Date:2/10/2009
Expiration Date: 2/24/2009

FROM: David M. Moore

SUBJECT: **IRB Expedited Approval:** "Feasibility of Transdermal Ethanol Sensing for Estimating Blood Alcohol Concentrations" , IRB # 08-100

This memo is regarding the above-mentioned protocol. The proposed research is eligible for expedited review according to the specifications authorized by 45 CFR 46.110 and 21 CFR 56.110. As Chair of the Virginia Tech Institutional Review Board, I have granted approval to the study for a period of 12 months, effective February 25, 2008.

As an investigator of human subjects, your responsibilities include the following:

1. Report promptly proposed changes in previously approved human subject research activities to the IRB, including changes to your study forms, procedures and investigators, regardless of how minor. The proposed changes must not be initiated without IRB review and approval, except where necessary to eliminate apparent immediate hazards to the subjects.
2. Report promptly to the IRB any injuries or other unanticipated or adverse events involving risks or harms to human research subjects or others.
3. Report promptly to the IRB of the study's closing (i.e., data collecting and data analysis complete at Virginia Tech). If the study is to continue past the expiration date (listed above), investigators must submit a request for continuing review prior to the continuing review due date (listed above). It is the researcher's responsibility to obtained re-approval from the IRB before the study's expiration date.
4. If re-approval is not obtained (unless the study has been reported to the IRB as closed) prior to the expiration date, all activities involving human subjects and data analysis must cease immediately, except where necessary to eliminate apparent immediate hazards to the subjects.

Important:
If you are conducting **federally funded non-exempt research**, this approval letter must state that the IRB has compared the OSP grant application and IRB application and found the documents to be consistent. Otherwise, this approval letter is invalid for OSP to release funds. Visit our website at http://www.irb.vt.edu/pages/newstudy.htm#OSP for further information.

cc: File

VirginiaTech

Office of Research Compliance
Institutional Review Board
2000 Kraft Drive, Suite 2000 (0497)
Blacksburg, Virginia 24061
540/231-4991 Fax 540/231-0959
e-mail moored@vt.edu
www.irb.vt.edu
FWA00000572(expires 1/20/2010)
IRB # is IRB00000667

DATE: April 2, 2008

MEMORANDUM

TO: Clay Gabler
Gregory Webster
Stephanie Comas

FROM: David M. Moore

Approval date: 2/25/2008
Continuing Review Due Date:2/10/2009
Expiration Date: 2/24/2009

SUBJECT: **IRB Amendment 1 Approval:** "Feasibility of Transdermal Ethanol Sensing for Estimating Blood Alcohol Concentrations" , IRB # 08-100

This memo is regarding the above referenced protocol which was previously granted approval by the IRB on February 25, 2008. You subsequently requested permission to amend your IRB application. Since the requested amendment is nonsubstantive in nature, I, as Chair of the Virginia Tech Institutional Review Board, have granted approval for requested protocol amendment, effective as of April 2, 2008. The anniversary date will remain the same as the original approval date.

As an investigator of human subjects, your responsibilities include the following:

1. Report promptly proposed changes in previously approved human subject research activities to the IRB, including changes to your study forms, procedures and investigators, regardless of how minor. The proposed changes must not be initiated without IRB review and approval, except where necessary to eliminate apparent immediate hazards to the subjects.
2. Report promptly to the IRB any injuries or other unanticipated or adverse events involving risks or harms to human research subjects or others.
3. Report promptly to the IRB of the study's closing (i.e., data collecting and data analysis complete at Virginia Tech). If the study is to continue past the expiration date (listed above), investigators must submit a request for continuing review prior to the continuing review due date (listed above). It is the researcher's responsibility to obtain re-approval from the IRB before the study's expiration date.
4. If re-approval is not obtained (unless the study has been reported to the IRB as closed) prior to the expiration date, all activities involving human subjects and data analysis must cease immediately, except where necessary to eliminate apparent immediate hazards to the subjects.

cc: File

Appendix B. Sensor Diagrams

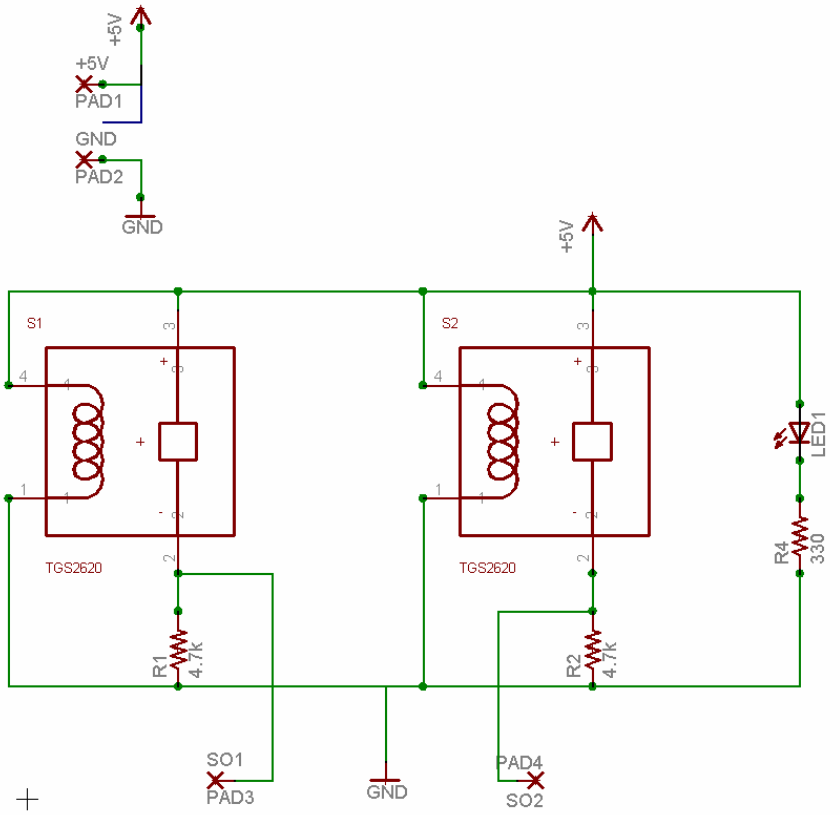

Figure B-1. Transdermal Sensor Electrical Schematic

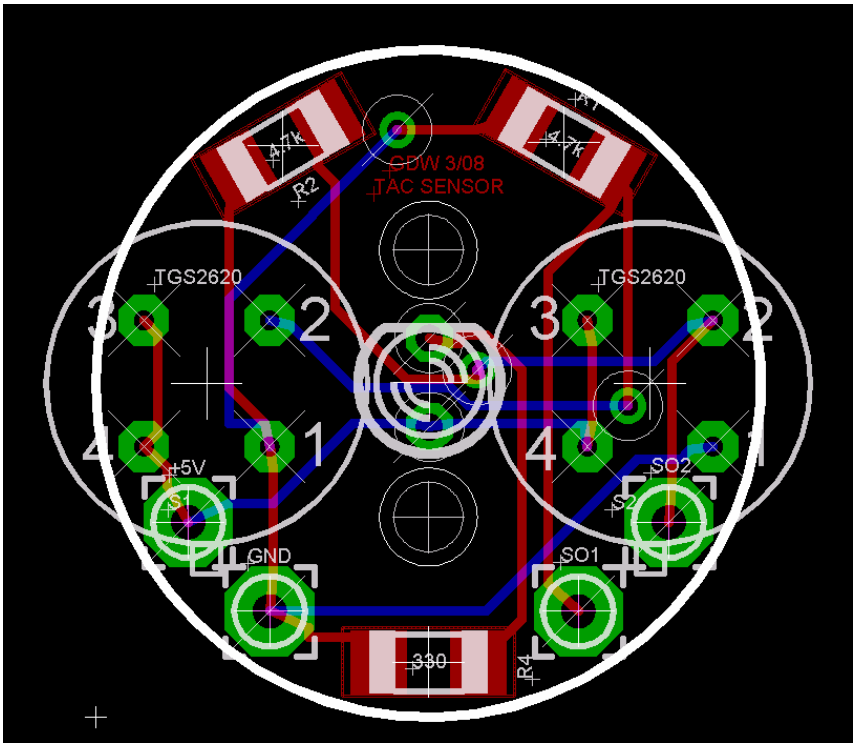

Figure B-2. Printed Circuit Board Layout

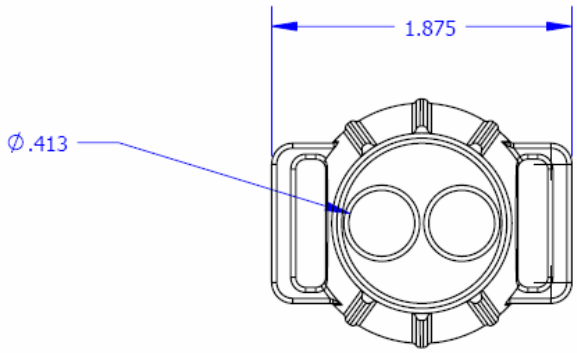

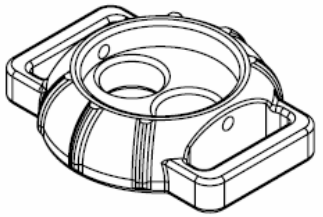

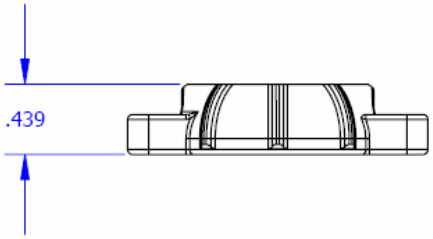

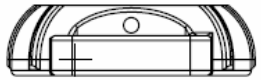

CENTER FOR INJURY BIOMECHANICS

Virginia Tech
VIRGINIA POLYTECHNIC INSTITUTE AND STATE UNIVERSITY

BASE
ALCOHOL SENSOR BRACELET

DRAWN BY: GDW	MATERIAL: ABS
DATE PRINTED: 3/10/2008	PRINT TYPE: REFERENCE
SCALE: 1:1	SIZE: A
	DWG. NO.: Housing3-base

5 4 3 2 1

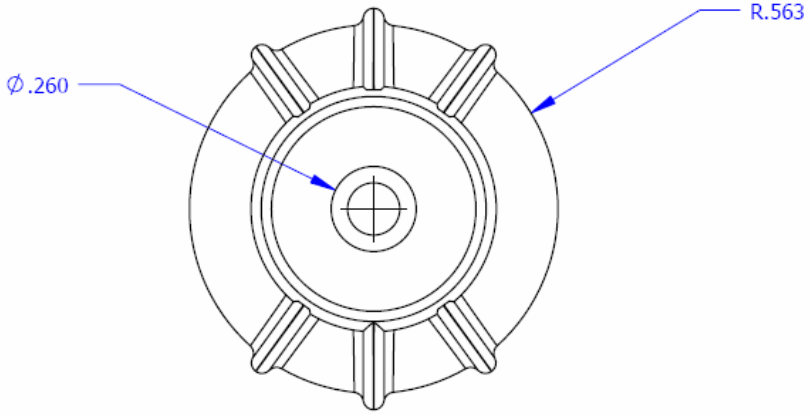

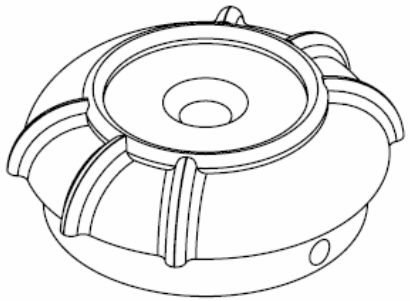

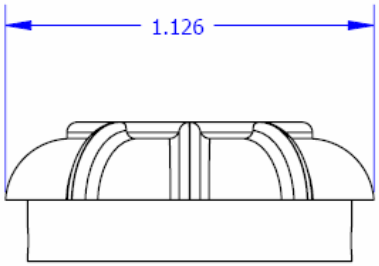

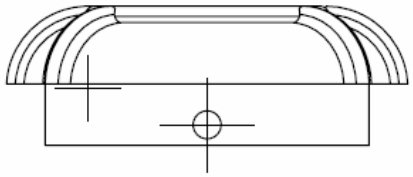

CENTER FOR INJURY BIOMECHANICS

Virginia Tech

VIRGINIA POLYTECHNIC INSTITUTE AND STATE UNIVERSITY

TOP
ALCOHOL SENSOR BRACELET

DRAWN BY: GDW	MATERIAL: ABS
DATE PRINTED: 3/10/2008	PRINT TYPE: REFERENCE
SCALE: 2:1	SIZE: A
	DWG. NO.: Housing3-top3

5 4 3 2 1

Appendix C. Experimental Data

Subject 001: Dose 1 Drink

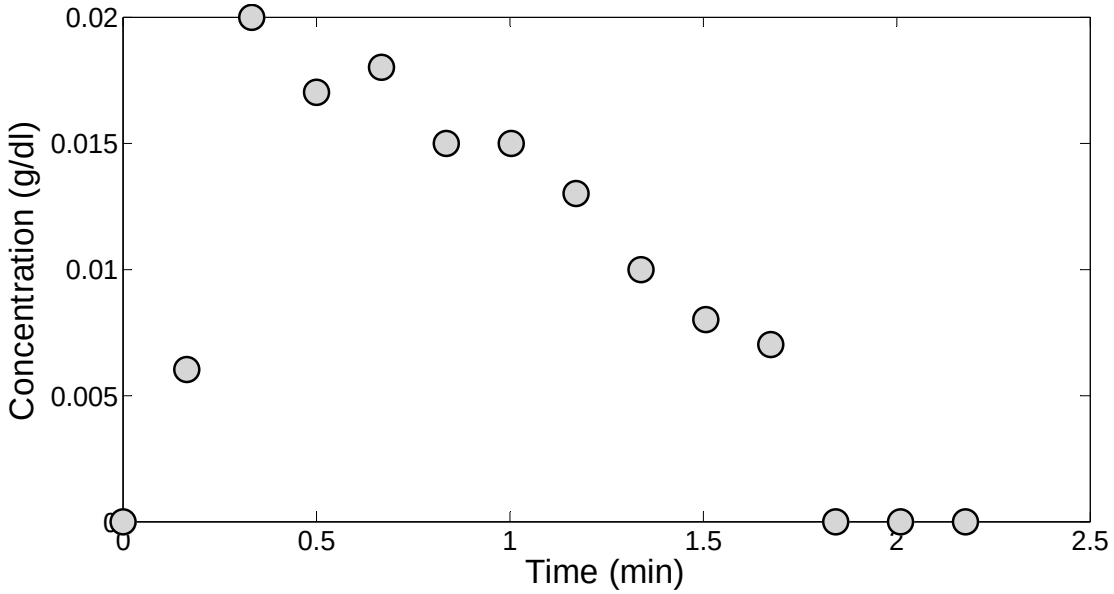

Figure C-1. Subject 001 | Dose: 1 Drink | BAC

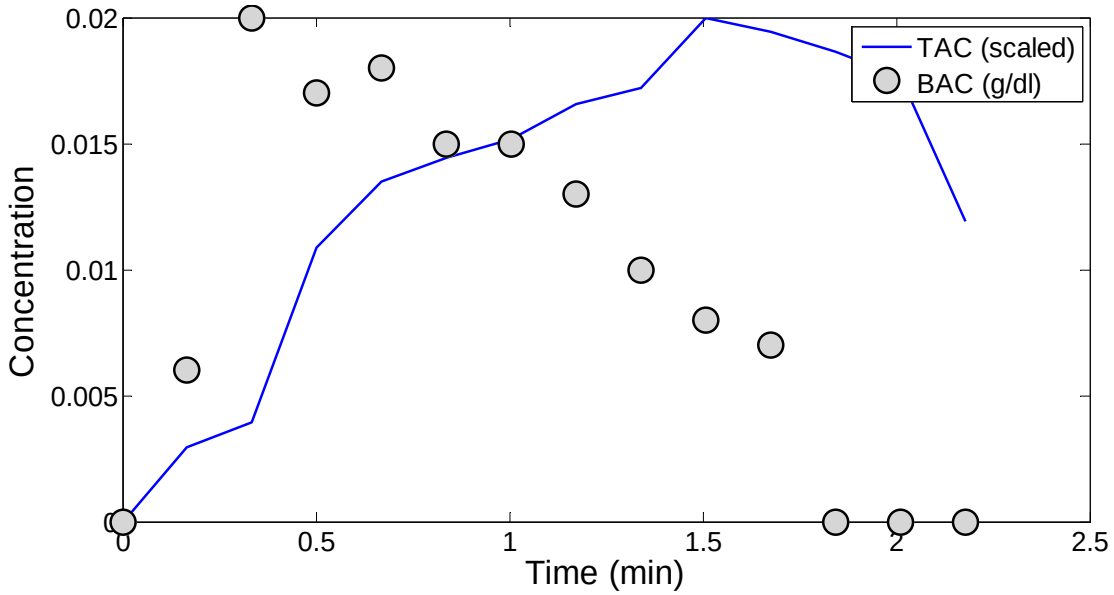

Figure C-2. Subject 001 | Dose: 1 Drink | Palm 1

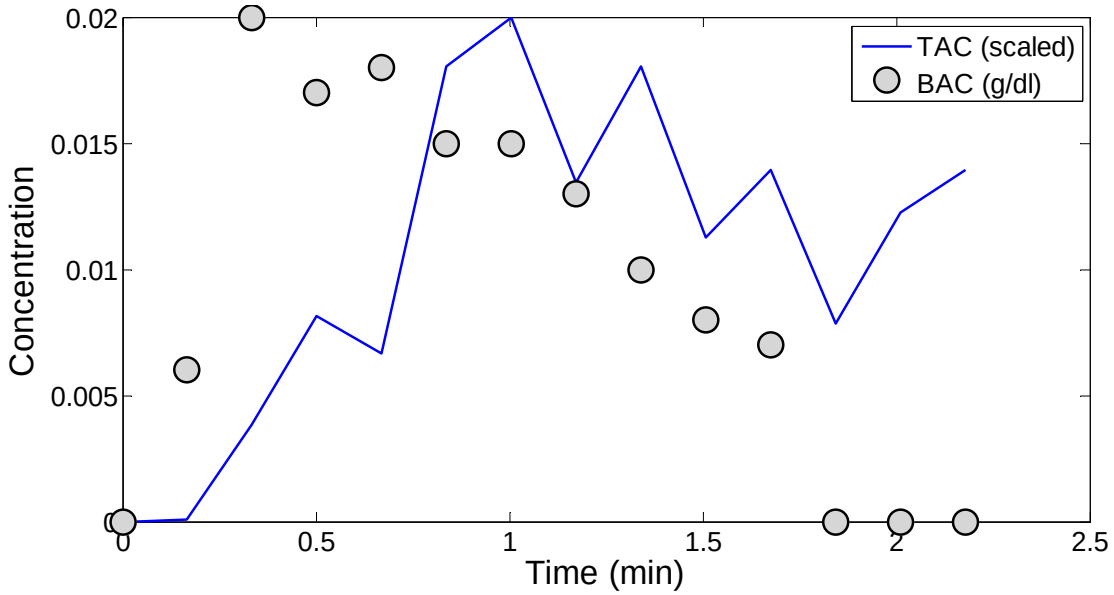

Figure C-3. Subject 001 | Dose: 1 Drink | Palm 2

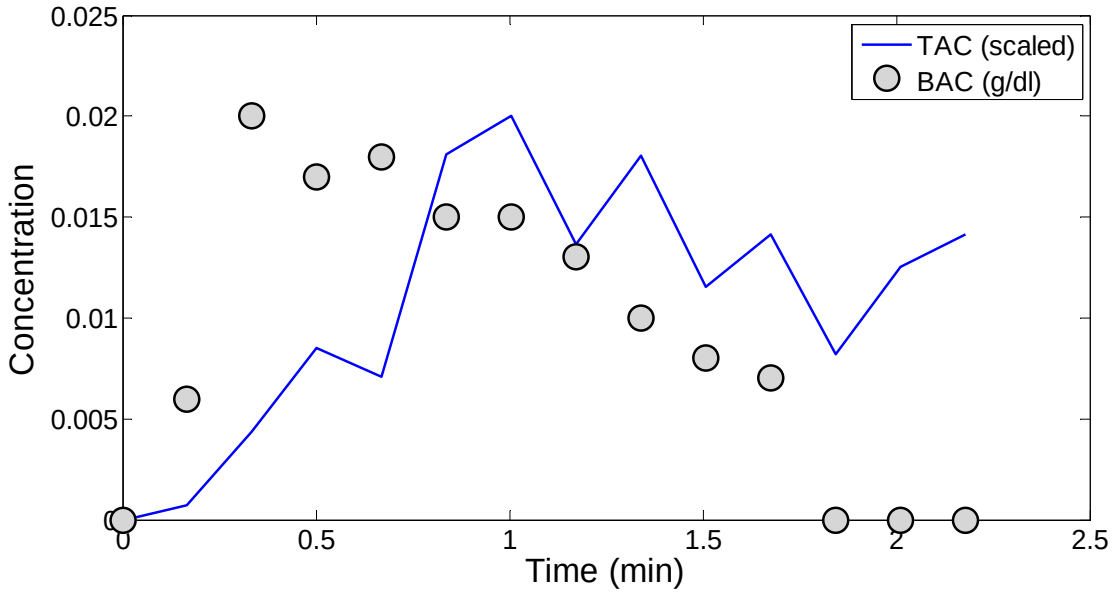

Figure C-4. Subject 001 | Dose: 1 Drink | Right Wrist

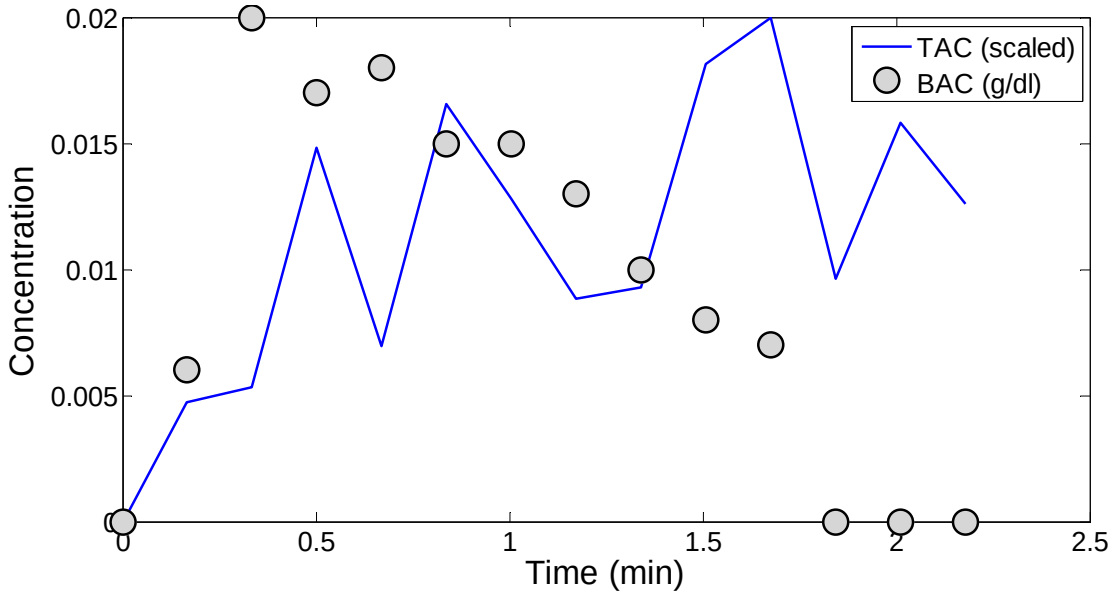

Figure C-5. Subject 001 | Dose: 1 Drink | Left Wrist

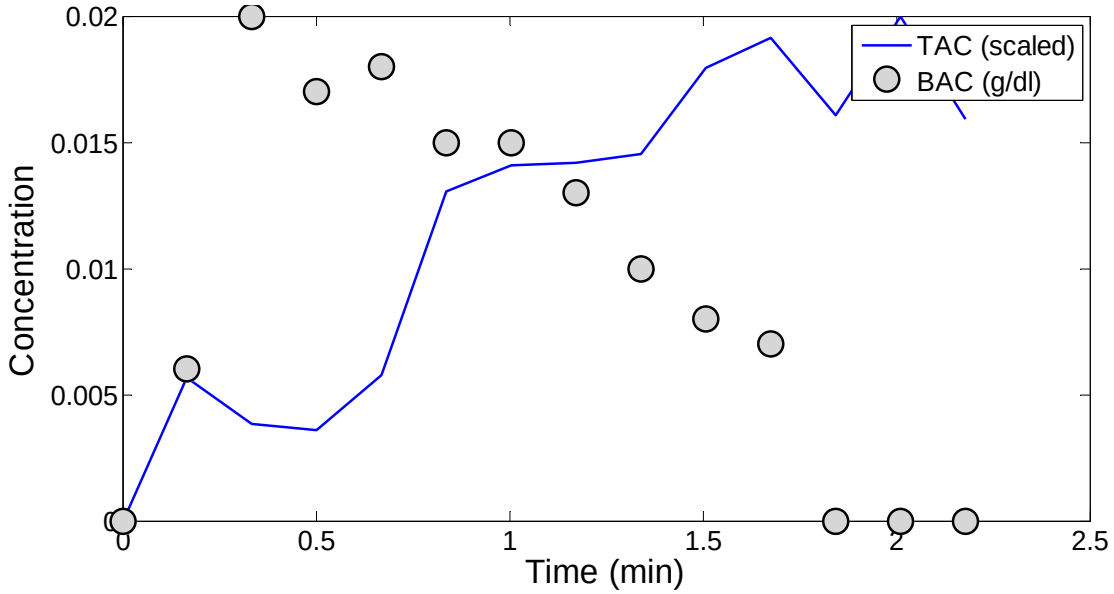

Figure C-6. Subject 001 | Dose: 1 Drink | Ankle

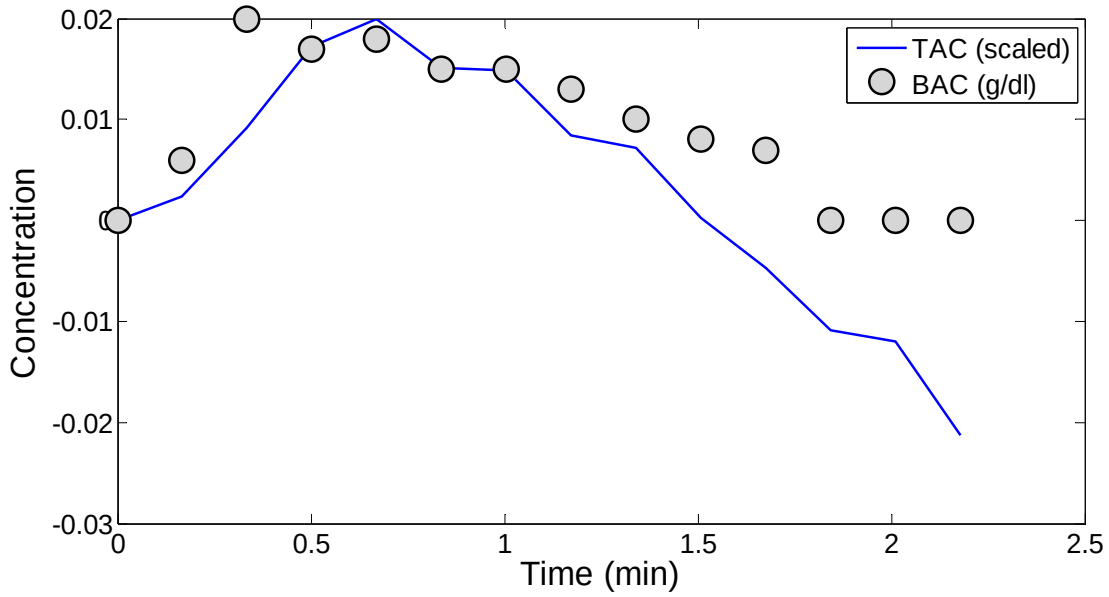

Figure C-7. Subject 001 | Dose: 1 Drink | Forehead

Subject 001: Dose 2 Drinks

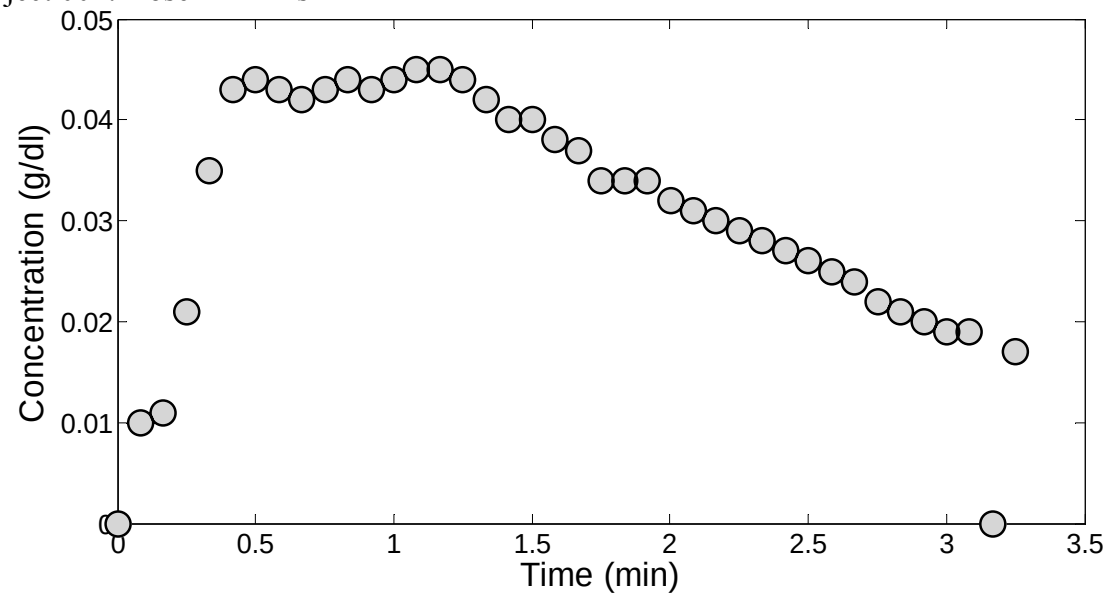

Figure C-8. Subject 001 | Dose: 2 Drinks | BAC

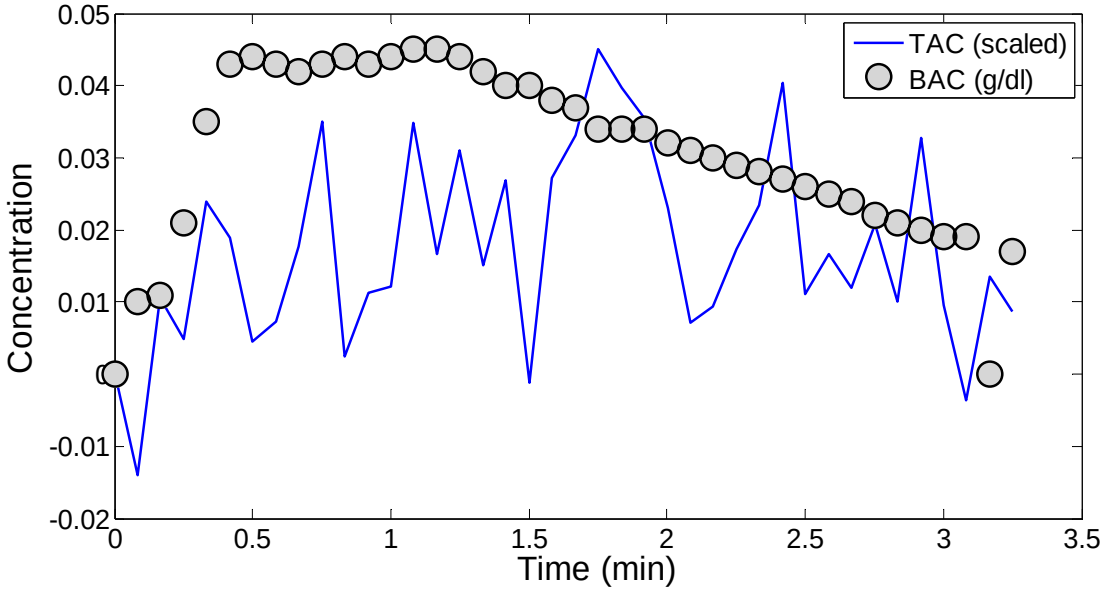

Figure C-9. Subject 001 | Dose: 2 Drinks | Palm 1

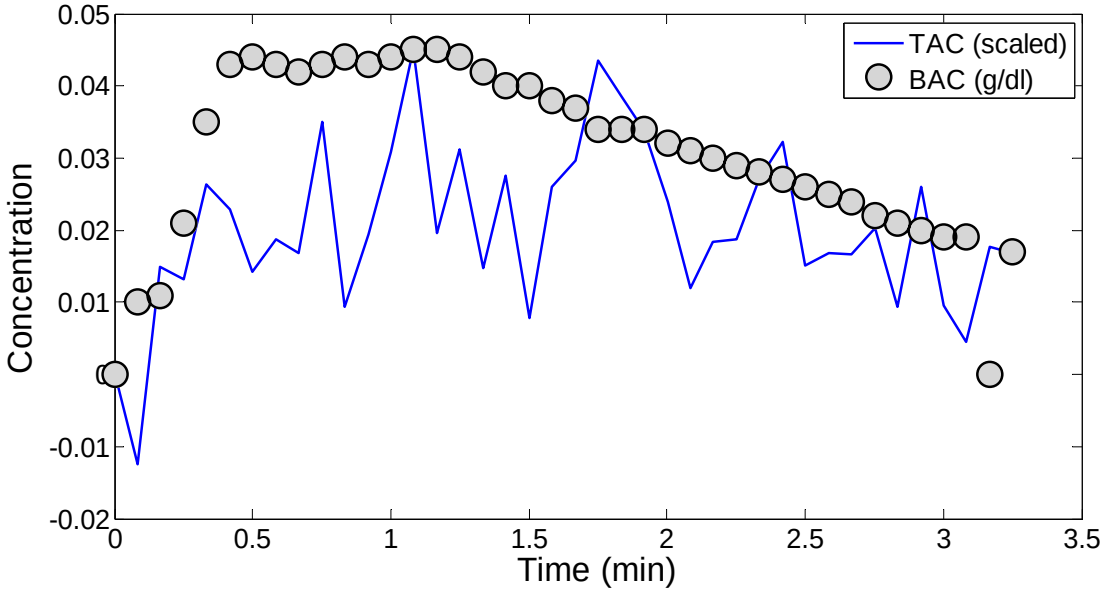

Figure C-10. Subject 001 | Dose: 2 Drinks | Palm 2

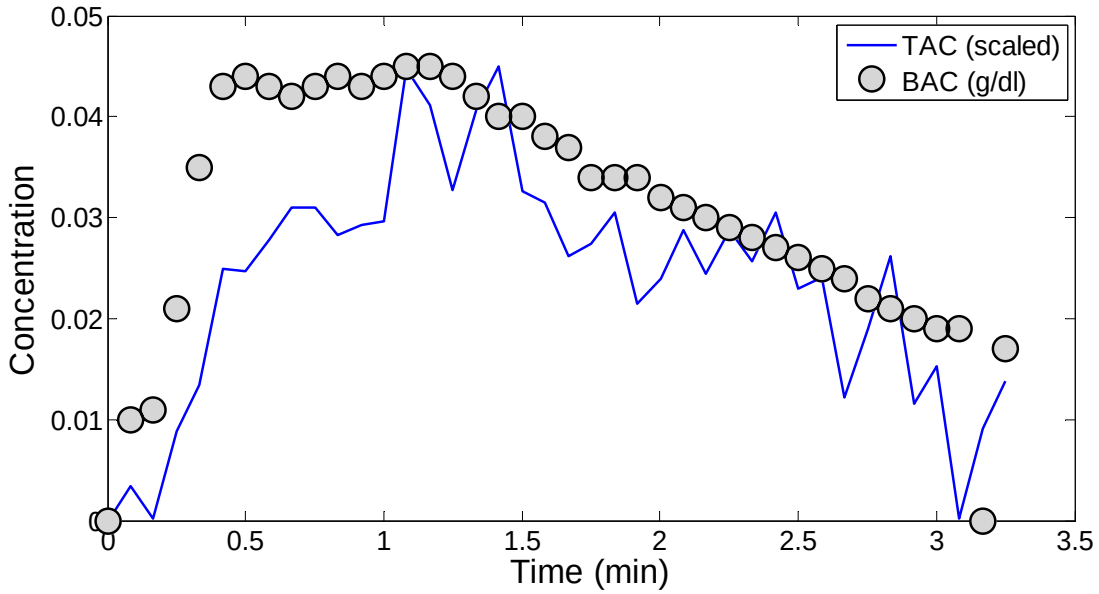

Figure C-11. Subject 001 | Dose: 2 Drinks | Right Wrist

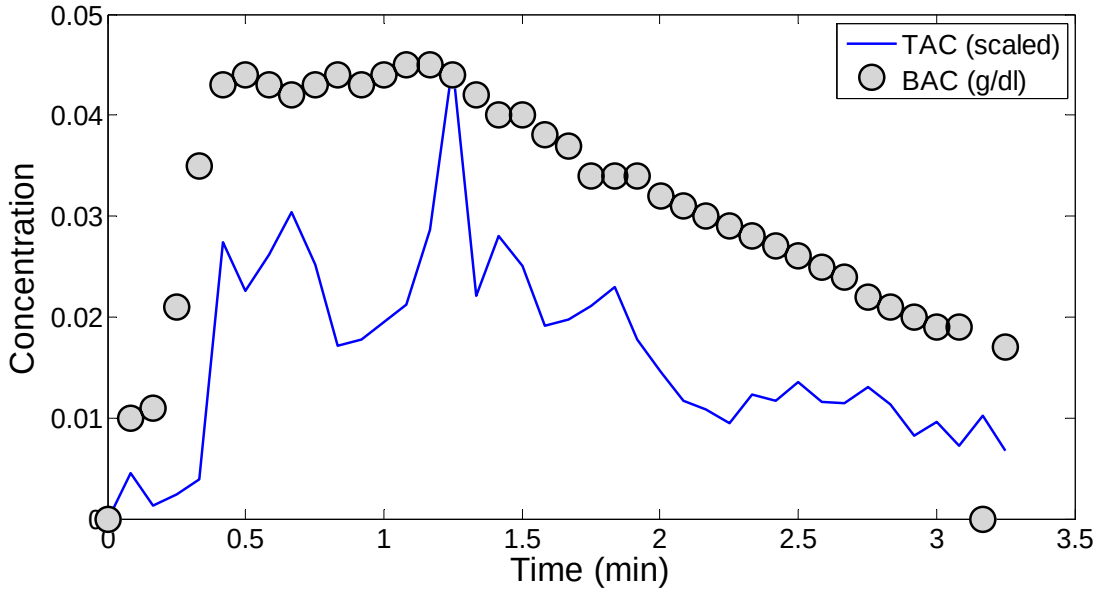

Figure C-12. Subject 001 | Dose: 2 Drinks | Left Wrist

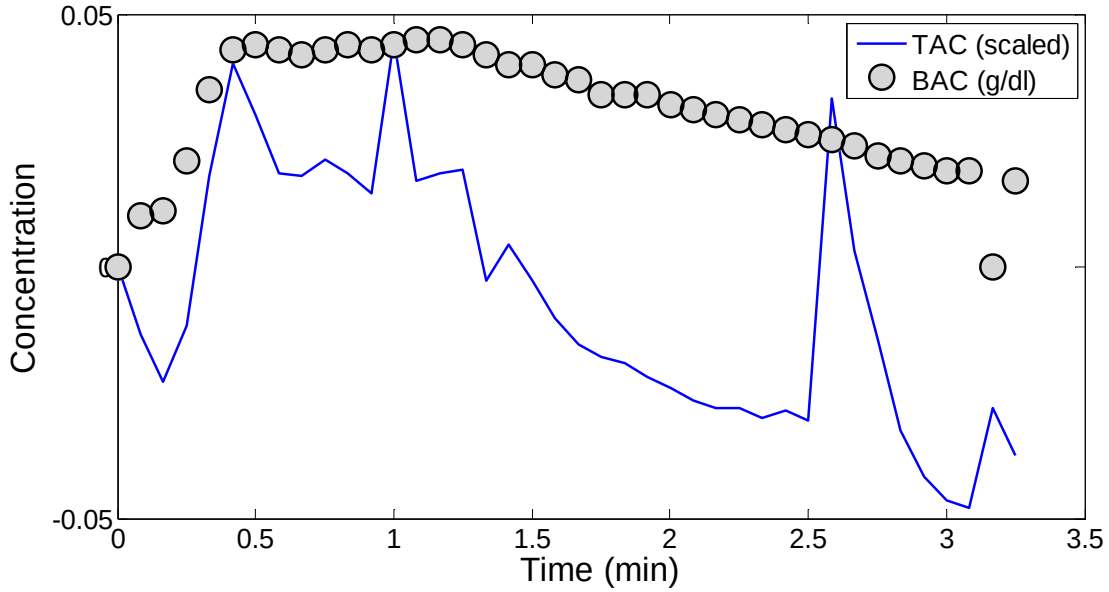

Figure C-13. Subject 001 | Dose: 2 Drinks | Ankle

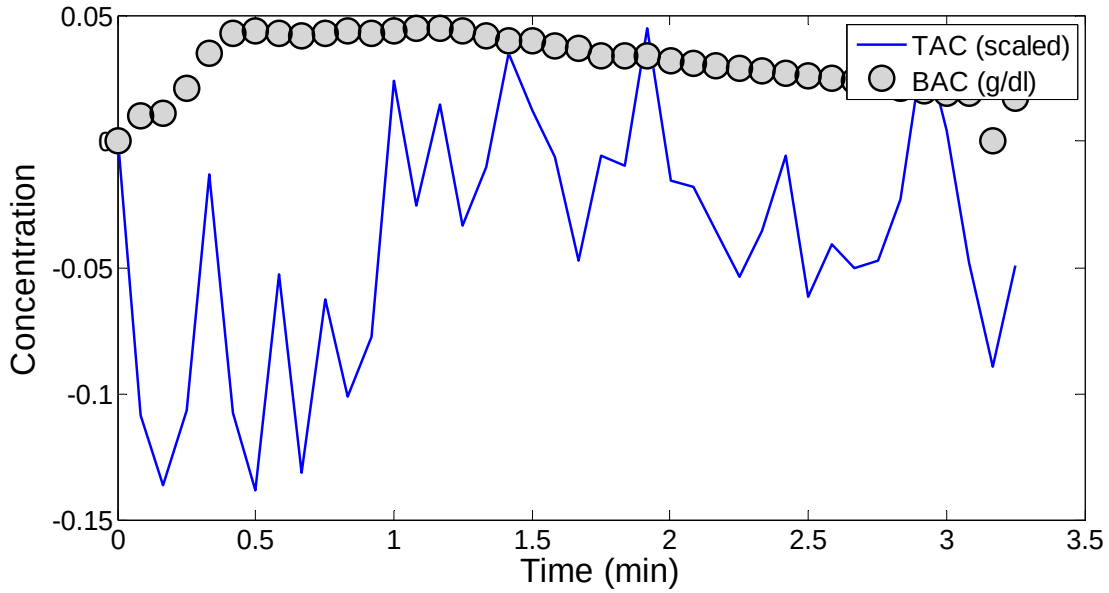

Figure C-14. Subject 001 | Dose: 2 Drinks | Forehead

Subject 001: Dose 3 Drinks

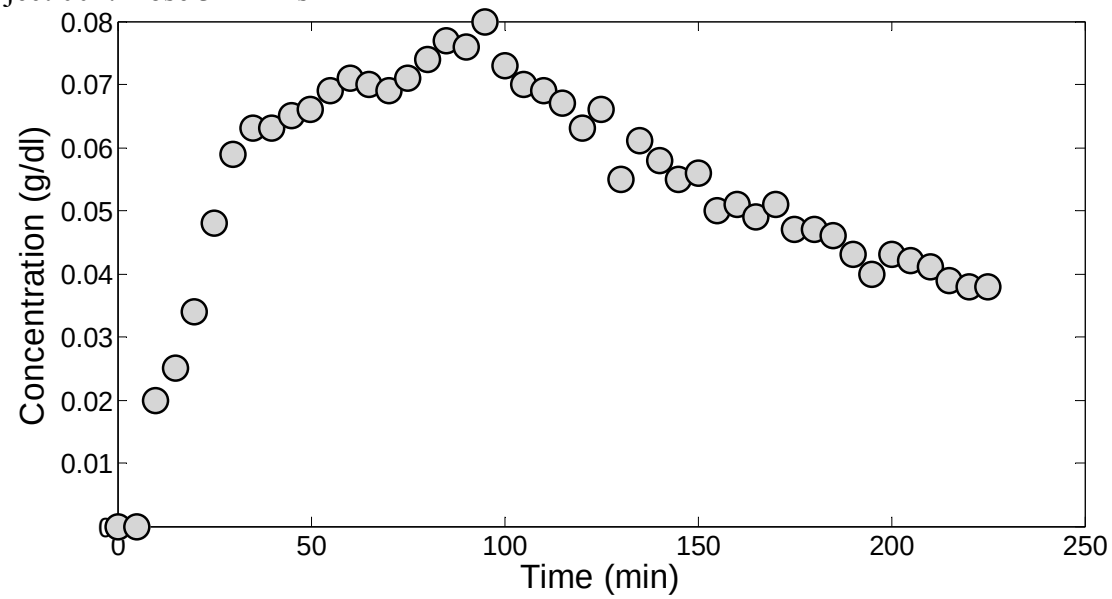

Figure C-15. Subject 001 | Dose: 3 Drinks | BAC

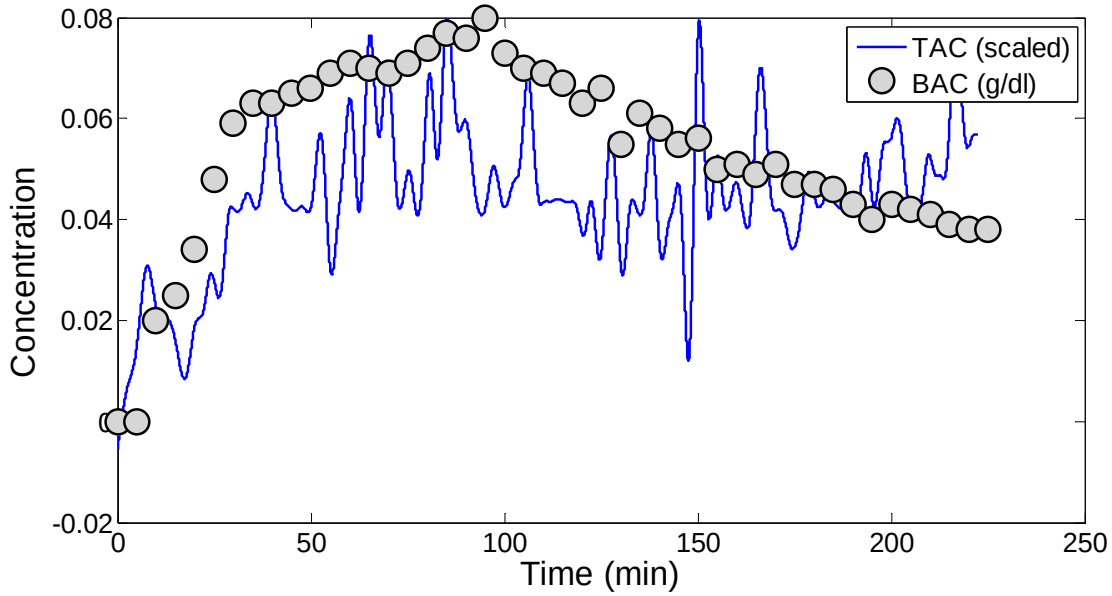

Figure C-16. Subject 001 | Dose: 3 Drinks | Palm 1

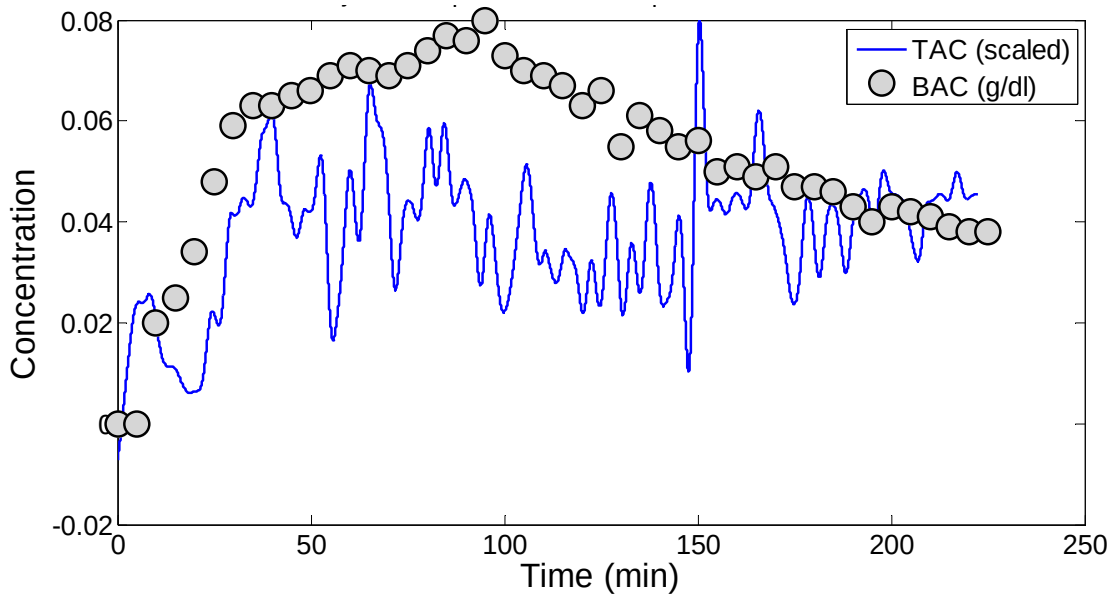

Figure C-17. Subject 001 | Dose: 3 Drinks | Palm 2

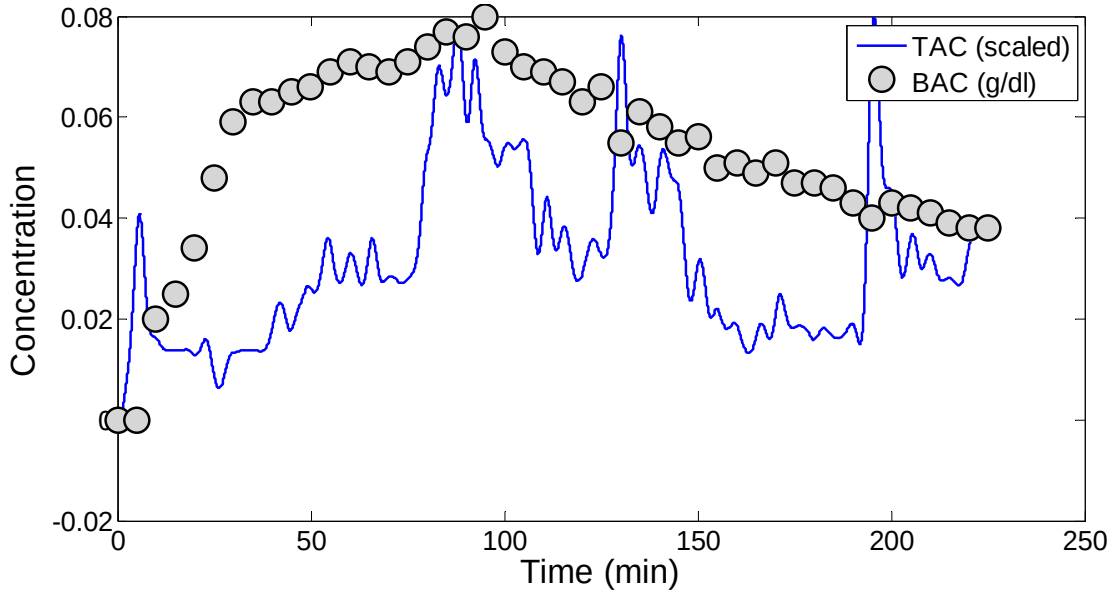

Figure C-18. Subject 001 | Dose: 3 Drinks | Forehead 1

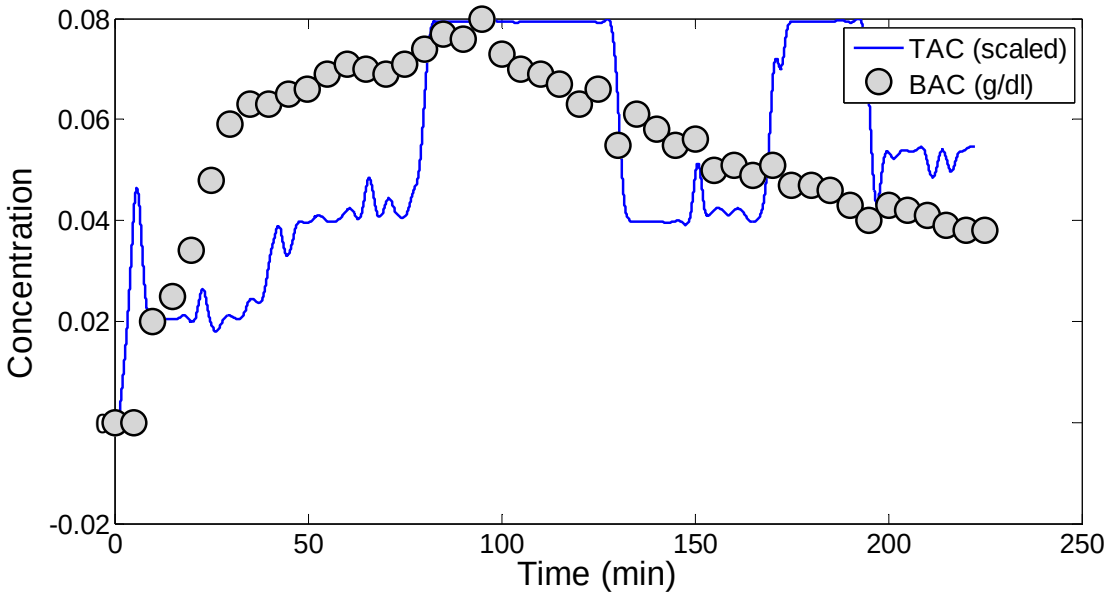

Figure C-19. Subject 001 | Dose: 3 Drinks | Forehead 2

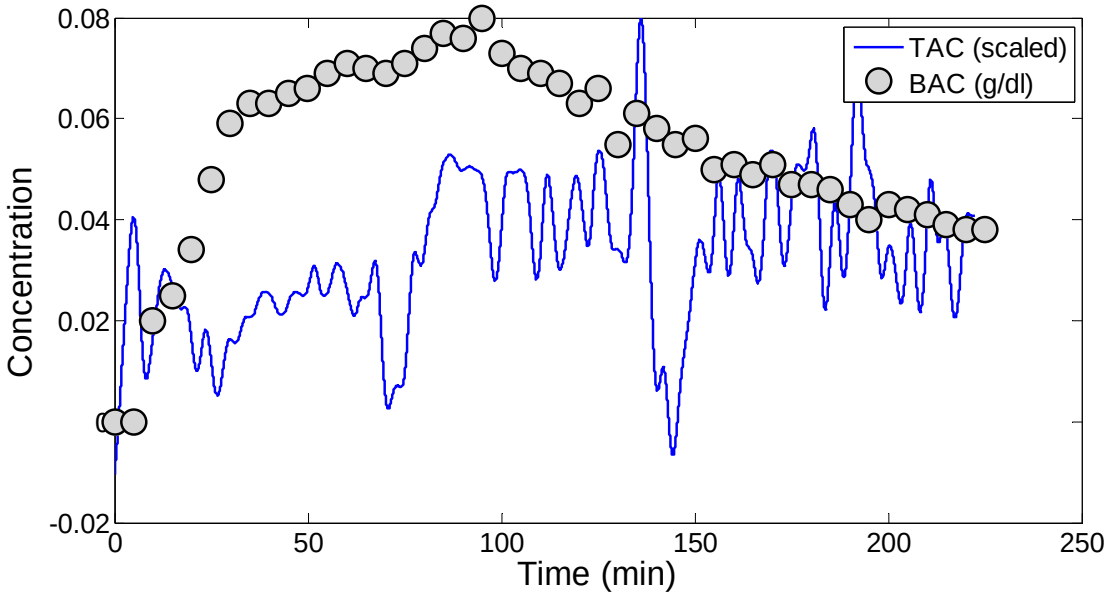

Figure C-20. Subject 001 | Dose: 3 Drinks | Neck 1

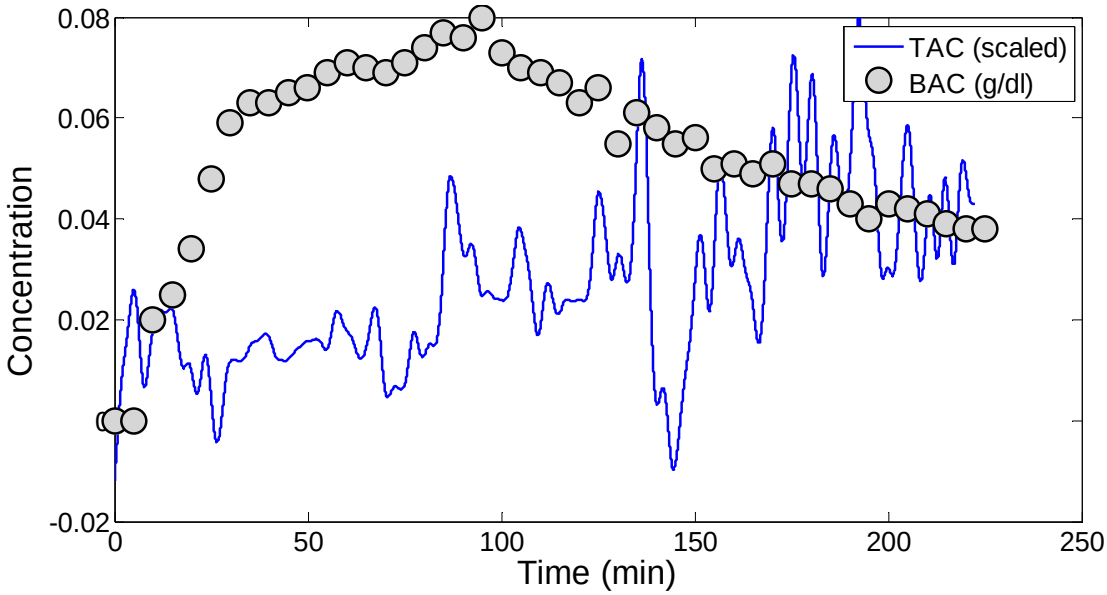

Figure C-21. Subject 001 | Dose: 3 Drinks | Neck 2

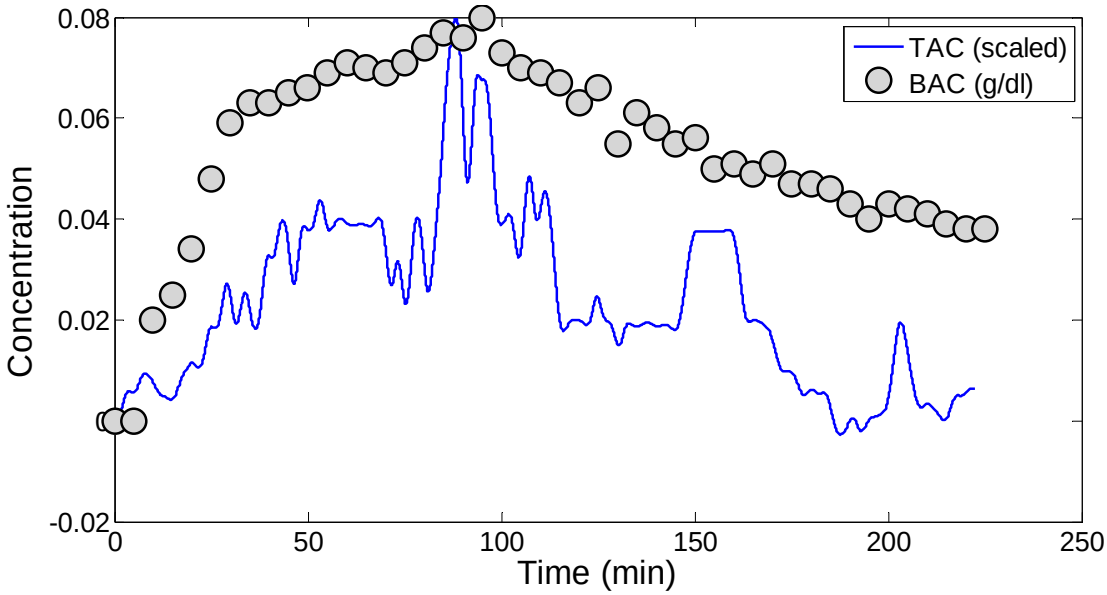

Figure C-22. Subject 001 | Dose: 3 Drinks | Left Wrist

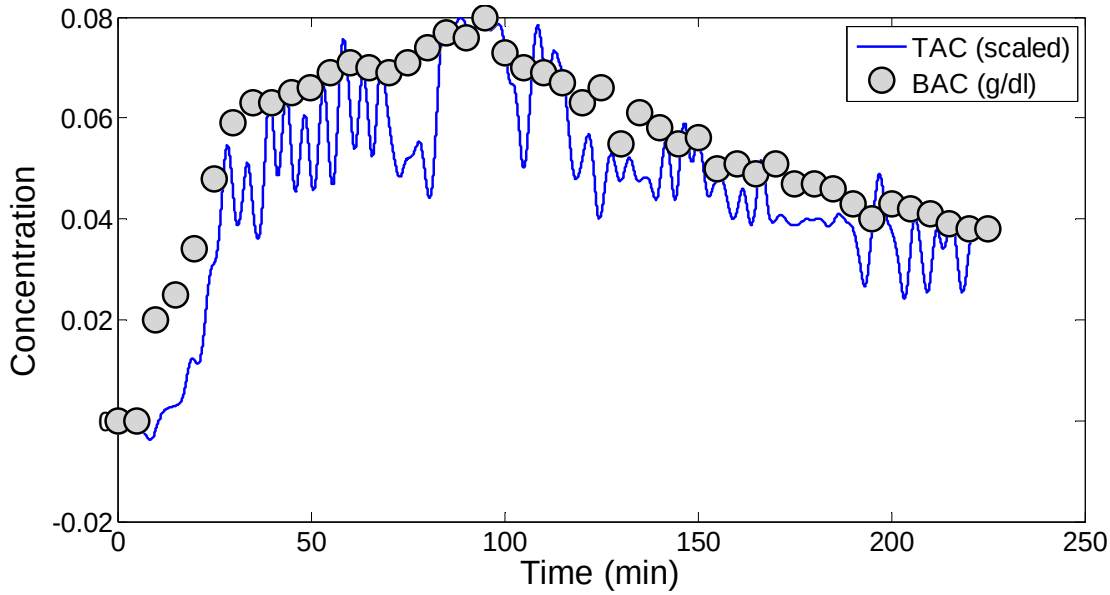

Figure C-23. Subject 001 | Dose: 3 Drinks | Right Wrist

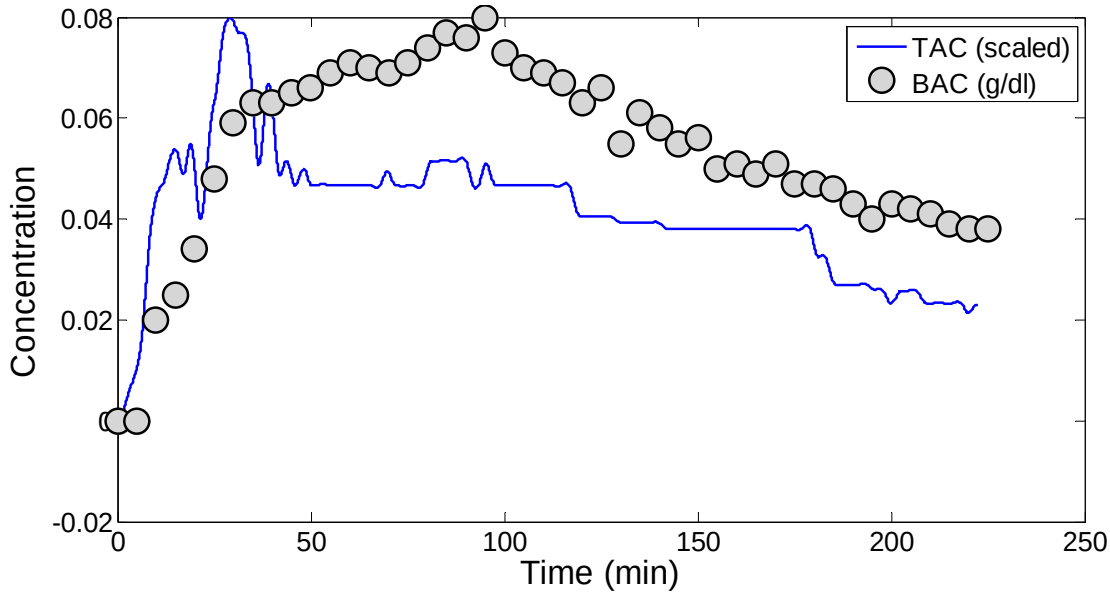

Figure C-24. Subject 001 | Dose: 3 Drinks | Left Ankle

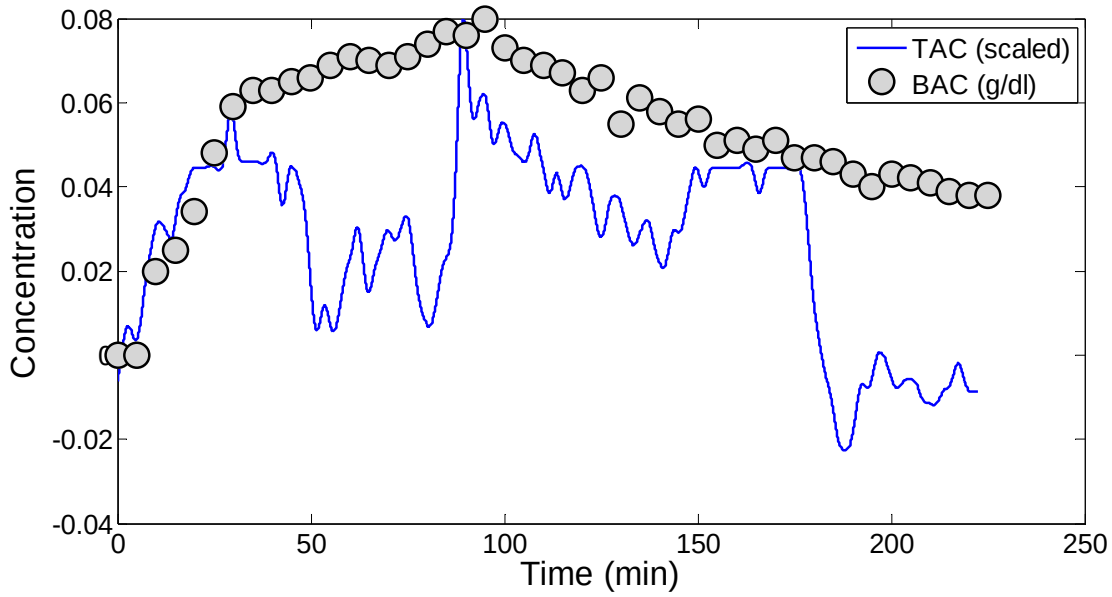

Figure C-25. Subject 001 | Dose: 3 Drinks | Right Ankle

Subject 004: Dose 1 Drink

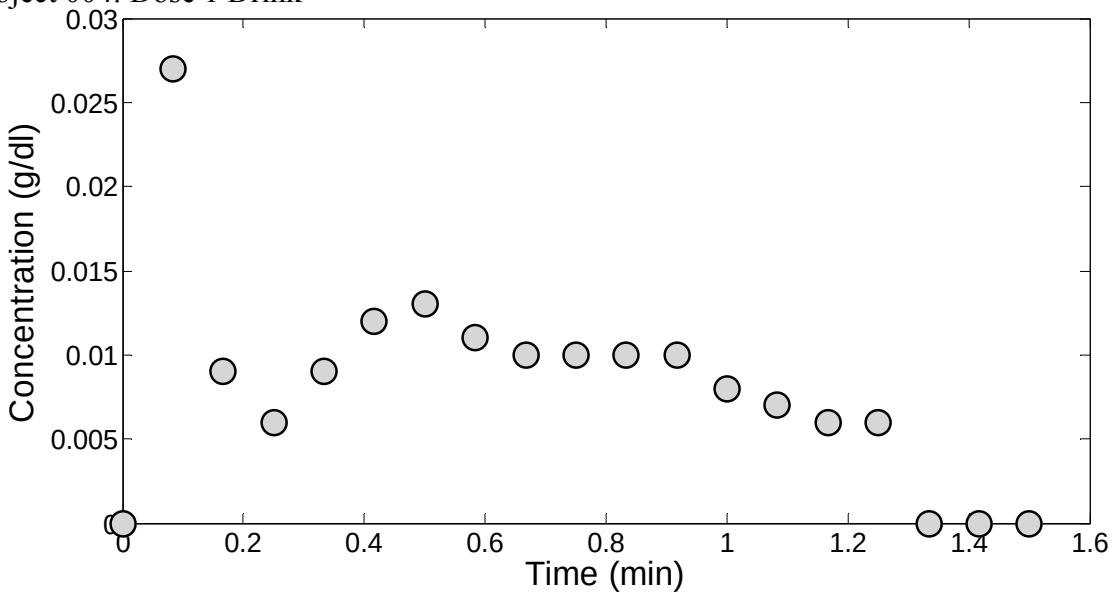

Figure C-26. Subject 004 | Dose: 1 Drink | BAC

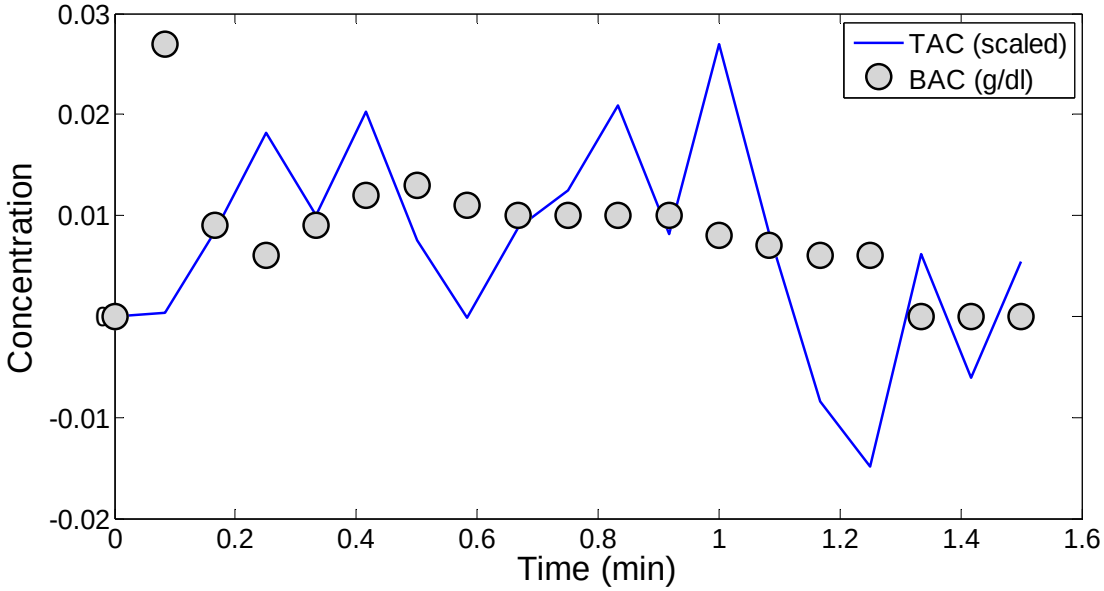

Figure C-27. Subject 004 | Dose: 1 Drink | Palm 1

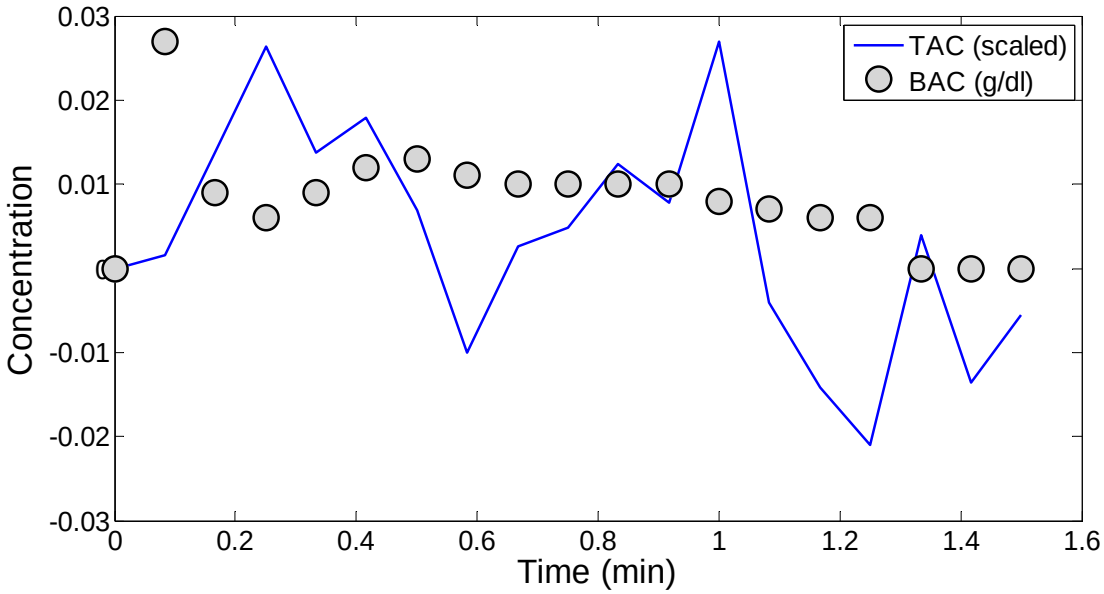

Figure C-28. Subject 004 | Dose: 1 Drink | Palm 2

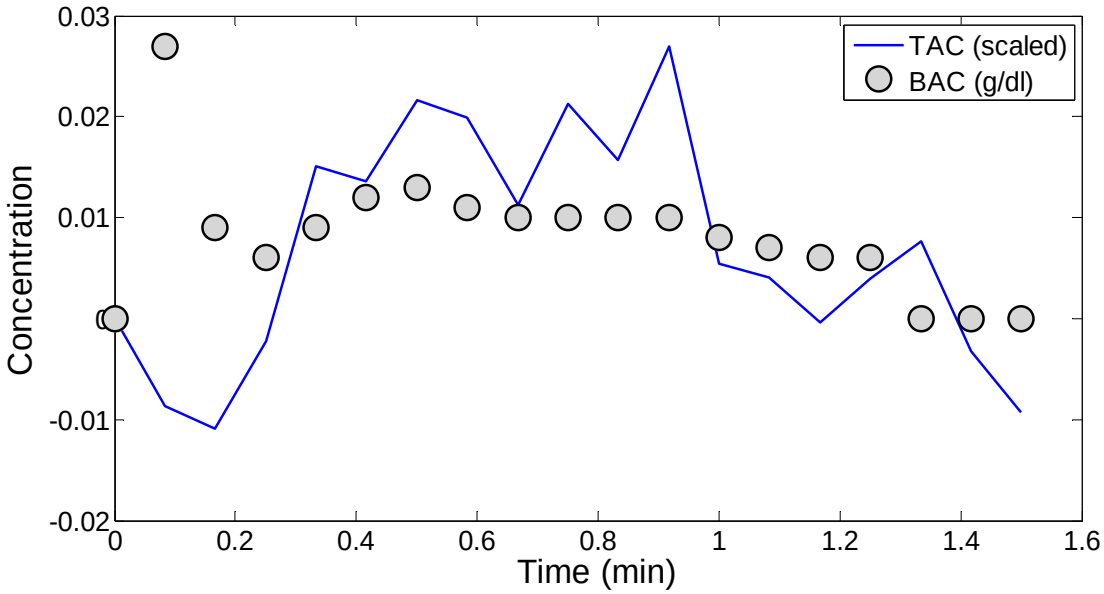

Figure C-29. Subject 004 | Dose: 1 Drink | Right Wrist

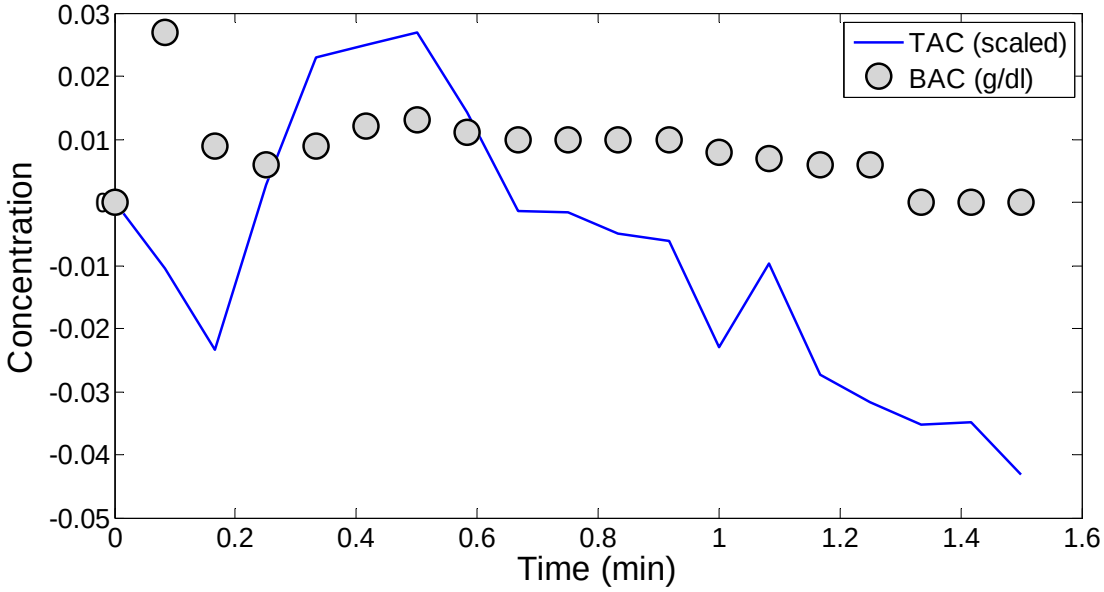

Figure C-30. Subject 004 | Dose: 1 Drink | Left Wrist

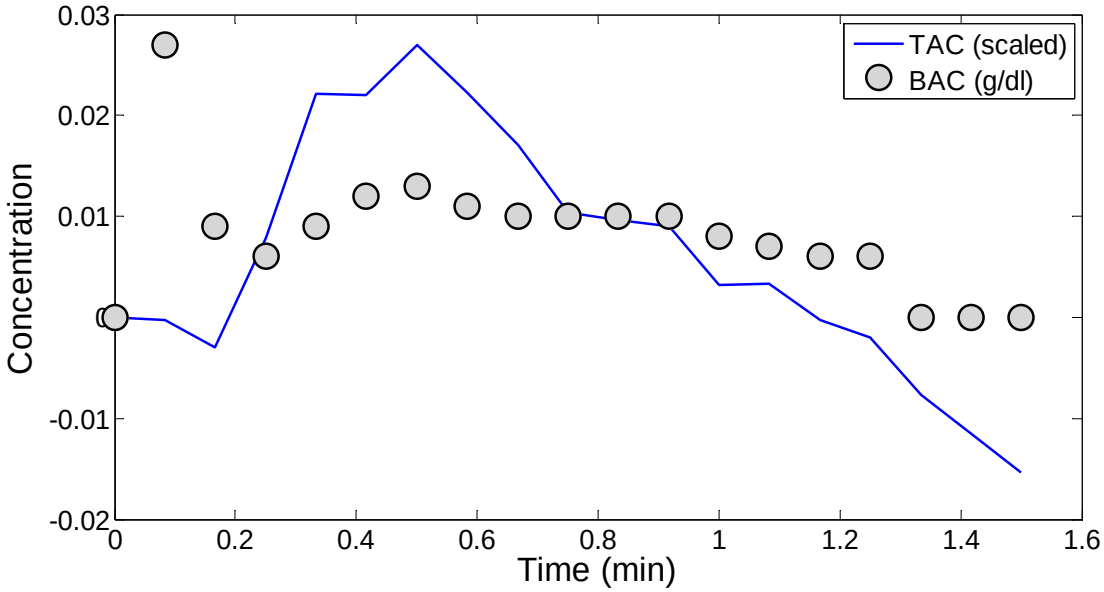

Figure C-31. Subject 004 | Dose: 1 Drink | Ankle

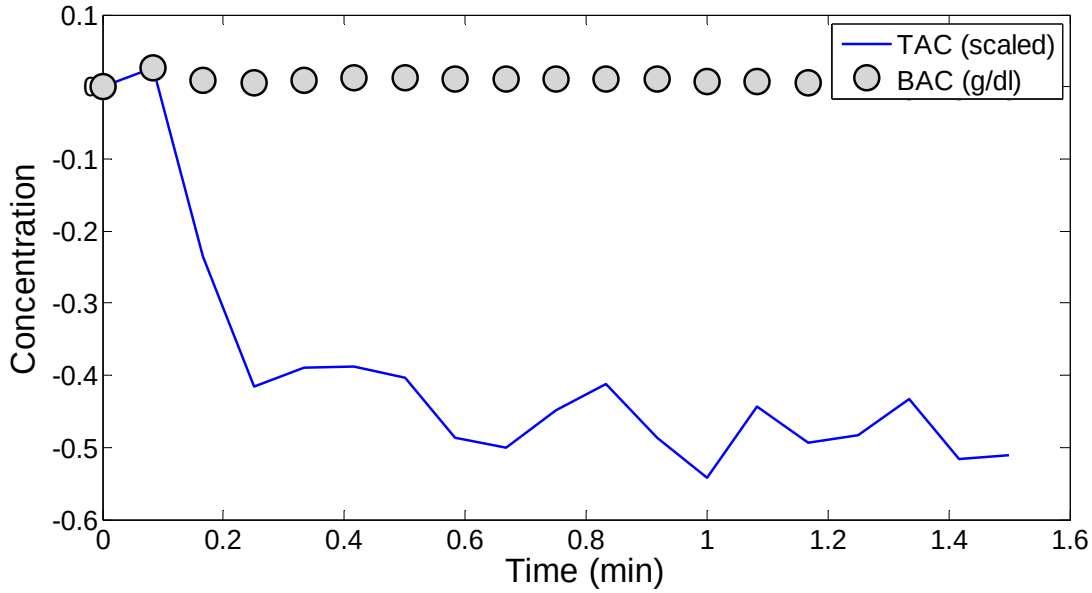

Figure C-32. Subject 004 | Dose: 1 Drink | Forehead

Subject 006: Dose: 1 Drink

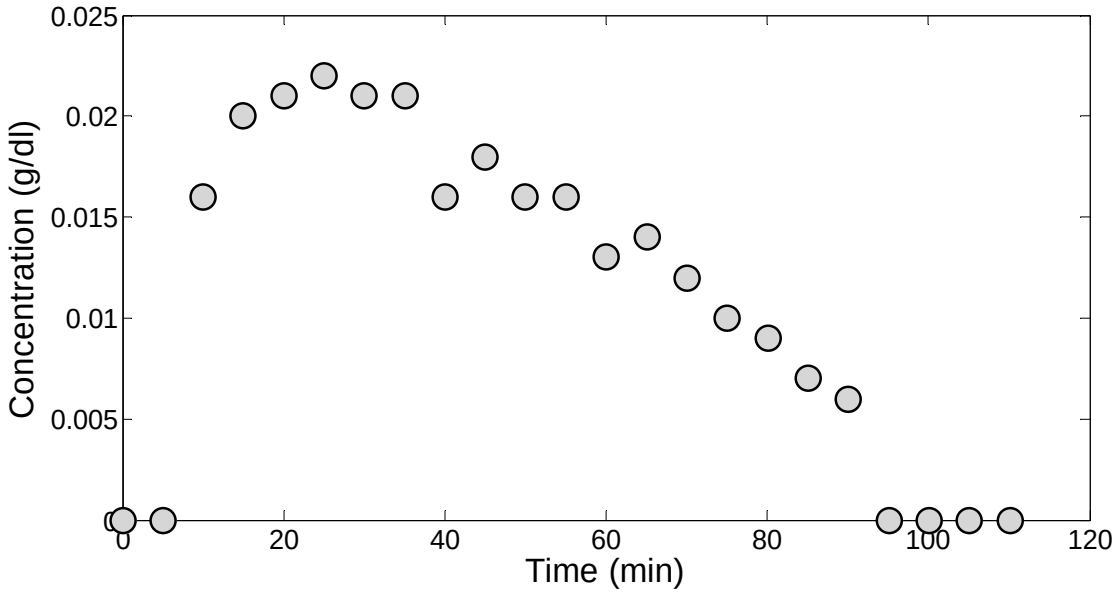

Figure C-33. Subject 006 | Dose: 1 Drink | BAC

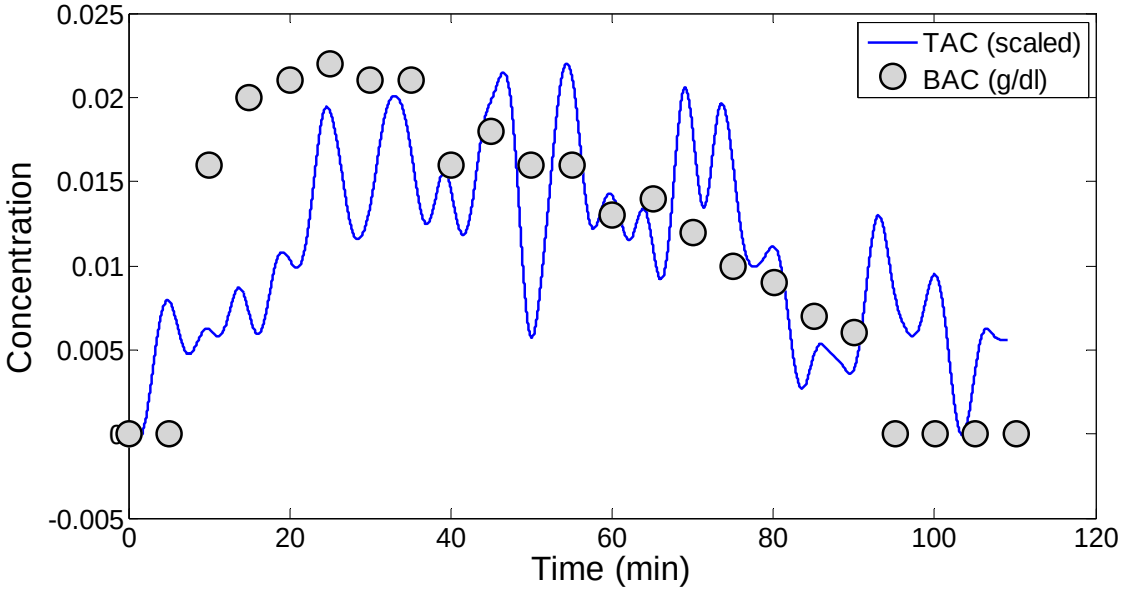

Figure C-34. Subject 006 | Dose: 1 Drink | Palm 1

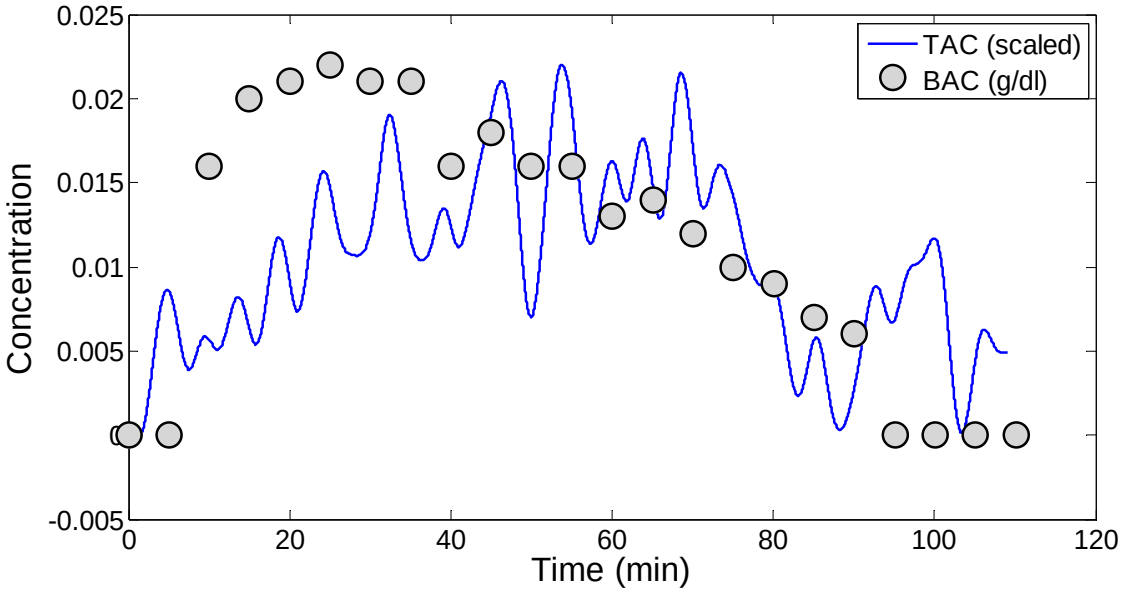

Figure C-35. Subject 006 | Dose: 1 Drink | Palm 2

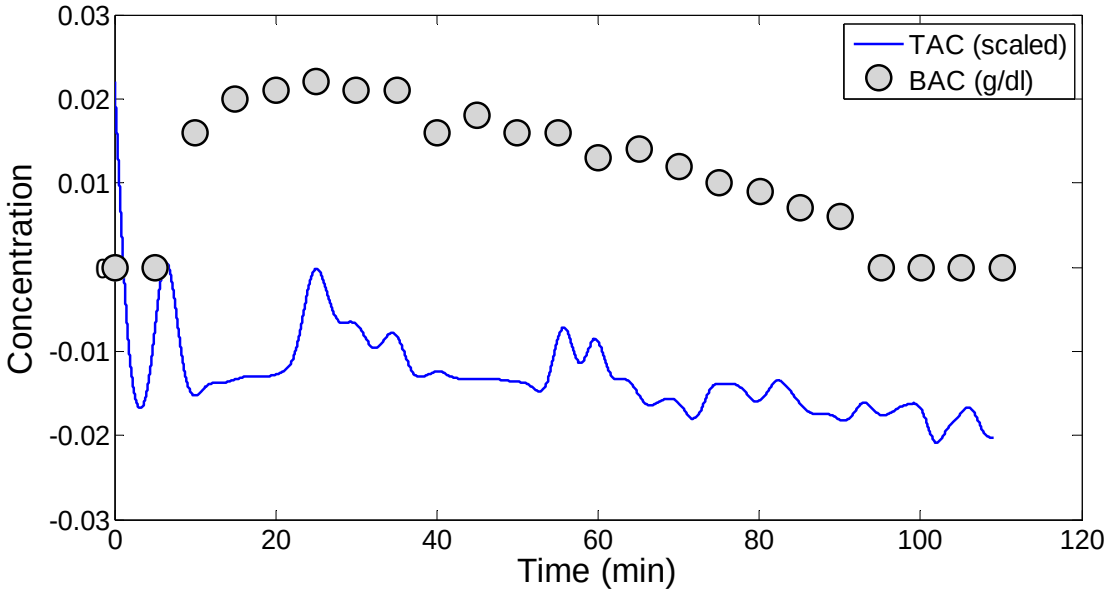

Figure C-36. Subject 006 | Dose: 1 Drink | Forehead 1

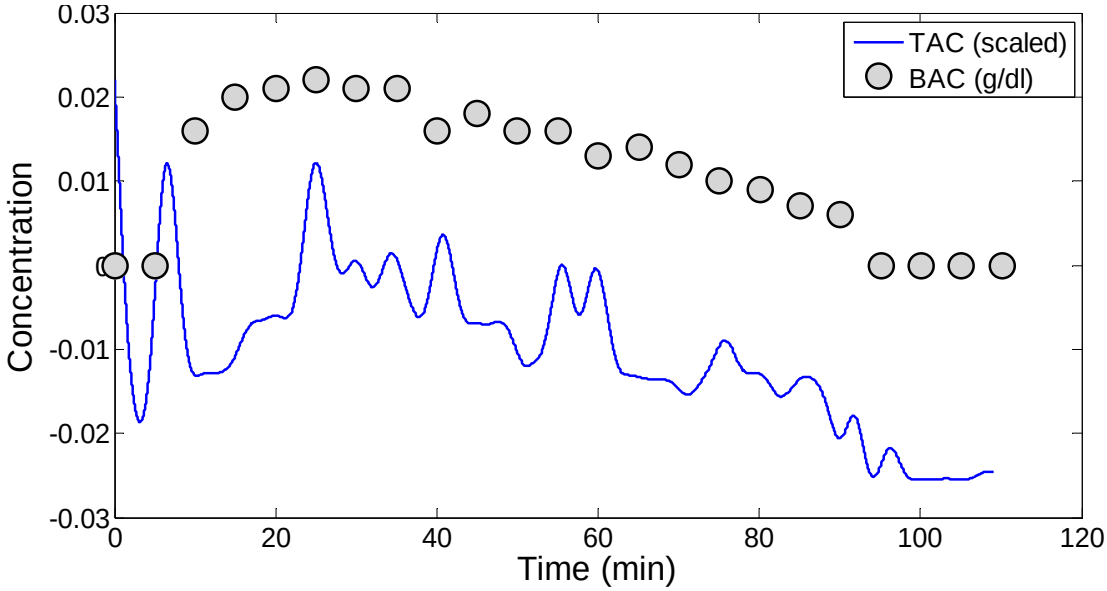

Figure C-37. Subject 006 | Dose: 1 Drink | Forehead 2

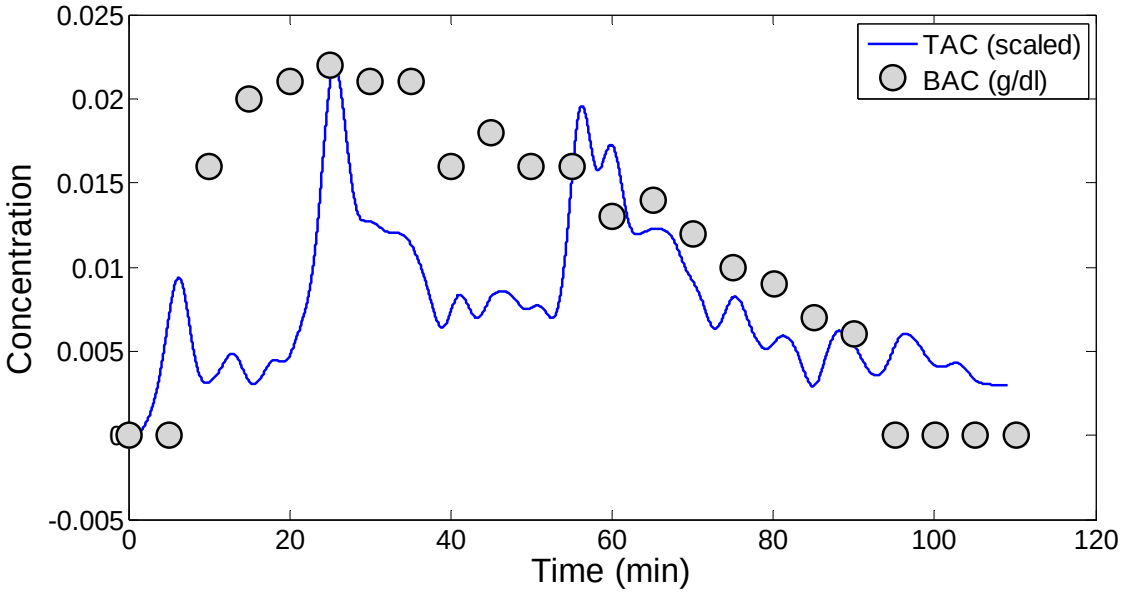

Figure C-38. Subject 006 | Dose: 1 Drink | Neck 1

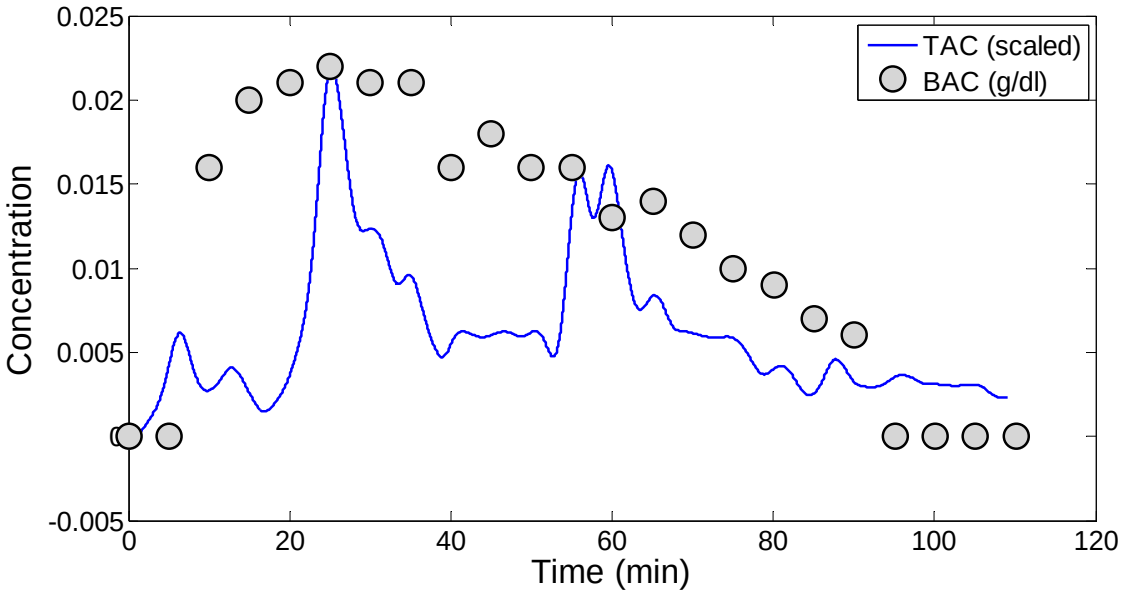

Figure C-39. Subject 006 | Dose: 1 Drink | Neck 2

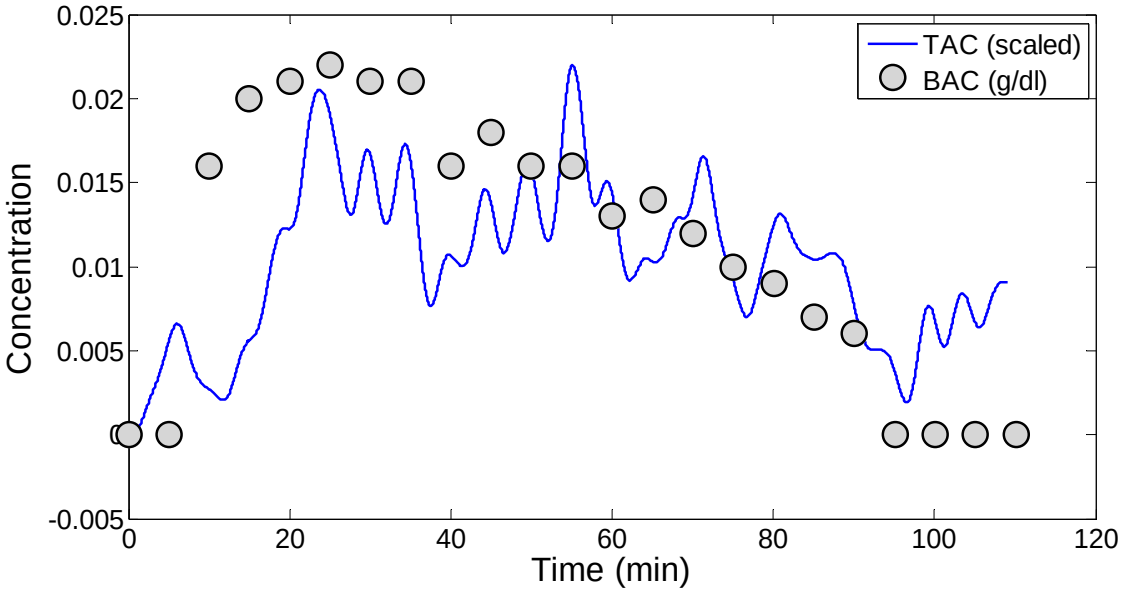

Figure C-40. Subject 006 | Dose: 1 Drink | Left Wrist

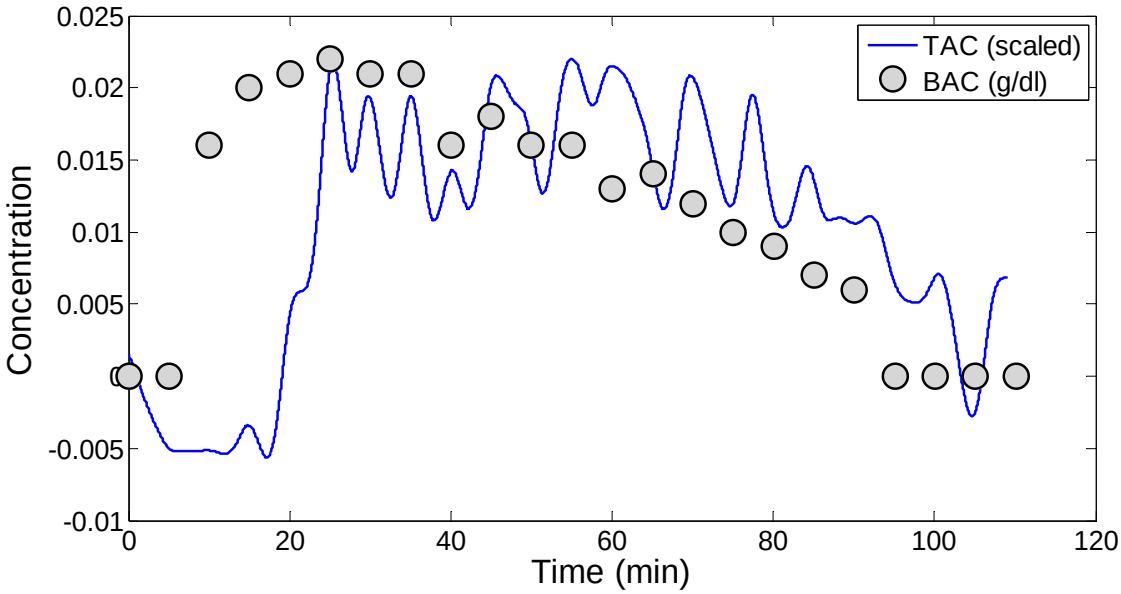

Figure C-41. Subject 006 | Dose: 1 Drink | Right Wrist

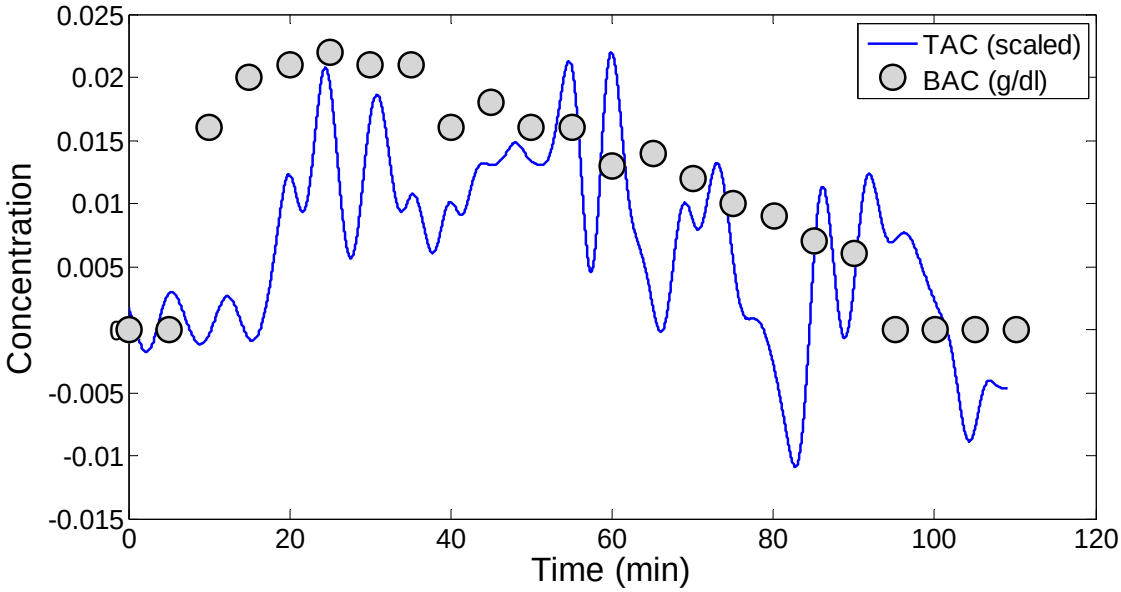

Figure C-42. Subject 006 | Dose: 1 Drink | Left Ankle

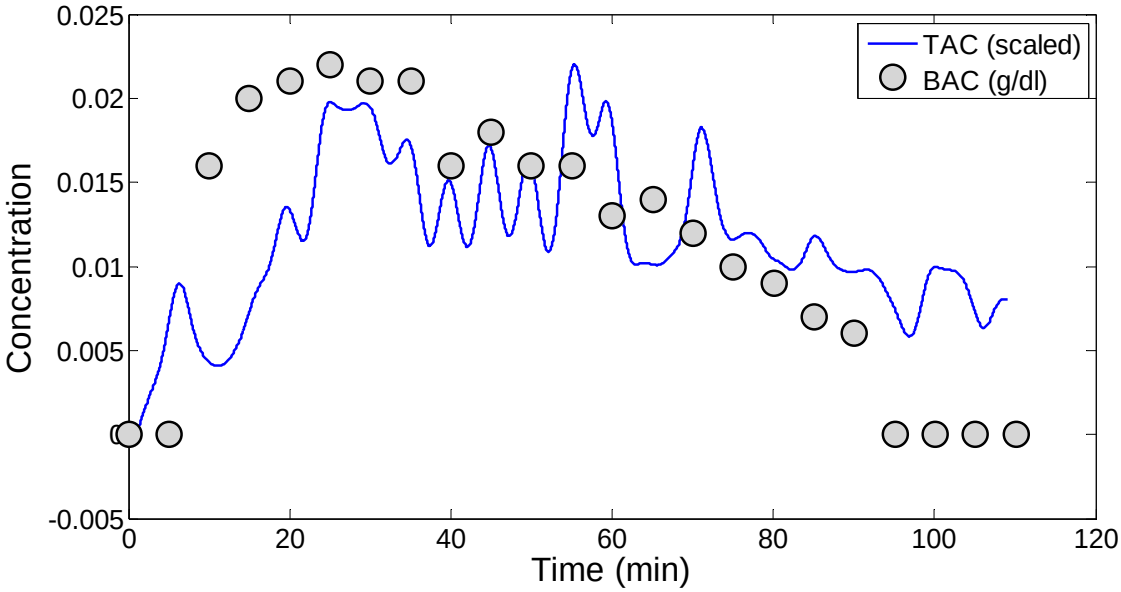

Figure C-43. Subject 006 | Dose: 1 Drink | Right Ankle

Subject 006: Dose 2 Drinks

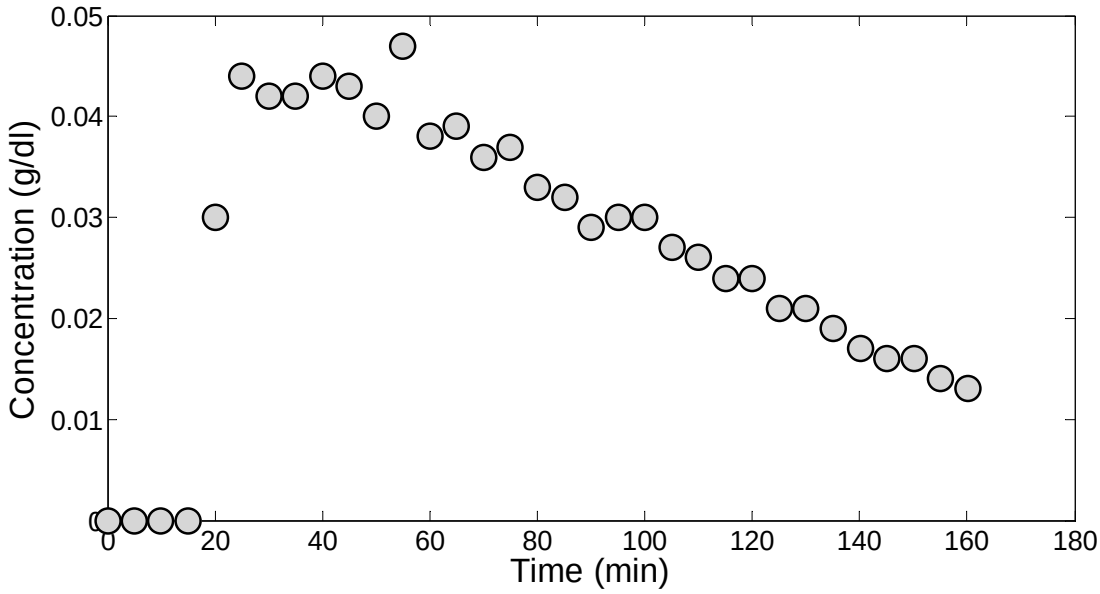

Figure C-44. Subject 006 | Dose: 2 Drinks | BAC

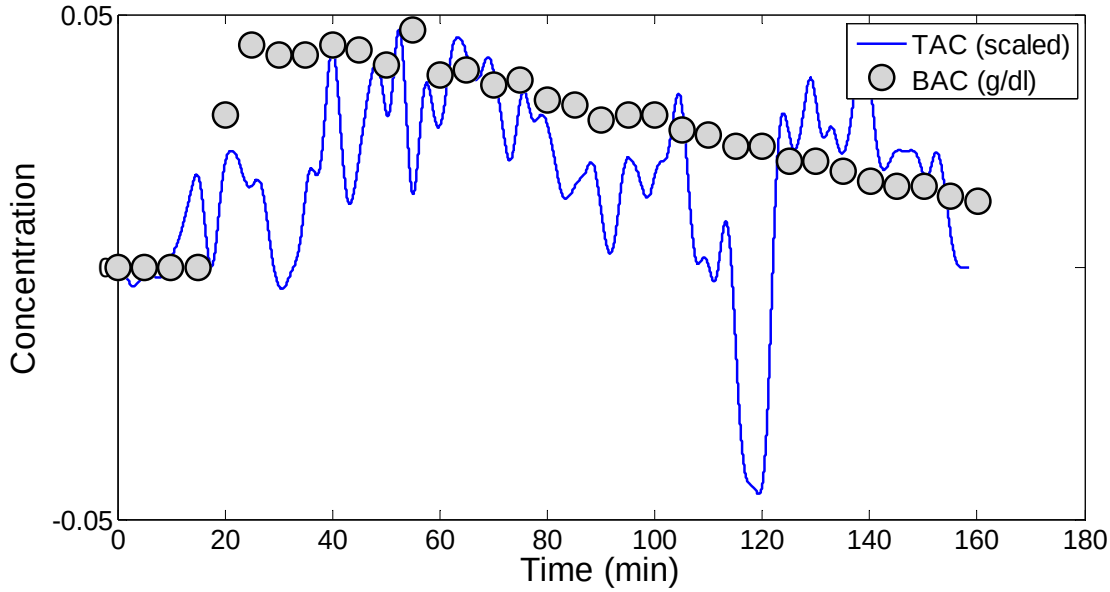

Figure C-45. Subject 006 | Dose: 2 Drinks | Palm 1

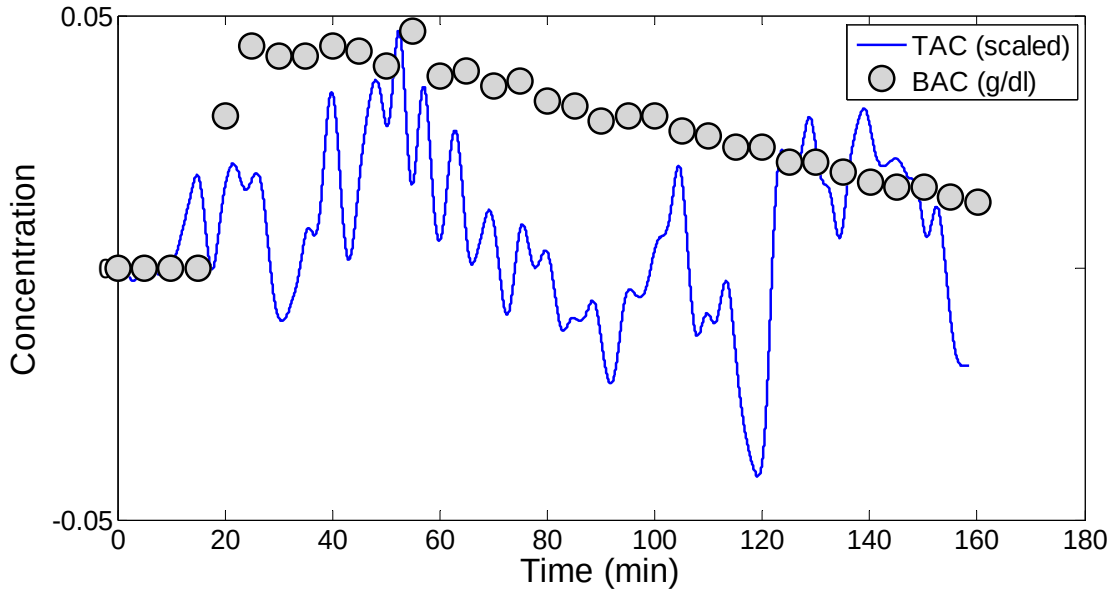

Figure C-46. Subject 006 | Dose: 2 Drinks | Palm 2

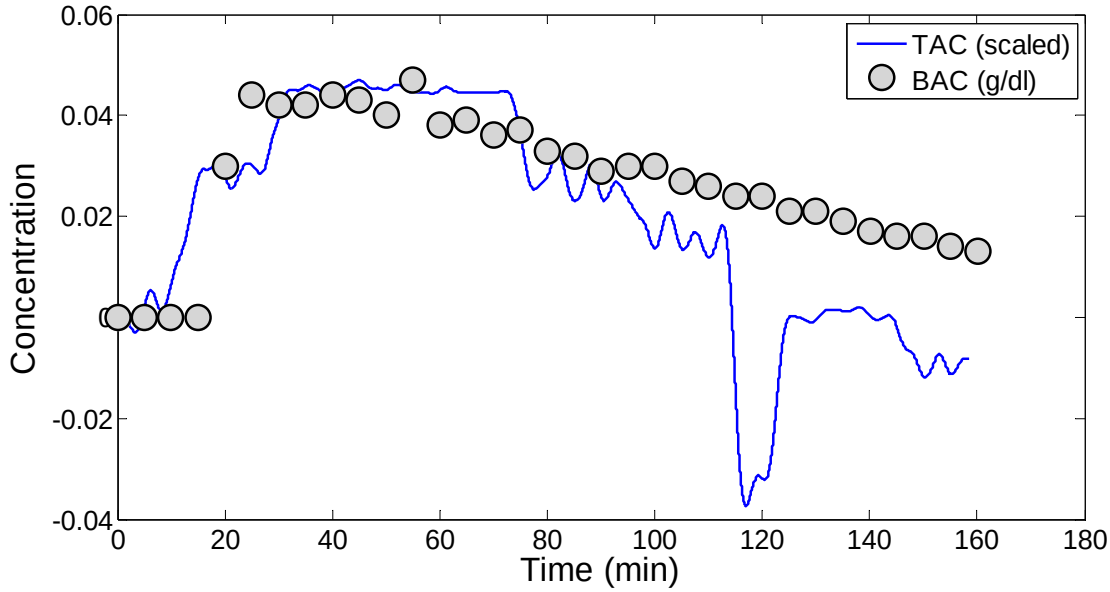

Figure C-47. Subject 006 | Dose: 2 Drinks | Forehead 1

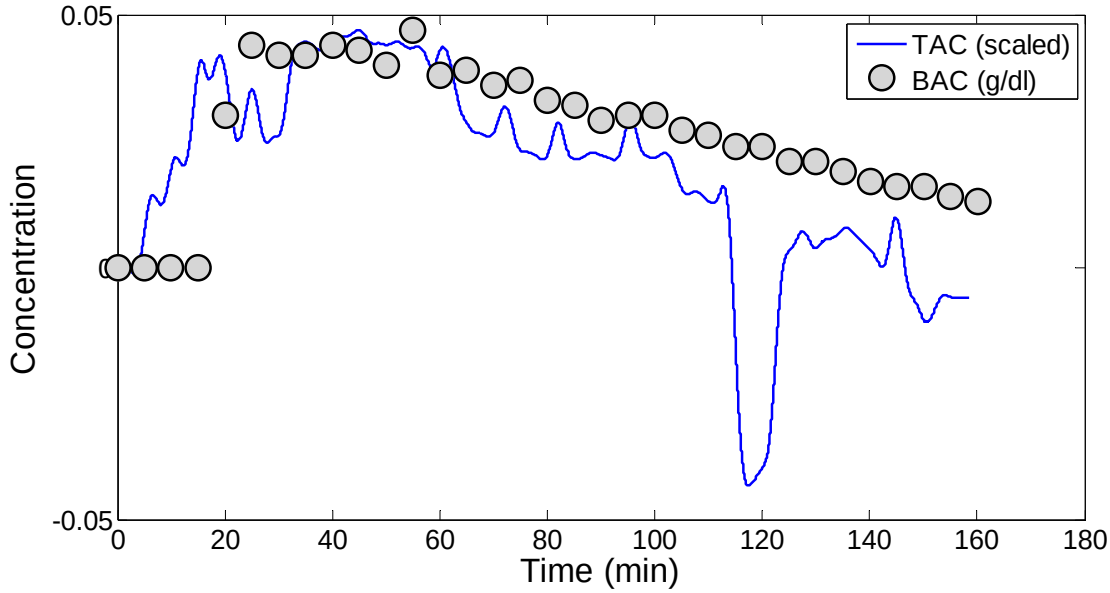

Figure C-48. Subject 006 | Dose: 2 Drinks | Forehead 2

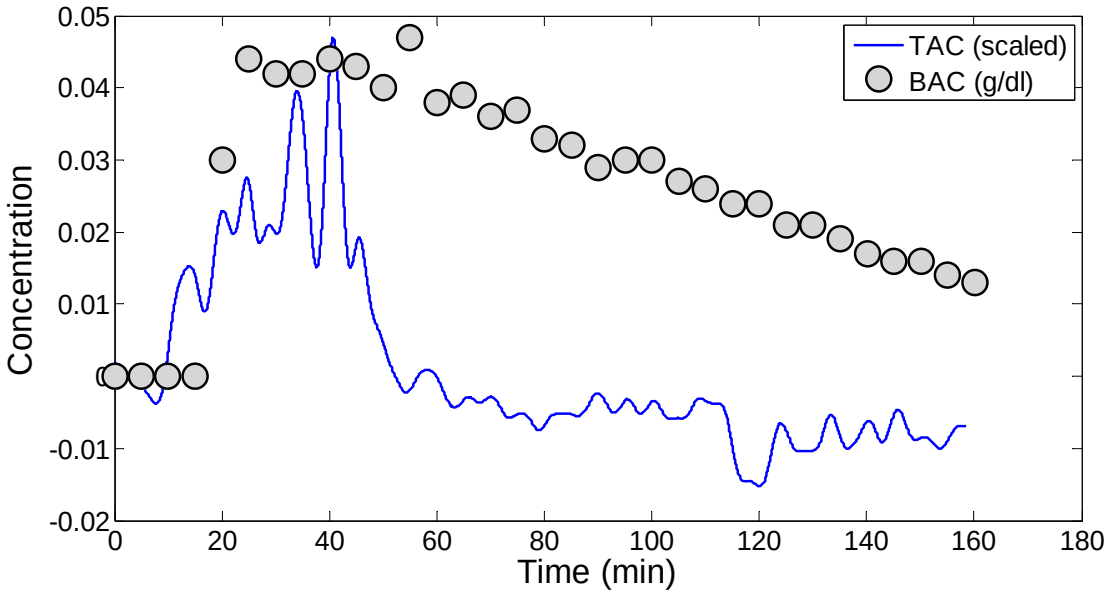

Figure C-49. Subject 006 | Dose: 2 Drinks | Neck 1

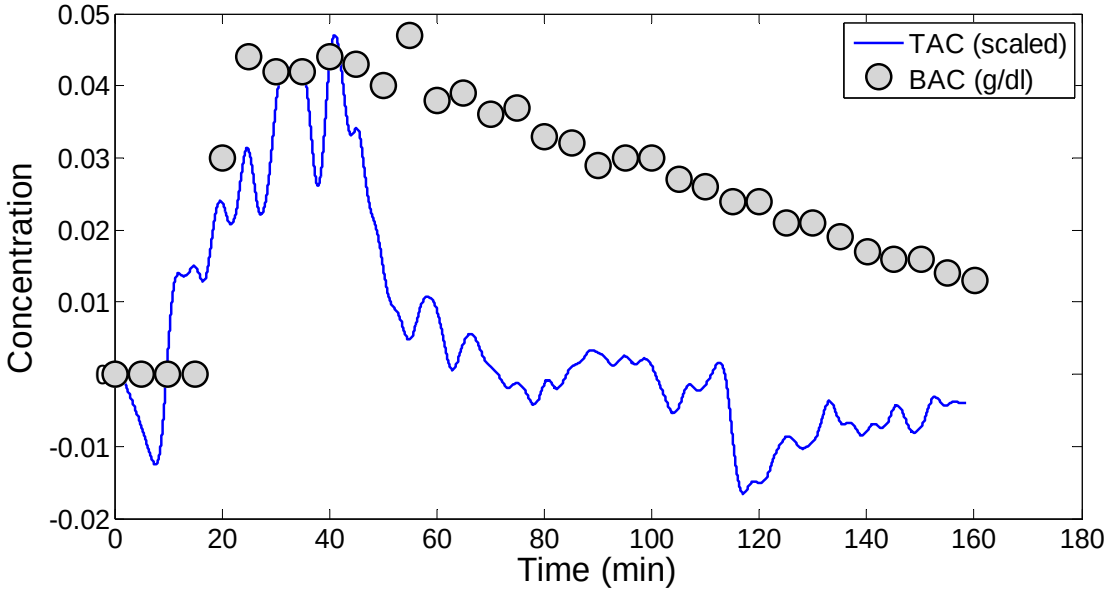

Figure C-50. Subject 006 | Dose: 2 Drinks | Neck 2

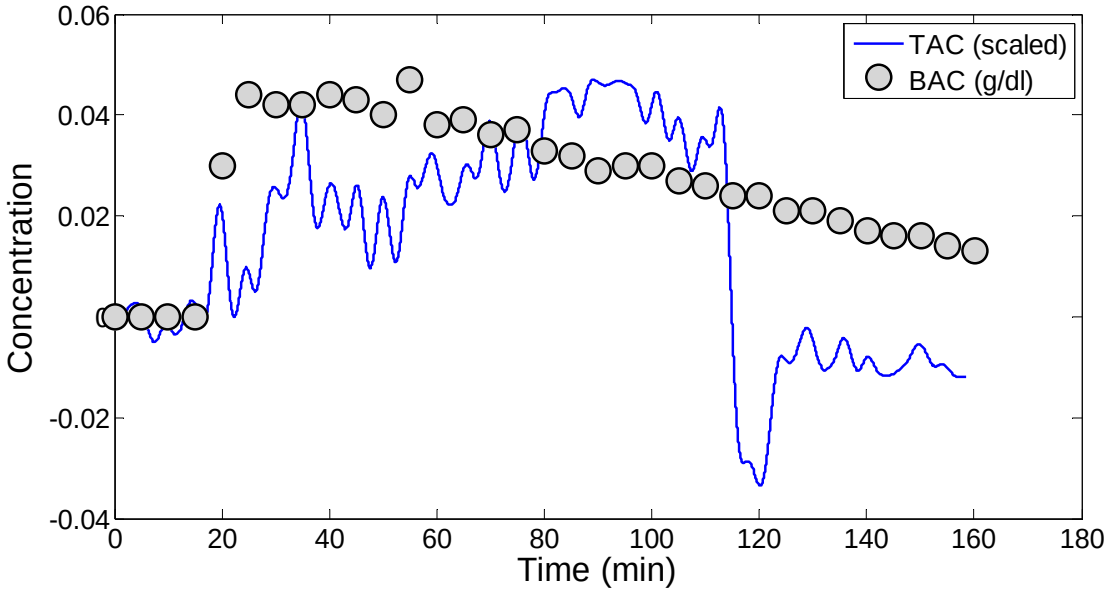

Figure C-51. Subject 006 | Dose: 2 Drinks | Left Wrist

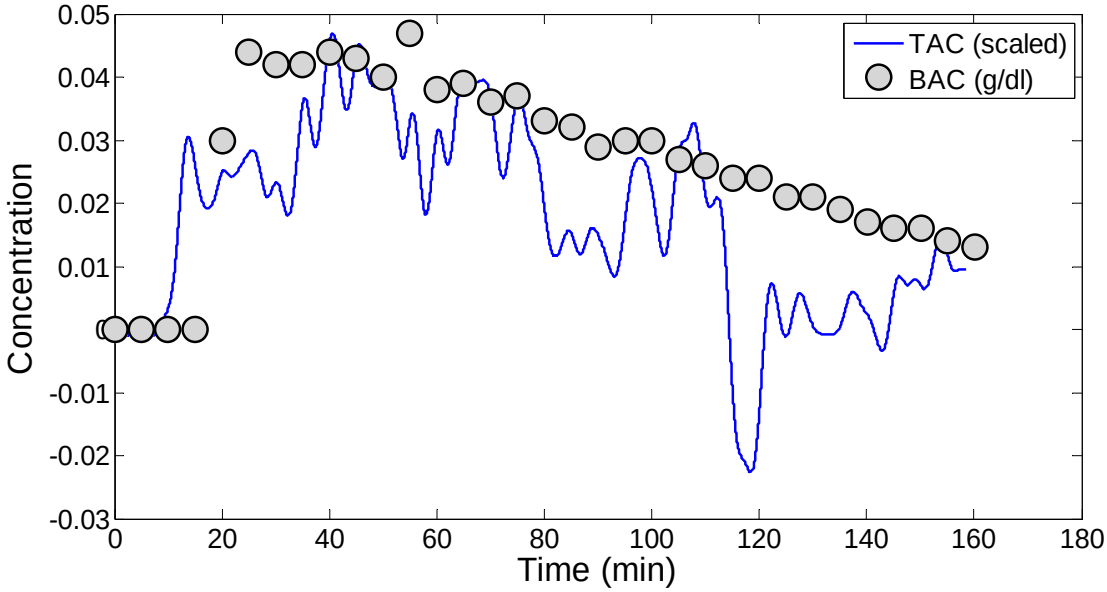

Figure C-52. Subject 006 | Dose: 2 Drinks | Right Wrist

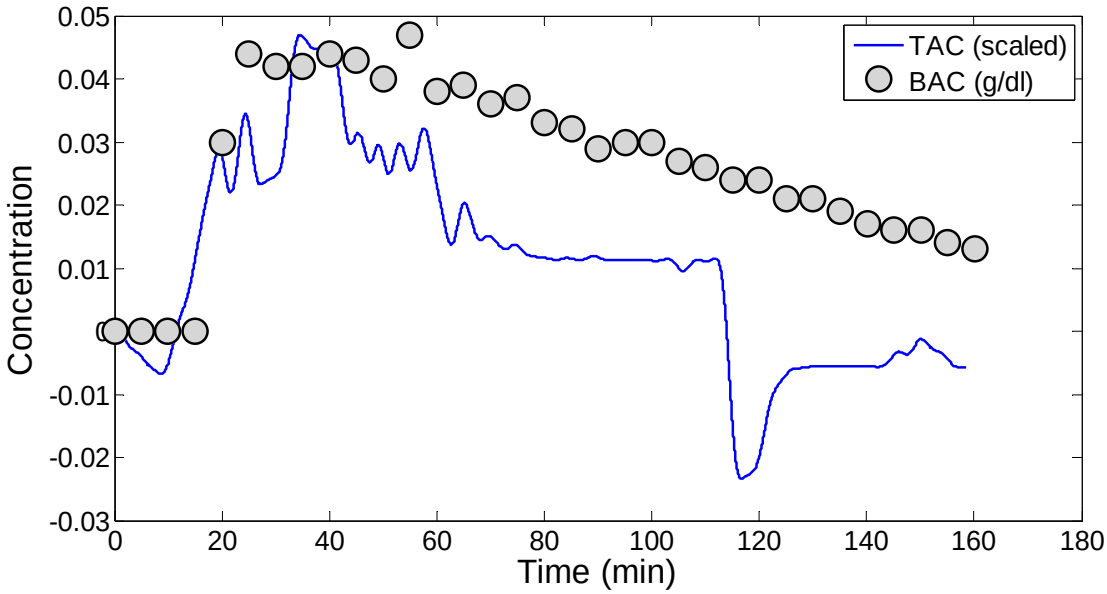

Figure C-53. Subject 006 | Dose: 2 Drinks | Left Ankle

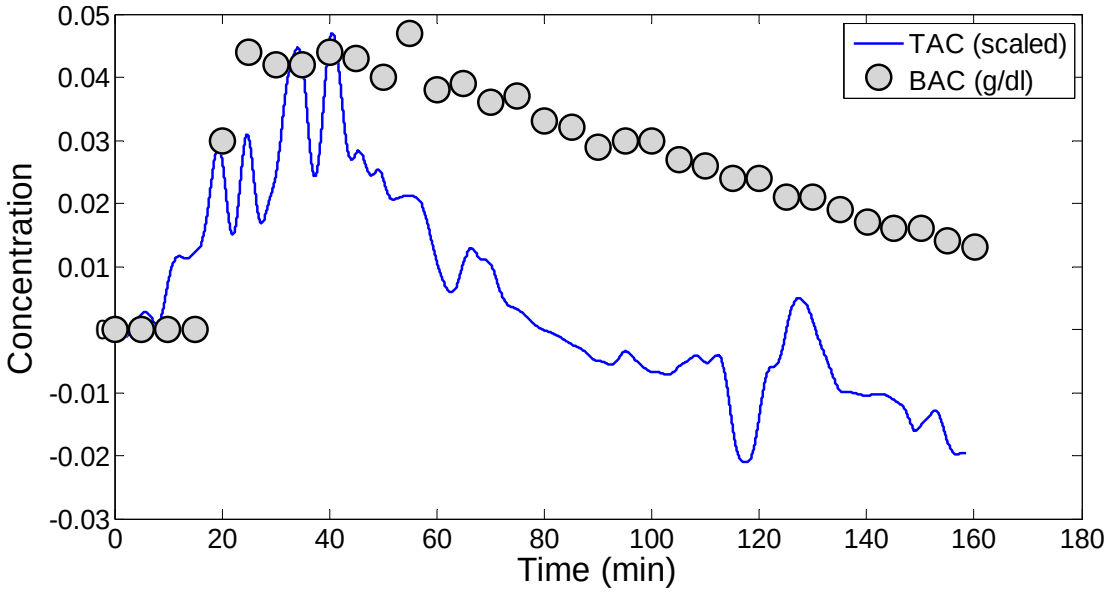

Figure C-54. Subject 006 | Dose: 2 Drinks | Right Ankle

Subject 006: Dose 3 Drinks

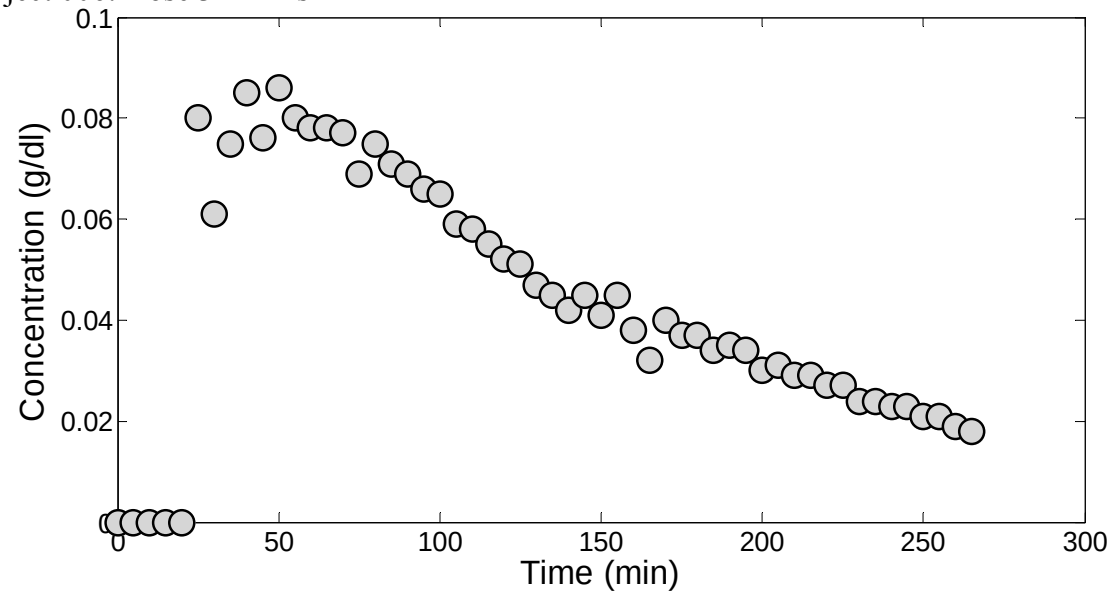

Figure C-55. Subject 006 | Dose: 3 Drinks | BAC

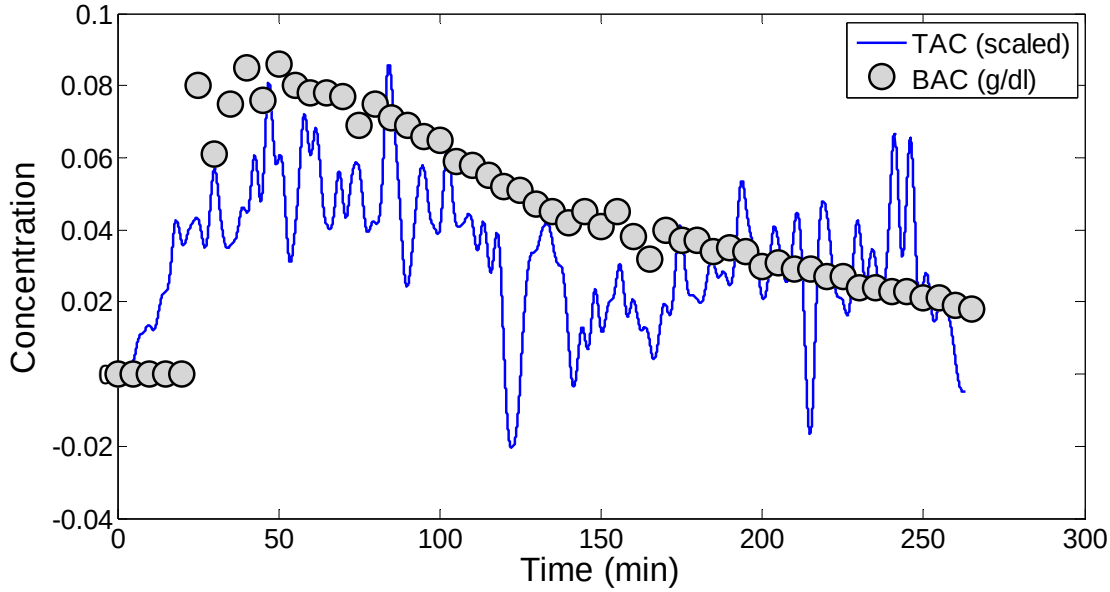

Figure C-56. Subject 006 | Dose: 3 Drinks | Palm 1

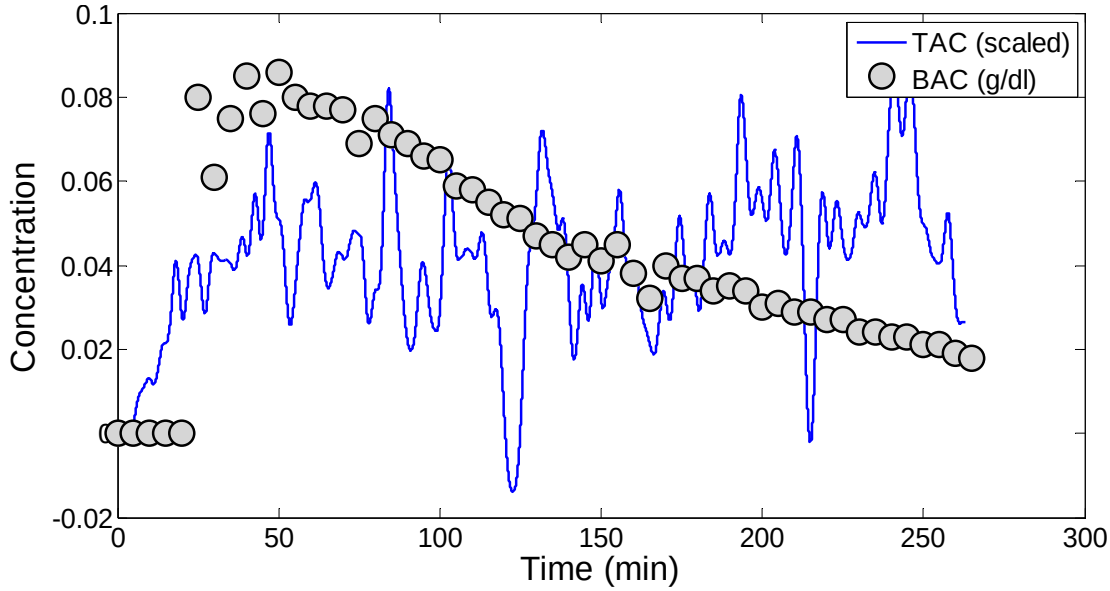

Figure C-57. Subject 006 | Dose: 3 Drinks | Palm 2

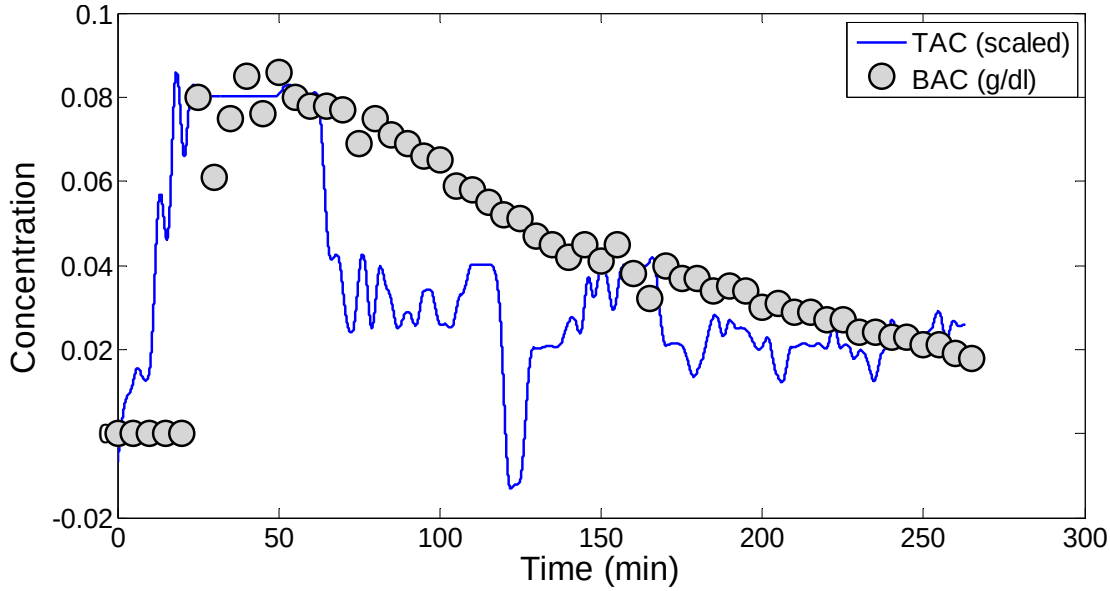

Figure C-58. Subject 006 | Dose: 3 Drinks | Forehead 1

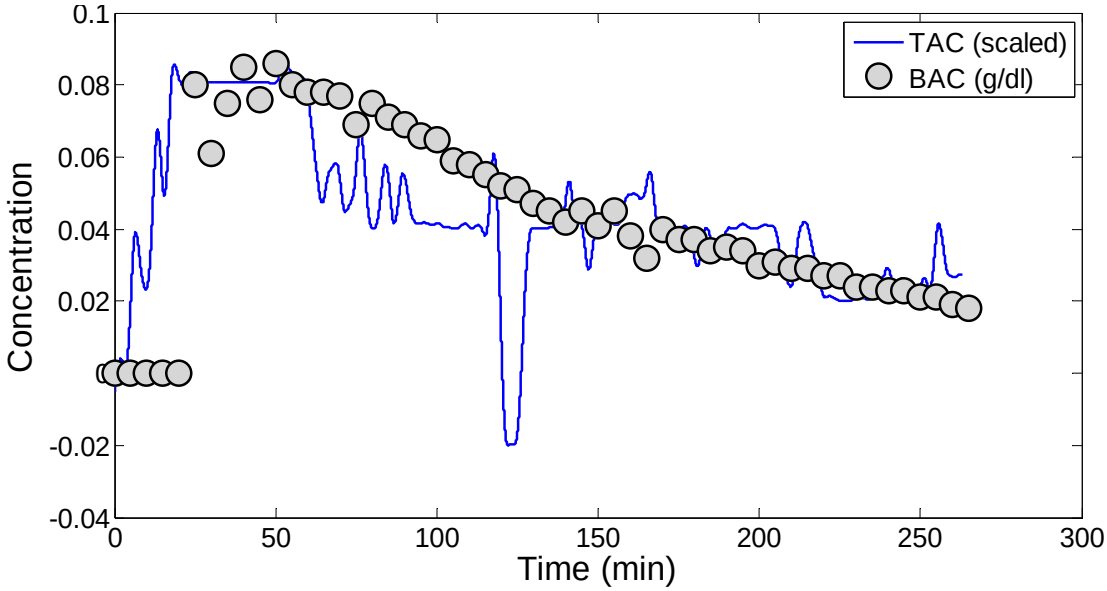

Figure C-59. Subject 006 | Dose: 3 Drinks | Forehead 2

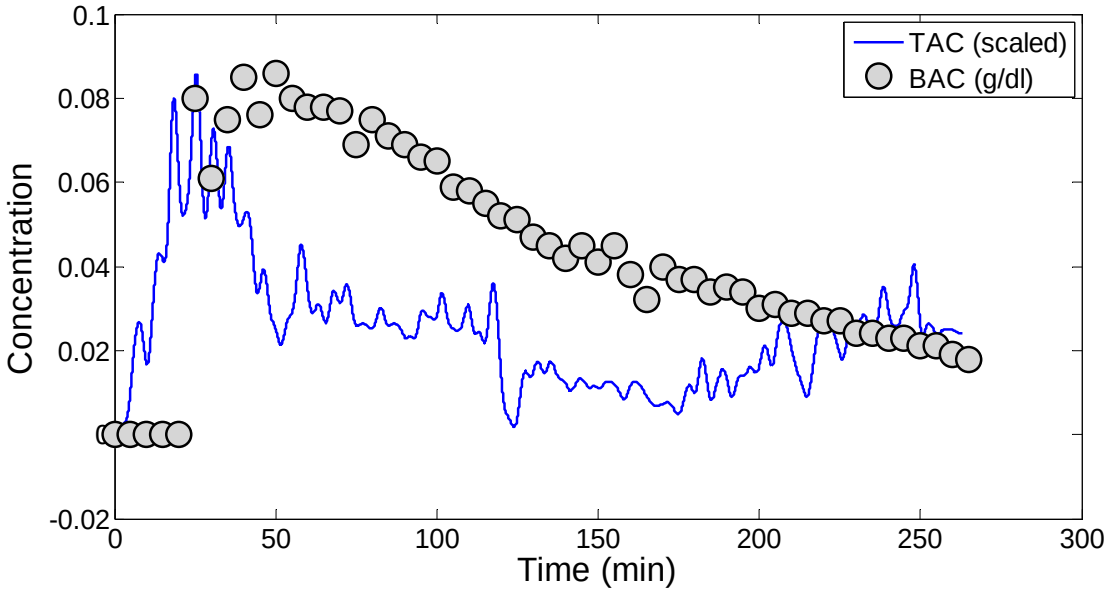

Figure C-60. Subject 006 | Dose: 3 Drinks | Neck 1

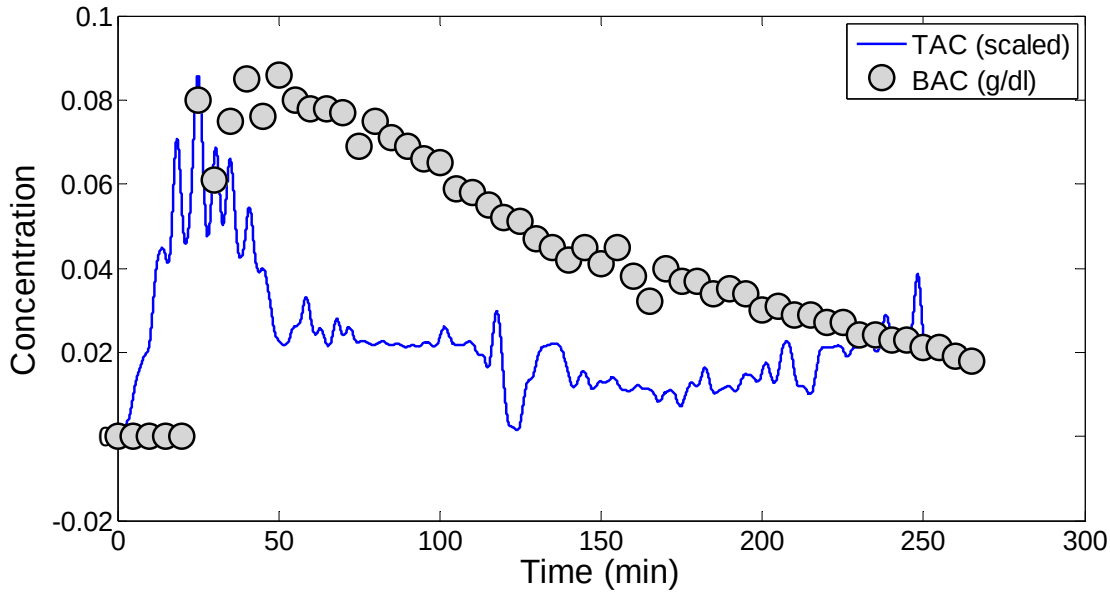

Figure C-61. Subject 006 | Dose: 3 Drinks | Neck 2

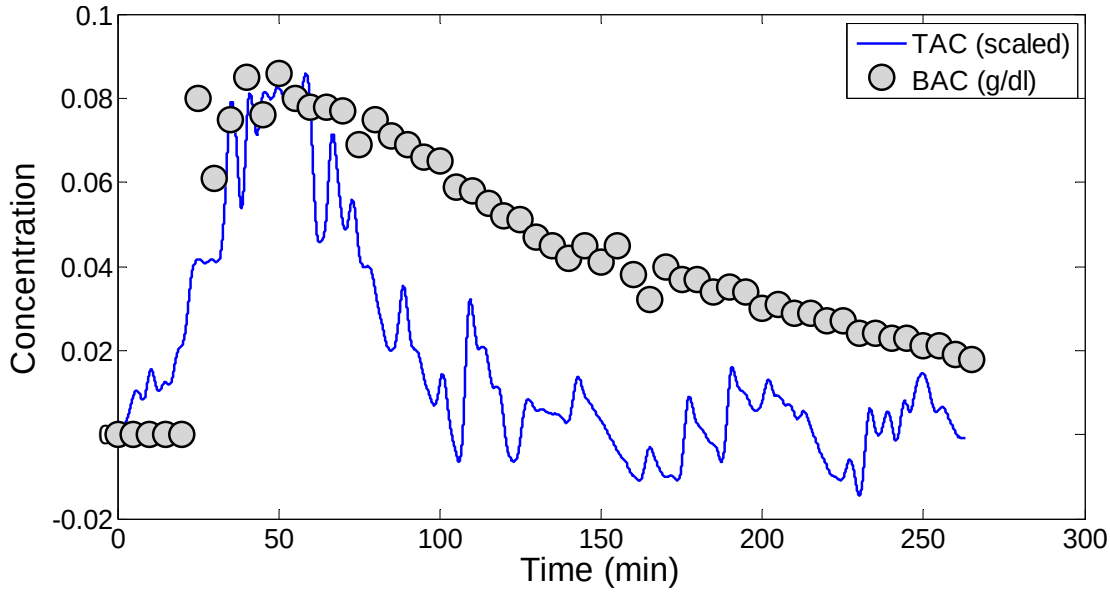

Figure C-62. Subject 006 | Dose: 3 Drinks | Left Wrist

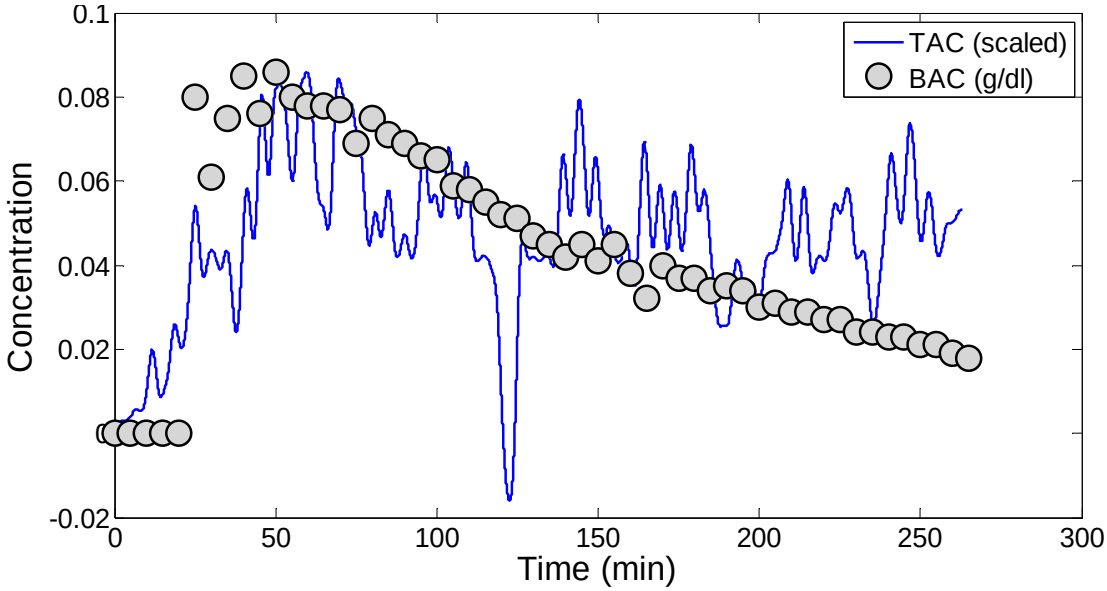

Figure C-63. Subject 006 | Dose: 3 Drinks | Right Wrist

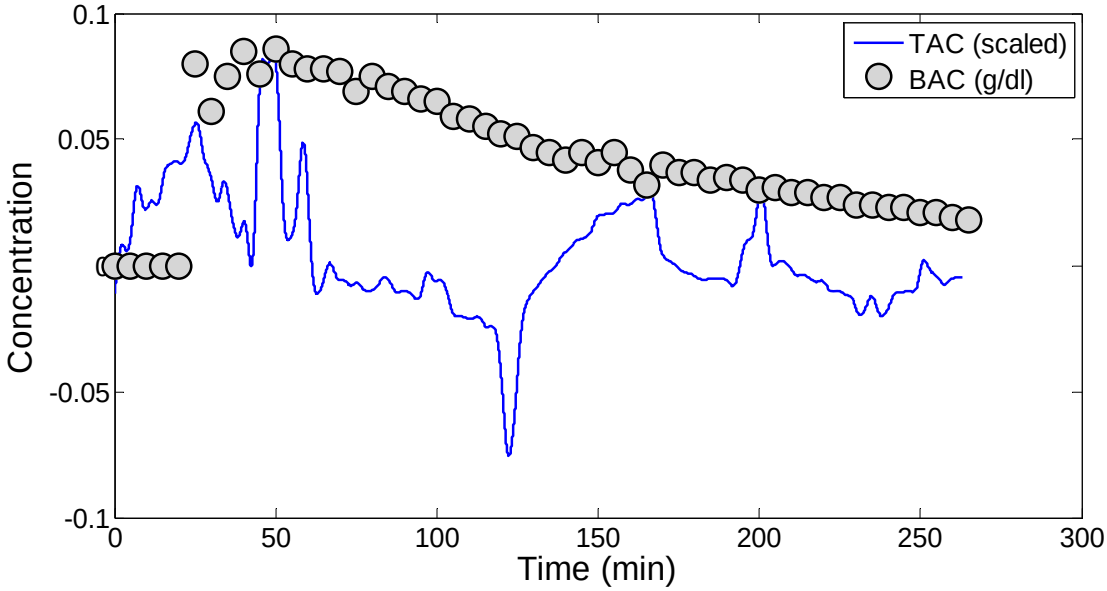

Figure C-64. Subject 006 | Dose: 3 Drinks | Left Ankle

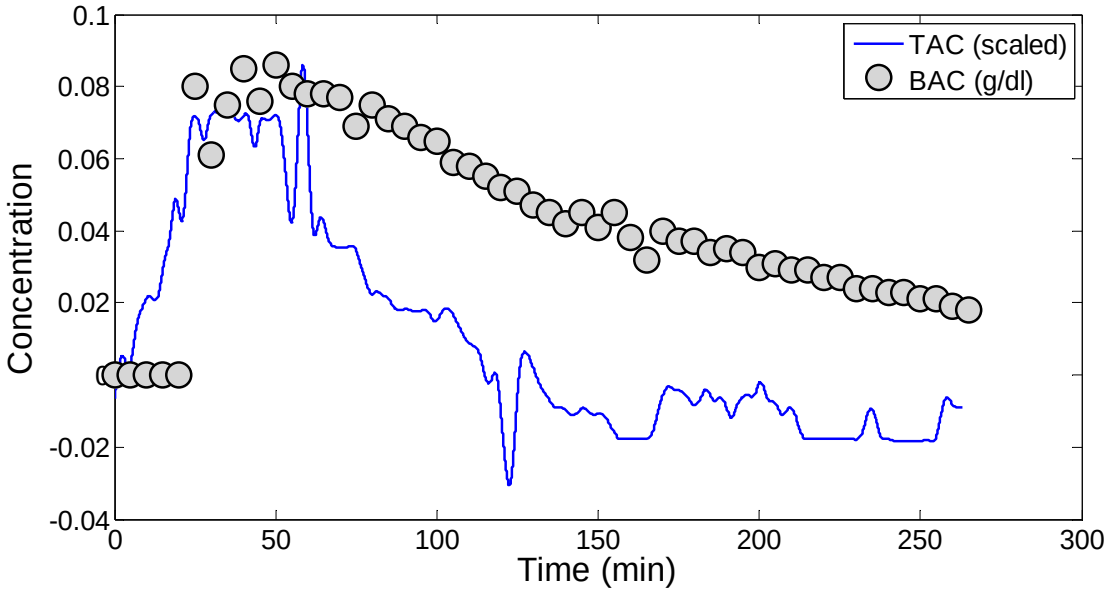

Figure C-65. Subject 006 | Dose: 3 Drinks | Right Ankle